

---

Doctoral Dissertations

Student Theses and Dissertations

---

1970

## A quasi-lattice model of simple liquids

Jesse Herbert Collins

Follow this and additional works at: [https://scholarsmine.mst.edu/doctoral\\_dissertations](https://scholarsmine.mst.edu/doctoral_dissertations)

 Part of the [Physics Commons](#)

Department: Physics

---

### Recommended Citation

Collins, Jesse Herbert, "A quasi-lattice model of simple liquids" (1970). *Doctoral Dissertations*. 2108.  
[https://scholarsmine.mst.edu/doctoral\\_dissertations/2108](https://scholarsmine.mst.edu/doctoral_dissertations/2108)

This thesis is brought to you by Scholars' Mine, a service of the Missouri S&T Library and Learning Resources. This work is protected by U. S. Copyright Law. Unauthorized use including reproduction for redistribution requires the permission of the copyright holder. For more information, please contact [scholarsmine@mst.edu](mailto:scholarsmine@mst.edu).

A QUASI-LATTICE MODEL OF SIMPLE LIQUIDS

by

JESSE HERBERT COLLINS, II, 1938-

A DISSERTATION

Presented to the Faculty of the Graduate School of the

UNIVERSITY OF MISSOURI - ROLLA

In Partial Fulfillment of the Requirements for the Degree

DOCTOR OF PHILOSOPHY

in

PHYSICS

1970

T2405

121 pages

c. I

Louis N. Lund  
Advisor

Ralph E. Lee

W. J. James

Richard Anderson

J. J. Rivers

Otto H. Hill

193972

## ABSTRACT

A cellular model of simple liquids is proposed which eliminates the objectionable feature of long range order found in other cell models. The volume is divided into  $N$  identical spherically symmetric cells, each occupied by one molecule. The cell-center density distribution relative to an average given cell center forms a series of Gaussian peaks whose width is proportional to the square root of the distance from the given cell center. The number of cell centers and average radial distance represented by each of the peaks correspond to a face-centered cubic lattice.

The molecular pair distribution function is determined for several temperatures and densities from the cell-center pair distribution and the molecular interaction through an integral relationship. The molecules are assumed to interact according to the Lennard-Jones 12-6 potential. The calculated molecular pair distribution functions agree qualitatively with experiment in most respects.

Thermodynamic functions are then calculated for liquid argon from the molecular pair distribution and comparison made with results of experiment and other models. Reasonable agreement with experimental values is obtained near the triple point where the assumptions

made are most valid. Extension of the range of densities for which this model gives meaningful values of the thermodynamic properties is achieved by a slight modification of the molecular pair distribution at small radial distances.

## ACKNOWLEDGEMENT

The author wishes to thank Dr. Louis H. Lund for suggesting the main features of the model considered in this work. His interest and encouragement throughout this study are greatly appreciated. The many stimulating and fruitful discussions with him were a major factor in the successful conclusion of this work.

## TABLE OF CONTENTS

	Page
ABSTRACT	ii
ACKNOWLEDGEMENT	iv
LIST OF ILLUSTRATIONS	vii
LIST OF TABLES	ix
I. INTRODUCTION	1
II. THEORY AND DESCRIPTION OF THE MODEL	6
A. The Cell-Center Distribution	6
B. The Molecular Interaction	8
C. The Potential and Probability Density Within a Cell	9
D. The Molecular Pair Distribution Function	13
E. Application to Argon	21
III. DETERMINATION OF THERMODYNAMIC PROPERTIES	24
IV. COMPUTER CALCULATIONS	26
A. General	26
B. The Cell-Center Pair Distribution Function	26
C. Normalization of Probability Density Within the Cell	27
D. The Molecular Pair Distribution Function	27
E. Thermodynamic Functions	28
V. RESULTS	34

	Page
VI. DISCUSSION OF RESULTS	66
A. The Molecular Pair Distribution Function	66
B. Thermodynamic Functions for Unadjusted $\rho(R)$	70
C. Thermodynamic Functions for Adjusted $\rho(R)$	75
D. Comparison of This Model to Other Cell Models	77
E. Accuracy of Results	80
F. Selection of Parameters	82
G. Possible Improvements in the Model	83
VII. CONCLUSIONS	86
VIII. APPENDICES	88
A. Square Root of R Dependence of Peak Width	88
B. Reduced Quantities	89
C. Computer Programs	91
IX. BIBLIOGRAPHY	109
X. VITA	112

## LIST OF ILLUSTRATIONS

Figure		Page
1	Lennard-Jones Potential	10
2	Relationship of Molecules and Cell Centers and the Bipolar Coordinate System	22
3	Molecular Pair Distribution for $T^* = .7$ , $V^* = 1.0$	35
4	Molecular Pair Distribution for $T^* = .7$ , $V^* = 1.2$	36
5	Molecular Pair Distribution for $T^* = .7$ , $V^* = 1.4$	37
6	Molecular Pair Distribution for $T^* = .7$ , $V^* = 1.6$	38
7	Molecular Pair Distribution for $T^* = 1.2$ , $V^* = 1.0$	39
8	Molecular Pair Distribution for $T^* = 1.2$ , $V^* = 1.2$	40
9	Molecular Pair Distribution for $T^* = 1.2$ , $V^* = 1.4$	41
10	Molecular Pair Distribution for $T^* = 1.2$ , $V^* = 1.6$	42
11	Molecular Pair Distribution for $T^* = 2.0$ , $V^* = 1.0$	43
12	Molecular Pair Distribution for $T^* = 2.0$ , $V^* = 1.2$	44
13	Molecular Pair Distribution for $T^* = 2.0$ , $V^* = 1.4$	45
14	Molecular Pair Distribution for $T^* = 2.0$ , $V^* = 1.6$	46
15	$\rho(R)$ and $\rho_C(R)$ , $D = .06$ , $T^* = .7$ , $V^* = 1.0$	47
16	$\rho(R)$ and $\rho_C(R)$ , $D = .02$ , $T^* = 2.0$ , $V^* = 1.6$	48



Figure		Page
17	Cell Potential, $D = 0$ , $T^* = 2.0$	49
18	Cell Potential, $D = .06$ , $T^* = .7$	50
19	Calculated $\rho(R)$ Compared to Experimental $\rho(R)$	51
20	Admusement of $\rho(R)$ in the Most Extreme Case	52
21	Comparison of $U_c/NKT$ at $T^* = 1.2$ with Results of Experiment and Other Models	53
22	Comparison of $PV/NKT$ at $T^* = 1.2$ with Results of Experiment and Other Models	54
23	Comparison of Adjusted Values of $U_c/NKT$ with Results of Experiment and Other Models	55
24	Comparison of Adjusted Values of $PV/NKT$ with Results of Experiment and Other Models	56

## LIST OF TABLES

Table		Page
I	Face-Centered Cubic Lattice	23
II	Values of Parameters Used	30
III	Fixed Programming Parameters	31
IV	Varying Programming Parameters	32
V	$U_c/NKT$ at $T^* = .7$	57
VI	$U_c/NKT$ at $T^* = 1.2$	58
VII	$U_c/NKT$ at $T^* = 2.0$	59
VIII	$PV/NKT$ at $T^* = .7$	60
IX	$PV/NKT$ at $T^* = 1.2$	61
X	$PV/NKT$ at $T^* = 2.0$	62
XI	$C_v/NK$ at $T^* = .7$	63
XII	$C_v/NK$ at $T^* = 1.2$	64
XIII	$C_v/NK$ at $T^* = 2.0$	65
XIV	Comparison of $U_c/NKT$ Near the Triple Point	73
XV	Comparison of $PV/NKT$ Near the Triple Point	74
XVI	Factors Used for Reduction	90

## I. INTRODUCTION

Advancement in the understanding of the liquid state has not been as great as that of the solid or rarefied gas states. The properties of these three states of matter can be deduced from a knowledge of their structure and of the interaction and properties of their structural units, atoms, molecules, and ions. The absence of an idealized model of general applicability for the case of liquids, such as the perfect crystal or ideal gas in the solid and gaseous states, is the chief reason for this lower degree of progress. Most theories of solids and gases consist of corrections, perturbations, etc., of the ideal model. With no "perfect liquid" model to use as a starting point, a lack of comprehensive understanding of the liquid state is not surprising.

A great deal has been achieved in spite of this handicap, especially of a qualitative nature. Liquids have properties which are intermediate to those of solids and those of rarefied gases. Furthermore, X-ray and neutron diffraction studies<sup>1,2,3,4</sup> show that liquid structure is characterized by short range order; that is, the arrangement of molecules near any given molecule has a high degree of regularity similar to a solid, but order decreases rapidly as one moves away from the given molecule, approaching the randomness of a gas structure.

Liquid theories thus usually take the form of extrapolations of the theories of gases or solids.

Theories in which the structure and properties are calculated from some assumed knowledge of the molecular interactions are usually gas-like. The most prominent are based on the cluster theory of Meyer<sup>5,6</sup> or on determination of distribution functions from integral equations by use of approximations introduced by Kirkwood<sup>7</sup>, Yvon<sup>8</sup>, Born and Green<sup>9</sup>, and Bogolyubov<sup>10</sup>. More recently, the integral equation developed by Percus and Yevick<sup>11</sup> and the hypernetted chain integral equation developed by several workers<sup>12</sup> have been used. Mathematical intractability has handicapped the applicability of all these methods to liquids.

Another general category of approaches to the study of liquids consists of "lattice theories". Each molecule is assumed to be confined to a limited volume or "cell" by its neighbors. The cells customarily are centered on the points of a regular lattice. Transfer of molecules between cells is infrequent and considered negligible in many models. The theory of Lennard-Jones and Devonshire<sup>13,14</sup> is the classic example, most lattice theories being modifications of this particular model.

As one would expect, lattice theories tend to exaggerate the solid-like properties of liquids; however, these theories are usually more amenable to calculation than other methods although less rigorously founded.

Frequently classed with lattice theories are the Monto Carle<sup>15,16</sup> and molecular dynamic<sup>17</sup> methods which consider large cells with many molecules and determine physical properties by direct numerical averaging. Very large amounts of machine calculations are required and, up to the present, this has limited the usefulness of these methods.

The "tunnel" model<sup>18,19</sup> which divides the volume into long, essentially one dimensional cells has shown promise of significantly improved results over earlier models.

The cell model of Lennard-Jones and Devonshire (hereafter called the LJD model) has been particularly useful in calculating thermodynamic and equilibrium properties of liquids in view of its relative simplicity and mathematical tractability. Although lacking physical rigor, the validity of this approach was enhanced when Kirkwood<sup>20</sup> showed it was equivalent to the first approximation of an integral equation approach based on a number of reasonable well defined assumptions.

In this study, we seek to develop a theory of the liquid state which, while retaining some of the simplicity and mathematical tractability of a cell model of the LJD type, will at the same time eliminate some of the more physically objectionable features of such a model. In particular, the long range order, inherent in the LJD model, is to be removed.

A model for liquid structure proposed by Prins and developed by Frenkel<sup>21</sup> gives a somewhat more realistic structure. Called the "structural diffusion" model, it has the desirable property of short range order.

The structure of a liquid is conveniently described by the molecular pair distribution function,  $\rho(R)$ , defined so that

$$N_R = 4\pi \int_0^R \rho(R) R^2 dR \quad (1)$$

where  $N_R$  is the number of molecules within radial distance  $R$  of an average molecule in the liquid. This function can be obtained experimentally from X-ray<sup>22</sup> and neutron<sup>3</sup> scattering data. Together with the molecular interaction,  $\rho(R)$  can be used to calculate the equilibrium thermodynamic properties<sup>23</sup>. A cell-center pair distribution function,  $\rho_c(R)$ , is defined in a similar manner.

Lund<sup>24</sup> has shown that the actual molecular pair distribution is related through an integral equation to the distribution of the cells.

We shall restrict the considerations in this study to "simple" liquids, i.e., those with spherically symmetrical molecules interacting with non-directional, non-saturating, van der Waals forces. A commonly used molecular interaction is the Lennard-Jones 12-6 potential<sup>25</sup>.

The only real liquids which are closely approximated by simple liquids are the condensed noble gases

(except helium for which quantum effects are significant). A few polyatomic liquids also meet these conditions to some extent, the usual example being carbon tetrachloride.

More particularly, we consider argon as a specific example since more experimental as well as theoretical calculations are available than for any other real substance reasonably described by our model. Application to other noble gas liquids can be made by use of appropriate constants in the intermolecular potential function according to the law of corresponding states<sup>26,27</sup>.

In summary, a model for simple liquids is proposed using the basic assumptions of the LJD model, but with cells distributed according to the structural diffusion approach, rather than in a perfectly regular array. The molecular pair distribution function can be determined by Lund's integral relationship from the cell-center distribution and the molecular interaction which we assume is described by the Lennard-Jones 12-6 potential. Equilibrium thermodynamic properties can then be calculated.

## II. THEORY AND DESCRIPTION OF THE MODEL

### A. The Cell-Center Distribution

The LJD theory assumes that the available volume  $V$  in a system of  $N$  molecules is divided into  $N$  identical cells each containing one molecule. The cells are distributed such that their centers lie on the points of a virtual face-centered cubic lattice. Each molecule is confined in a potential well formed by its neighbors. The potential within a cell is calculated assuming all other molecules are at their cell centers and there is no coordination between the motion of the molecules.

For mathematical convenience the cell potential is averaged over all angles or "spherically" so that it is a function of radial distance from the cell center with no angular dependence. This is equivalent to distributing each shell of neighboring molecules continuously and uniformly over a spherical shell, hence the term "smearing approximation" is applied to this procedure.

With a spherically symmetric cell potential, it is also convenient to consider the cells spherical in shape. Obviously spherical cells will not completely fill a volume without overlap. This turns out to be not too serious since the potential wells are sufficiently narrow to restrict the molecules to a fraction of the cell volume



near the center. Usually the cell radius is chosen so the cell volume is  $V/N$ .

Mathematically one can express the cell-center pair distribution function in the LJD model as a sum of Dirac delta functions

$$\rho_c(R) = \sum_m z_m \delta(a_m - R)/(4\pi R^2) \quad (2)$$

where  $a_m$  is the  $m^{\text{th}}$  neighbor distance and  $z_m$  is the coordination number of the  $m^{\text{th}}$  shell. Such a model based on a regular lattice will, of course, retain long range order.

Prins<sup>21</sup> introduced the idea that a liquid structure might be represented as quasi-crystalline with the distribution of molecules relative to a given molecule as successive Gaussian curves with width increasing as the square root of the radial distance  $R$ . This concept was developed by Frenkel into the "structural diffusion" model of liquids.

The width of the peaks of the pair distribution function for such a model arises from two sources<sup>28</sup>. The first is from thermal vibrations as in a crystal, the second is due to spatial disorder of the centers of vibration. The former should provide a constant contribution to the disorder, i.e., independent of  $R$ . The latter, assuming independent disorder in separation of pairs of molecules, is proportional to the square root of  $R$  (see Appendix A).

In this study we consider a model with essentially the same assumptions as the LJD model except the cell-centers are distributed as postulated by the structural diffusion model, that is, the cell-center pair distribution function is a series of Gaussian curves with width proportional to  $\sqrt{R}$ .

Mathematically,  $\rho_c(R)$  can then be expressed in normalized form as follows:

$$\rho_c(R) = \sum_m z_m [\sqrt{2\pi D a_m} (a_m^2 + D a_m)]^{-1} \exp[-(R - a_m)^2 / 2 D a_m] \quad (3)$$

where  $D$  is a constant specifying the degree of local order. Larger values of  $D$  indicate less order. Considering the Dirac delta function as the limiting case of a Gaussian curve of zero width<sup>29</sup>, we see Equation (3) reduces to Equation (2), the LJD form of  $\rho_c(R)$ , for  $D = 0$ .

The disorder in position due to thermal oscillations is accounted for by the molecular motion within the cell, not in the cell-center distribution.

#### B. The Molecular Interaction

The molecular interaction most frequently applied to simple liquids is the Lennard-Jones 12-6 potential<sup>25</sup> which may be written

$$u(R) = 4\epsilon [(\sigma/R)^{12} - (\sigma/R)^6] \quad (4)$$

where  $u(R)$  is the intermolecular potential for molecules whose centers are separated a distance  $R$ ,  $\epsilon$  is the

absolute value of the potential minimum and  $\sigma$  is the distance at which the potential is zero (see Figure 1). Rowlinson<sup>30</sup> gives a detailed and well documented justification for choosing this particular form of the potential.

### C. The Potential and Probability Density Within a Cell

The potential  $\Phi(\bar{r}_j)$  of the  $j^{\text{th}}$  molecule at a vector position  $\bar{r}_j$  from its cell center relative to the potential at the cell center is given by

$$\begin{aligned}\Phi(\bar{r}_j) &= \sum_{\substack{i=1 \\ i \neq j}}^N u(|\bar{R}_{ij} + \bar{r}_j|) - u(|\bar{R}_{ij}|) \\ &= \sum_{\substack{i=1 \\ i \neq j}}^N u(\sqrt{R_{ij}^2 + r_j^2 - 2R_{ij}r_j \cos \theta}) - u(R_{ij})\end{aligned}\quad (5)$$

where  $\bar{R}_{ij}$  is the position of the  $j^{\text{th}}$  cell center relative to the  $i^{\text{th}}$  cell center,  $\theta$  is the angle between  $\bar{r}_j$  and  $\bar{R}_{ij}$  and  $u(x)$  is the pair interaction potential for molecules whose centers are separated a distance  $x$ . We consider only potentials that are functions of distance only with no angular dependence.

Averaging over all angles yields

$$\begin{aligned}\langle \Phi(r_j) \rangle &= \sum_{\substack{i=1 \\ i \neq j}}^N (1/2) \int_0^\pi [u(\sqrt{R_{ij}^2 + r_j^2 - 2R_{ij}r_j \cos \theta}) \\ &\quad - u(R_{ij})] \sin \theta \, d\theta\end{aligned}\quad (6)$$

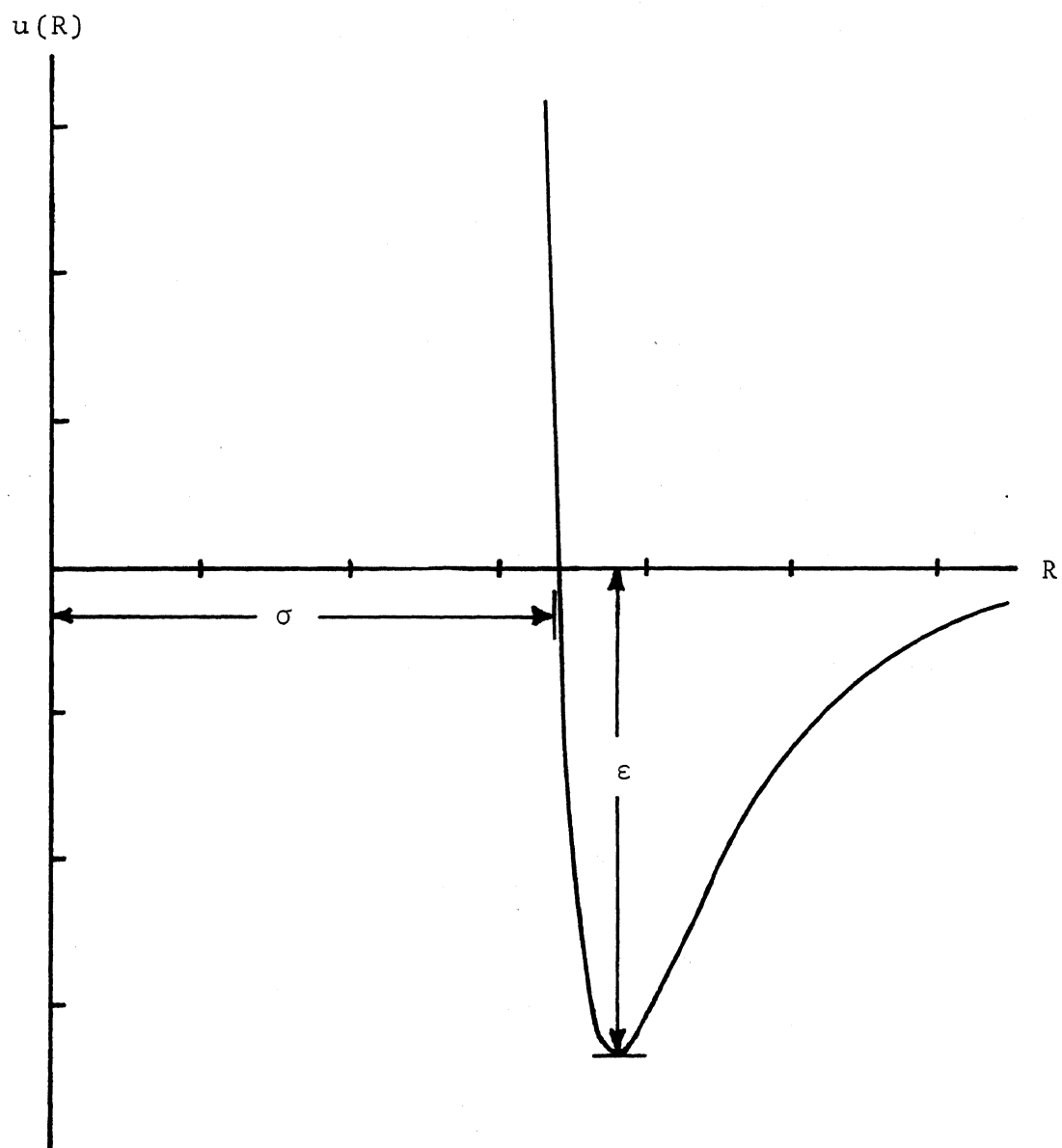


Figure 1. Lennard-Jones Potential

In the case of a discrete cell-center distribution arranged on a regular lattice and using the fact that all cells are identical

$$\begin{aligned} \langle \Phi(r) \rangle = \sum_m (Z_m/2) \int_0^\Pi [u(\sqrt{a_m^2 + r^2 - 2ra_m \cos \theta}) \\ - u(a_m)] \sin \theta \, d\theta \end{aligned} \quad (7)$$

where  $Z_m$  is the number of  $m^{\text{th}}$  neighbors and  $a_m$  is the  $m^{\text{th}}$  neighbor distance.

For a continuous cell-center density distribution  $\rho_c(R)$  we have

$$\langle \Phi(r) \rangle = \int \rho_c(R) [u(\sqrt{R^2 + r^2 - 2rR \cos \theta}) - u(R)] d\bar{R} \quad (8)$$

where the integration is over all volume.

Using the Lennard-Jones 12-6 potential (Equation (4)) gives

$$\begin{aligned} \langle \Phi(r) \rangle = 4\epsilon(2\Pi) \int_0^\infty \int_0^\Pi \rho_c(R) [\sigma^{12}(R^2 + r^2 - 2rR \cos \theta)^{-6} \\ - \sigma^6(R^2 + r^2 - 2rR \cos \theta)^{-3} - (\sigma/R)^{12} \\ + (\sigma/R)^6] R^2 \sin \theta \, d\theta \, dR \end{aligned} \quad (9)$$

Performing the  $\theta$  integration

$$\begin{aligned}
\langle \Phi(r) \rangle = 16\pi\epsilon \int_0^\infty \rho_c(R) [ & \sigma^{12} (R^8 + 12R^6 r^2 + 25.2R^4 r^4 \\
& + 12R^2 r^6 + r^8) (R^2 - r^2)^{-10} - \sigma^6 (R^2 + r^2) (R^2 \\
& - r^2)^{-4} - (\sigma/R)^{12} + (\sigma/R)^6 ] R^2 dR . \quad (10)
\end{aligned}$$

In the LJD model  $\rho_c(R)$  is given by Equation (2) or  $\Phi$  by Equation (6), so Equation (10) becomes

$$\begin{aligned}
\langle \Phi(r) \rangle = 4\epsilon \sum_m Z_m \sigma^{12} ( & a_m^8 + 12a_m^6 r^2 + 25.2a_m^4 r^4 + 12a_m^2 r^6 \\
& + r^8) (a_m^2 - r^2)^{-10} - \sigma^6 (a_m^2 + r^2) (a_m^2 - r^2)^{-4} \\
& - (\sigma/a_m)^{12} + (\sigma/a_m)^6 . \quad (11)
\end{aligned}$$

In the literature this equation is usually expressed in terms of  $V^* = a_1^3 (\sqrt{2} \sigma^3)^{-1}$  and  $y = r^2/a_1^2$ , resulting in the form<sup>31,32</sup>

$$\langle \Phi(r) \rangle = \epsilon Z_1 [L(y) (V^*)^{-4} - 2M(y) (V^*)^{-2}] \quad (12)$$

where

$$L(y) = \sum_m (Z_m/Z_1) (a_1/a_m)^{12} \ell(ya_1^2/a_m^2) \quad (13)$$

$$M(y) = \sum_m (Z_m/Z_1) (a_1/a_m)^6 m(ya_1^2/a_m^2) \quad (14)$$

and

$$\ell(y) = (1 + 12y + 25.2y^2 + 12y^3 + y^4) (1 - y)^{-10} - 1 \quad (15)$$

$$m(y) = (1 + y)(1 - y)^{-4} - 1. \quad (16)$$

Let  $p(\bar{r}_j, \bar{R}_{1j}, \dots, \bar{R}_{Nj})$  be the probability density that molecule  $j$  is located at vector position  $\bar{r}_j$  from its cell center,  $\bar{R}_{ij}$  is the vector position of the  $j^{\text{th}}$  cell center relative to the  $i^{\text{th}}$  cell center, and  $N$  is the total number of molecules. We choose  $p(\bar{r}_j, \bar{R}_{1j}, \dots, \bar{R}_{Nj})$  proportional to  $\exp[-\langle\Phi(r_j)\rangle/KT]$  where  $K$  is Boltzmann's constant and  $T$  the absolute temperature. Recall  $\Phi$  is actually a function of the other cell-center positions as well as  $\bar{r}_j$ .

The requirement that each cell contain one molecule, assuming all cells identical and spherical, can be expressed

$$\int_{\text{cell}} p(\bar{r}_j, \bar{R}_{1j}, \dots, \bar{R}_{Nj}) d\bar{r}_j = c \int_{\text{cell}} \exp[-\langle\Phi\rangle/KT] d\bar{r} = 1 \quad (17)$$

where  $c$  is the normalizing constant and a function of the  $\bar{R}_{ij}$ 's or  $\rho_c(R)$ .

#### D. The Molecular Pair Distribution Function

The molecular pair distribution function can be calculated from the cell-center pair distribution  $\rho_c(R)$  and the positional probability density within a cell  $p(r)$  by an integral formula developed by Lund. He assumes the following model. The liquid consists of  $N$  identical monatomic molecules and is spanned by a virtual lattice

of  $N$  spherically symmetric cells, each of volume  $\Delta = V/N$ . Each cell is occupied by a single molecule and there is no correlation between the positions of molecules in different cells. Note these assumptions are in common with those of the LJD model and the model considered in this study.

Following Lund, we assume there is a probability per unit volume  $p(\bar{x})$  of a vector position  $\bar{x}$  for a molecule relative to an arbitrary origin. Let  $h(\bar{k})$  be the Fourier transform of  $p(\bar{x})$ . One thus has the Fourier transform pair

$$h(\bar{k}) = \int p(\bar{x}) \exp(-i\bar{k} \cdot \bar{x}) d\bar{x} \quad (18)$$

$$p(\bar{x}) = (1/2\pi)^3 \int h(\bar{k}) \exp(i\bar{k} \cdot \bar{x}) d\bar{k} \quad (19)$$

where  $d\bar{x}$  and  $d\bar{k}$  are volume elements and the integrations are over all space.

The probability density of a vector displacement  $\bar{R}$  between two molecules is

$$p(R) = (1/N) \int p(\bar{x}) p(\bar{x} + \bar{R}) d\bar{x} . \quad (20)$$

Substituting Equation (19) into (20) and rearranging gives



$$\begin{aligned}
\rho(\bar{R}) &= (1/N) (1/2\pi)^6 \int \exp(i\bar{k} \cdot \bar{R}) h(\bar{k}) \int h^*(\bar{k}') \\
&\times \int \exp[i\bar{x} \cdot (\bar{k} - \bar{k}')] d\bar{x} d\bar{k}' d\bar{k} \\
&= (1/N) (1/2\pi)^3 \int \exp(i\bar{k} \cdot \bar{R}) h(\bar{k}) \int h^*(\bar{k}') \delta(\bar{k} - \bar{k}') d\bar{k}' d\bar{k} \\
&= (1/N) (1/2\pi)^3 \int \exp(i\bar{k} \cdot \bar{R}) [h(\bar{k})]^2 d\bar{k} \tag{21}
\end{aligned}$$

where the asterisk indicates complex conjugate and  $[h(\bar{k})]^2 = h(\bar{k})h^*(\bar{k})$ .

Let

$$p(\bar{x}) = \sum_{j=1}^N p(\bar{r}_j, \bar{R}_{1j}, \dots, \bar{R}_{Nj}) \tag{22}$$

where as before  $\bar{r}_j$  is the position of the  $j^{\text{th}}$  molecule relative to the  $j^{\text{th}}$  cell center and  $\bar{R}_{\ell j}$  is the vector position of the  $j$  cell center relative to the  $\ell^{\text{th}}$  cell center. Recall  $p(\bar{r}_j, \bar{R}_{1j}, \dots, \bar{R}_{Nj})$  is given by Equation (17) and is zero outside the  $j^{\text{th}}$  cell.

Substituting into Equation (18) and letting  $\bar{x} = \bar{R}_j + \bar{r}_j$  where  $\bar{R}_j$  is the position of the center of the  $j^{\text{th}}$  cell relative to the same origin as  $\bar{x}$ , gives

$$h(\bar{k}) = \sum_{j=1}^N \int p(\bar{r}_j, \bar{R}_{1j}, \dots, \bar{R}_{Nj}) \exp[-i\bar{k} \cdot (\bar{R}_j + \bar{r}_j)] d\bar{r}_j \tag{23}$$

$$\begin{aligned}
[h(\bar{k})]^2 = & \sum_{j=1}^N \sum_{q=1}^N \left\{ \int_{\Delta} p(\bar{r}_j, \bar{R}_{1j}, \dots, \bar{R}_{Nj}) \exp[-i\bar{k} \cdot (\bar{R}_j + \bar{r}_j)] d\bar{r}_j \right. \\
& \cdot \int_{\Delta} p(\bar{r}_q, \bar{R}_{1q}, \dots, \bar{R}_{Nq}) \exp[i\bar{k} \cdot (\bar{R}_q + \bar{r}_q)] d\bar{r}_q \left. \right\} . \quad (24)
\end{aligned}$$

Using Equations (5) and (17) we get

$$\begin{aligned}
[h(\bar{k})]^2 = & \sum_{j=1}^N \sum_{q=1}^N \int_{\Delta} c \exp\{(-1/kT) \sum_{\substack{\ell=1 \\ \ell \neq j}}^N [u(|\bar{r}_j + \bar{R}_{\ell j}|) \\
& - u(|\bar{R}_{\ell j}|)]\} \exp[-i\bar{k} \cdot (\bar{R}_j + \bar{r}_j)] d\bar{r}_j \int_{\Delta} c \exp\{(-1/kT) \\
& \sum_{\substack{\ell=1 \\ \ell \neq q}}^N [u(|\bar{r}_q + \bar{R}_{\ell q}|) - u(|\bar{R}_{\ell q}|)]\} \exp[i\bar{k} \cdot (\bar{R}_q + \bar{r}_q)] d\bar{r}_q . \quad (25)
\end{aligned}$$

We now average over the summations using distribution functions<sup>28</sup>. First averaging the  $q$  summation as one particle functions gives

$$\begin{aligned}
[h(\bar{k})]^2 = & \sum_{j=1}^N \int \int_{\Delta} c \exp\{(-1/KT) \sum_{\substack{\ell=1 \\ \ell \neq j}}^N [u(|\bar{r}_j + \bar{R}_{\ell j}|) \\
& - u(|\bar{R}_{\ell j}|)]\} \exp[-i\bar{k} \cdot (\bar{R}_j + \bar{r}_j)] d\bar{r}_j \int_{\Delta} c \exp\{(-1/KT) \\
& \cdot \sum_{\substack{\ell=1 \\ \ell \neq k}}^N [u(|\bar{r}_1 + \bar{R}_{\ell 1}|) - u(|\bar{R}_{\ell 1}|)]\} \\
& \exp[-i\bar{k} \cdot (\bar{R}_1 + \bar{r}_1)] d\bar{r}_1 \rho_c^{(1)}(\bar{R}_1) d\bar{R}_1 \quad (26)
\end{aligned}$$

where  $\rho_c^{(n)}$  is the generic n-particle distribution function<sup>23</sup>.

Averaging the j summation with one molecule fixed at  $\bar{R}_1$  yields

$$\begin{aligned}
[h(\bar{k})]^2 = & (N/V) \int \int \int_{\Delta} c \exp\{(-1/KT) \sum_{\substack{\ell=1 \\ \ell \neq 2}}^N [u(|\bar{r}_2 + \bar{R}_{\ell 2}|) \\
& - u(|\bar{R}_{\ell 2}|)]\} \exp[i\bar{k} \cdot (\bar{R}_2 + \bar{r}_2)] d\bar{r}_2 \\
& \int_{\Delta} c \exp\{(-1/KT) \sum_{\ell=2}^N [u(|\bar{r}_1 + \bar{R}_{\ell 1}|) - u(|\bar{R}_{\ell 1}|)]\} \\
& \exp[i\bar{k} \cdot (\bar{R}_1 + \bar{r}_1)] d\bar{r}_1 \rho_c^{(2)}(\bar{R}_1, \bar{R}_2) d\bar{R}_1 d\bar{R}_2 \quad (27)
\end{aligned}$$

Averaging over the  $\ell$  summations and using the fact that the averages must be independent of the origin

$$\begin{aligned}
& \sum_{\ell=2}^N u(|\bar{r}_1 + \bar{R}_{\ell 1}|) - u(|\bar{R}_{\ell 1}|) \\
&= \int [\rho_c^{(2)}(\bar{R}_1', \bar{R}_1) / \rho^{(1)}(\bar{R}_1)] \\
&\quad [u(|\bar{r}_1 + \bar{R}_1' - \bar{R}_1|) - u(|\bar{R}_1' - \bar{R}_1|)] d\bar{R}_1' \\
&= \int \rho_c(\bar{R}) [u(|\bar{r}_1 + \bar{R}|) - u(|\bar{R}|)] d\bar{R} \tag{28}
\end{aligned}$$

and

$$\begin{aligned}
& \sum_{\substack{\ell=1 \\ \ell \neq 2}}^N u(|\bar{r}_2 + \bar{R}_{\ell 2}|) - u(|\bar{R}_{\ell 2}|) \\
&= \int \rho_c(\bar{R}) [u(|\bar{r}_2 + \bar{R}|) - u(|\bar{R}|)] d\bar{R} . \tag{29}
\end{aligned}$$

The potential function is the same for every cell,  
hence

$$\Phi(\bar{r}_1, \bar{R}) = \Phi(\bar{r}_2, \bar{R}) = \Phi(\bar{r}, \bar{R}) \tag{30}$$

Let  $X(\bar{k})$  be defined by

$$X(\bar{k}) = \int_{\Delta} c \exp[-\langle \Phi(\bar{r}, \bar{R}) \rangle / kT] \exp(i\bar{k} \cdot \bar{r}) d\bar{r} \tag{31}$$

and if we let  $\bar{R} = \bar{R}_2 - \bar{R}_1$ , Equation (27) can be written

$$\begin{aligned}
[h(\bar{k})]^2 &= (N/V) \iint [X(\bar{k})]^2 \exp[-i\bar{k} \cdot (\bar{R}_2 - \bar{R}_1)] \\
&\quad \rho_C^{(2)}(\bar{R}_1, \bar{R}_2) d\bar{R}_1 d\bar{R}_2 \\
&= N \int [X(\bar{k})]^2 \exp(-i\bar{k} \cdot \bar{R}) \rho_C(\bar{R}) d\bar{R} .
\end{aligned} \tag{32}$$

Using this in Equation (21) gives

$$\begin{aligned}
\rho(R) &= (1/2\pi)^3 \iint \rho_C(\bar{R}') [X(\bar{k})]^2 \\
&\quad \exp(-i\bar{k} \cdot \bar{R}') d\bar{R}' \exp(i\bar{k} \cdot \bar{R}) d\bar{k} .
\end{aligned} \tag{33}$$

Let  $\bar{s} = \bar{R}' - \bar{R}$ , then

$$\begin{aligned}
\rho(\bar{R}) &= (1/2\pi)^3 \iint \rho_C(|\bar{R} + \bar{s}|) [X(\bar{k})]^2 \exp(-i\bar{k} \cdot \bar{s}) d\bar{k} d\bar{s} \\
&= \int \rho_C(|\bar{R} + \bar{s}|) F(\bar{s}) d\bar{s}
\end{aligned} \tag{34}$$

where

$$F(\bar{s}) = (1/2\pi)^3 \int [X(\bar{k})]^2 \exp(-i\bar{k} \cdot \bar{s}) d\bar{k} . \tag{35}$$

For calculations it is convenient to express Equation (34) in bipolar coordinates  $R$ ,  $s$  and  $t$ , (see Figure 2), that is

$$\rho(R) = (2\pi/R) \int_0^{\infty} \int_{|R-t|}^{|R+t|} \rho_c(t) F(s) s t ds dt \quad (36)$$

The thermodynamic functions are very sensitive to small changes in  $\rho(R)$ . A slight modification of  $\rho(R)$  gave significant improvement in the thermodynamic functions in comparison with experimental values. (See Chapter VI for detailed discussion.) This adjustment consisted of shifting the probability that a second molecule occur within a short distance,  $R < a_1$ , of a given molecule to a larger value of  $R$ , but still less than  $a$ , according to the formula

$$R_a = R_0 + (a_1^2 - R_0^2)B/a_1 \quad (37)$$

where  $R_0$  is the original value of  $R$ ,  $R_a$  is the adjusted value of  $R$  and  $B$  is a parameter indicating the degree of adjustment. Note that the adjustment is greatest for small  $R_0$  and is zero at  $R_0 = a_1$ .

The adjusted value of the molecular pair distribution function  $\rho(R_a)$  is written

$$\rho(R_a) = R_0^2 \rho(R_0)/R_n^2 \quad (38)$$

so that the total number of molecules remain the same. Although  $\rho(R_0)$  is calculated at discrete evenly spaced values of  $R_0$ , the corresponding  $\rho(R_a)$  is determined at the unevenly spaced values of  $R_a$ .

### E. Application to Argon

For purposes of specific calculations, liquid argon was selected as a typical example. As stated in the introduction, this choice is based on the larger quantity of experimental data and other model calculations available than for other reasonable choices.

The crystalline form of materials whose molecular interaction is of the Lennard-Jones type will be face-centered cubic<sup>33</sup>. Therefore, the average neighbor distances and coordination numbers used in our model correspond to this type of lattice (see Table I).

Two constants,  $\epsilon$  and  $\sigma$ , appear in the Lennard-Jones pair potential. The values for argon of Michels et al.<sup>34</sup>,  $\epsilon/K = 119.8^\circ K$  and  $\sigma = 3.405\text{\AA}$  were selected for this study which are also probably the most frequently used by other workers. Hirschfelder et al.<sup>32</sup> list several other published values for these constants.

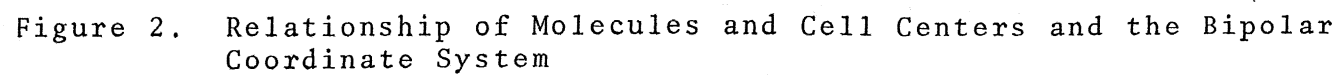




Table I. Face-Centered Cubic Lattice

m	$(a_m/a_1)^2$	$z_m$	m	$(a_m/a_1)^2$	$z_m$
1	1	12	21	22	24
2	2	6	22	23	48
3	3	24	23	24	8
4	4	12	24	25	84
5	5	24	25	26	24
6	6	8	26	27	96
7	7	48	27	28	48
8	8	6	28	29	24
9	9	36	29	31	96
10	10	24	30	32	6
11	11	24	31	33	96
12	12	24	32	34	48
13	13	72	33	35	48
14	15	48	34	36	36
15	16	12	35	37	120
16	17	48	36	38	24
17	18	30	37	39	48
18	19	72	38	40	24
19	20	24	39	41	48
20	21	48	40	42	48

m = shell number

$a_m$  = radius mth shell

$z_m$  = coordination number mth shell

### III. DETERMINATION OF THERMODYNAMIC PROPERTIES

If  $\rho(R)$  is known as a function of temperature and density and the intermolecular potential is also known, in principle, all equilibrium thermodynamic properties can be calculated<sup>28,35</sup>. Actually only three thermodynamic functions need be determined independently, then the rest are derivable from these.

Two thermodynamic properties are readily expressed, the internal energy  $U$  and the pressure-volume product  $PV$ <sup>23,35</sup>.

$$U = 3NKT/2 + (N/2) \int_0^{\infty} \rho(R) u(R) d\bar{R} \quad (39)$$

$$PV = NKT - (N/6) \int_0^{\infty} R\rho(R) \frac{\partial u(R)}{\partial R} d\bar{R} \quad (40)$$

where all symbols have their previously defined meaning.

In order to calculate a third thermodynamic property, one must determine the partial derivative of  $\rho(R)$  with respect to temperature or density<sup>23,28</sup>, which can be done conveniently only if  $\rho(R)$  is known in analytical form or at a large number of points over a sufficient range of temperature and density. Alternately the partial derivatives of  $U$  or  $PV$  can be used with the same restrictions.

Because of the complicated form of  $\rho_c(R)$ , the calculation of  $\rho(R)$  must be done numerically with the aid of a computer.  $\rho(R)$  and the thermodynamic functions determined from it are found only at a few discrete values of temperature and density. Considering this, the easiest third thermodynamic quantity to determine is the specific heat at constant volume,  $C_v$ , given by

$$C_v = \left( \frac{\partial U}{\partial T} \right)_v \quad (41)$$

Since the model considered gives only information about the molecular arrangement, not the kinetics of the molecules, we need only consider the structural related portion of the thermodynamic quantity or the configurational thermodynamic properties. This is given by the integral part of  $U$  in Equation (39). Likewise the configurational internal energy can be used in Equation (41) to find the configurational specific heat.

#### IV. COMPUTER CALCULATIONS

##### A. General

The molecular pair distribution function  $\rho(R)$ , reduced configurational internal energy  $U_c/NKT$ , configurational specific heat at constant volume  $C_v/NK$ , and the compressibility factor  $PV/NKT$  were determined for forty-eight combinations of the order parameter  $D$ , reduced temperature  $T^*$ , and reduced specific volume  $V^*$ . (See Appendix B for explanation of reduced units.) The particular values of these parameters are listed in Table II.

Calculations were performed using the IBM 360 Model 50 Digital Computer System of the UMR Computer Center. The principle computer programs used are given in Appendix C.

##### B. The Cell-Center Pair Distribution Function

The cell-center pair distribution function  $\rho_c(R)$  was determined for radial distances up to six times the nearest neighbor distance at intervals of approximately 1/100 of the nearest neighbor distance. The interval between points at which  $\rho_c(R)$  was evaluated, was chosen so that both  $R = \sigma$  and  $R = a_1$  were points at which  $\rho_c(R)$  was calculated. This results in an irregular interval between  $R = 0$  and

the first evaluated point, but this is unimportant since  $\rho_c(R)$  is zero for several points near  $R = 0$ .

It was found that an excessive number of cell centers were located at distances  $R < \sigma$  using Equation (3) as it stands. To correct this,  $\rho_c(R)$  was set to zero for  $R < \sigma$ . At the same time the contribution of the first shell for values of  $R \geq \sigma$  was increased so that the coordination numbers of the first shell (12) was perserved.

#### C. Normalization of Probability Density Within the Cell

The potential in the cell was determined and the normalization constant was determined by numerical integration of Equation (17) using Simpson's rule with increments of 1/100 of the nearest neighbor distance. The integration was carried out only to a point where the integrand became less than  $\exp(-25)$ . This resulted in 20 to 44 strips being used.

#### D. The Molecular Pair Distribution Function

The integrations required to calculate  $\rho(R)$  from  $\rho_c(R)$ , Equation (34), were performed by Simpson's rule using the increments and limits in Tables III and IV.

The integration over  $k$  (Equation (35)) requires special attention since the upper limit is infinite. The integrand is oscillatory and the integral converges, but nonuniformly. A finite upper limit was established such that the amplitude of the final oscillation was on the

order of  $10^{-5}$  or less times the maximum amplitude. The increment  $\Delta k$  was selected such that each cycle contained twelve or more strips.

The function  $F(s)$  is also oscillatory but decreases very fast with increasing  $s$ , usually only the first cycle being significant. Thus  $F(s)$  was considered zero for values of  $s$  such that the amplitude of the oscillations was on the order of  $10^{-5}$  or less of the amplitude of the first cycle.

In the integration over  $t$  (Equation (36)) a finite upper limit can be fixed, since contributions from higher values of  $t$  are zero. This upper limit was put at 25.0 Angstroms for all cases.

In all cases  $\rho(R)$  was evaluated in increments of approximately  $1/50$  the nearest neighbor distance up to  $R = 21.5 \rightarrow 22.0$  Angstroms. The maximum value of  $R$  is limited by the fact that shells beyond the fortieth begin to contribute at higher values and the finite upper limit in the  $t$  integration as discussed above.

#### E. Thermodynamic Functions

The reduced configurational internal energy  $U_c/NKT$ , and compressibility factor  $PV/NKT$  were determined again using Simpson's rule to perform the integrations in Equations (39) and (40) numerically. The increments in  $R$  were approximately  $1/50$  of the nearest neighbor distance. Some contribution occurs from  $\rho(R)$  for values of  $R > R_m$

where  $R_m$  is the maximum value of  $R$  for which  $\rho(R)$  was calculated. Therefore,  $\rho(R)$  was set equal to its average value for  $R > R_m$ . This is physically reasonable since order has largely disappeared for  $R > R_m$ . This portion of the integrals could be performed analytically.

In order to calculate  $U_c/NKT$  and  $PV/NKT$  using the adjusted  $\rho(R)$ , a slightly different approach was needed since the points at which  $\rho(R)$  was evaluated for  $R < a_1$  were no longer evenly spaced. The trapezoid rule was used to calculate the contributions to the integrals in Equations (30) and (40) for values of  $R < a_1$ .

The reduced configurational specific heat at constant volume  $C_v/NK$  was determined from the calculated values of  $U_c/N\epsilon$  ( $= T^* \times U_c/NKT$ ) as a function of  $T^*$  by use of a library subroutine which determines a parabola through the points  $(U_c/N\epsilon, T^*)$ . This curve is then differentiated to give  $C_v/NK$ .

Table II. Values of Parameters Used

Parameter	Symbol	Values Used
Reduced Temperature	$T^*$	.7, 1.2, 2.0
Reduced Specific Volume	$V^*$	1.0, 1.2, 1.4, 1.6
Order Parameter	D	0.0, .02, .04, .06
Adjustment Parameter	B	1/4, 1/3, 1/2, 2/3



Table III. Fixed Programming Parameters

Name	Value
$\Delta r$	$a_1/100$
$\Delta k$	.2
$t(\max)$	25.0
$R(\max)$	21.5 $\rightarrow$ 22.0

Table IV. Varying Programming Parameters

D	T*	V*	k (max)	s (max)	$\Delta R = \Delta t = 2\Delta s$
0.0	.7	1.0	24.0	1.223	.076440
		1.2	20.0	1.625	.081229
		1.4	16.0	2.394	.085512
		1.6	16.0	2.682	.089404
	1.2	1.0	24.0	1.223	.076440
		1.2	20.0	1.950	.081229
		1.4	16.0	2.394	.085512
		1.6	16.0	2.682	.089404
	2.0	1.0	24.0	1.223	.076440
		1.2	18.0	1.950	.081229
		1.4	16.0	2.565	.085512
		1.6	15.0	3.040	.089404
.02	.7	1.0	24.0	1.390	.069497
		1.2	24.0	1.641	.082058
		1.4	20.0	2.089	.087061
		1.6	16.0	2.486	.088768
	1.2	1.0	24.0	1.390	.069497
		1.2	20.0	1.969	.082058
		1.4	20.0	2.438	.087061
		1.6	16.0	2.486	.088768
	2.0	1.0	22.0	1.390	.069497
		1.2	20.0	1.805	.082058
		1.4	20.0	2.089	.087061
		1.6	16.0	2.486	.088768
.04	.7	1.0	24.0	1.390	.069497
		1.2	24.0	1.641	.082058
		1.4	20.0	1.741	.087061
		1.6	16.0	2.486	.088768
	1.2	1.0	24.0	1.390	.069497
		1.2	20.0	1.641	.082058
		1.4	16.0	2.089	.087061
		1.6	16.0	2.486	.088768
	2.0	1.0	20.0	1.668	.069497
		1.2	20.0	1.641	.082058
		1.4	20.0	1.741	.087061
		1.6	16.0	2.486	.088768
.06	.7	1.0	24.0	1.112	.069497
		1.2	20.0	1.641	.082058
		1.4	20.0	1.741	.087061
		1.6	16.0	2.486	.088768

Table IV. Varying Programming Parameters (Continued)

D	T*	V*	k (max)	s (max)	$\Delta R = \Delta t = 2\Delta s$
	1.2	1.0	20.0	1.668	.069497
		1.2	20.0	1.641	.082058
		1.4	20.0	1.741	.087061
		1.6	16.0	2.486	.088768
	2.0	1.0	22.0	1.529	.069497
		1.2	20.0	1.805	.082058
		1.4	18.0	2.089	.087061
		1.6	14.0	2.663	.088768

## V. RESULTS

The unadjusted molecular pair distribution functions are presented in Figures 3 to 14. The cell-center pair distribution is compared with the molecular distribution. In the two diverse cases  $D = .06$ ,  $T^* = .7$ ,  $V^* = 1.0$  and  $D = .02$ ,  $T^* = 2.0$ ,  $V^* = 1.6$  in Figures 15 and 16. Figures 17 and 18 show the potential well within the cell for the external situations  $D = 0.0$ ,  $T^* = 2.0$  and  $D = .06$ ,  $T = .7$ . Comparison with experimentally determined molecular pair distributions is shown in Figure 19. The first peak is compared in the adjusted and unadjusted form in Figure 20 for  $D = 0.0$ ,  $T^* = 2.0$ ,  $V^* = 1.6$ ,  $B = 2/3$ , which is the most radical alteration.

The calculated thermodynamic properties are given in Tables V through XIII. In the particularly interesting cases discussed in Section VI, graphical presentation is also given in Figures 21 through 24.

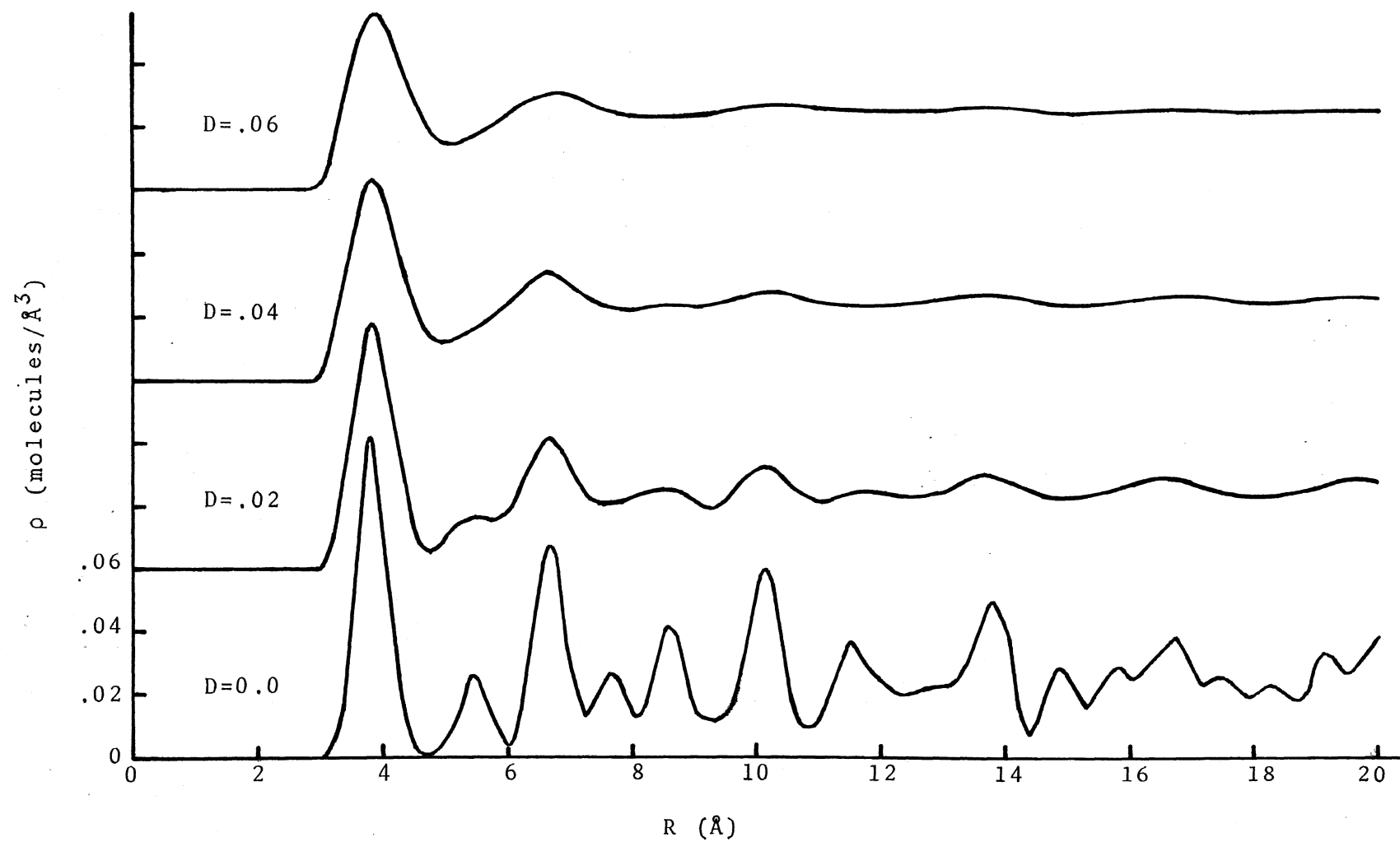


Figure 3. Molecular Pair Distribution,  $T^*=.7$ ,  $V^*=1.0$

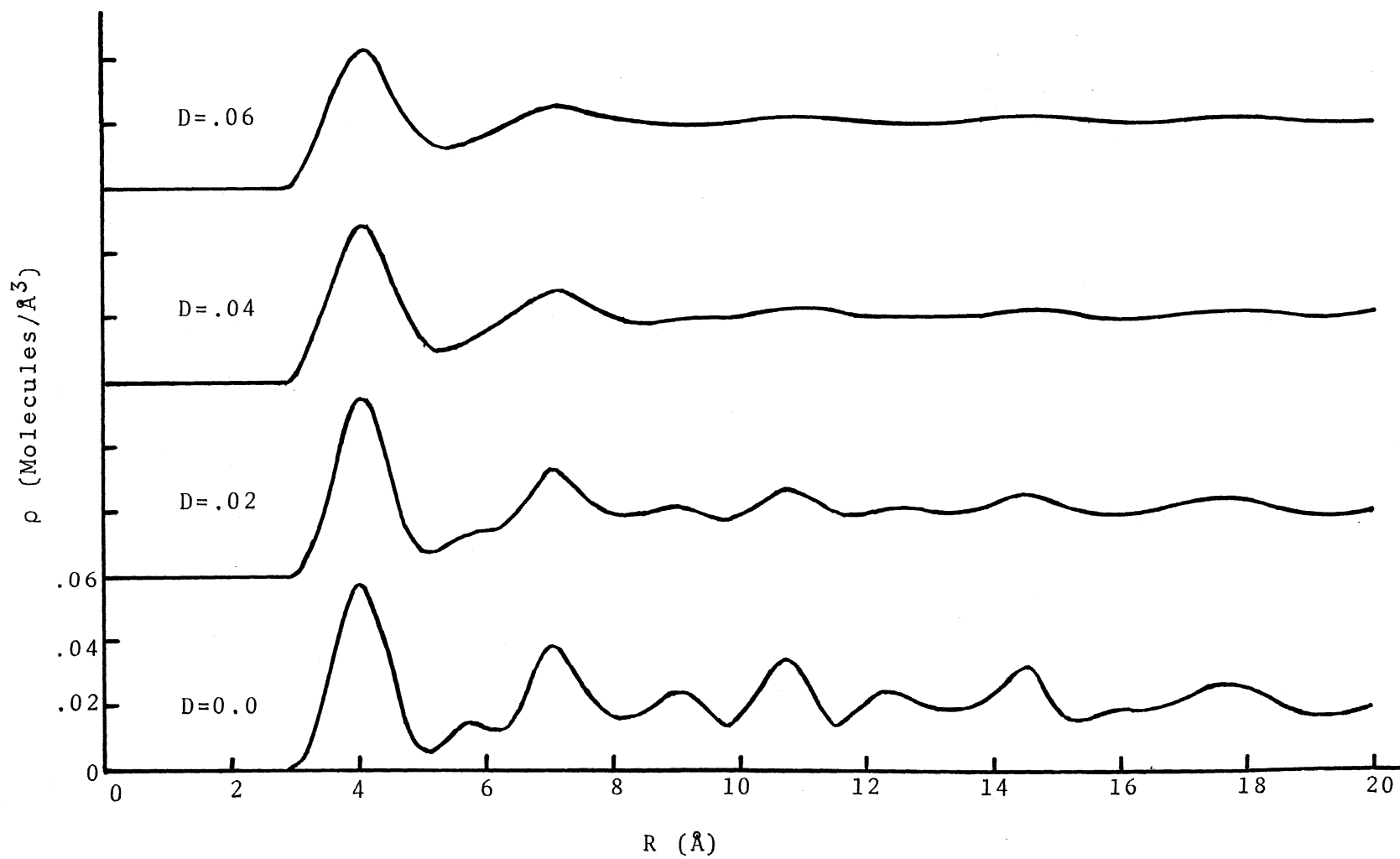


Figure 4. Molecular Pair Distribution,  $T^*=0.7$ ,  $V^*=1.2$

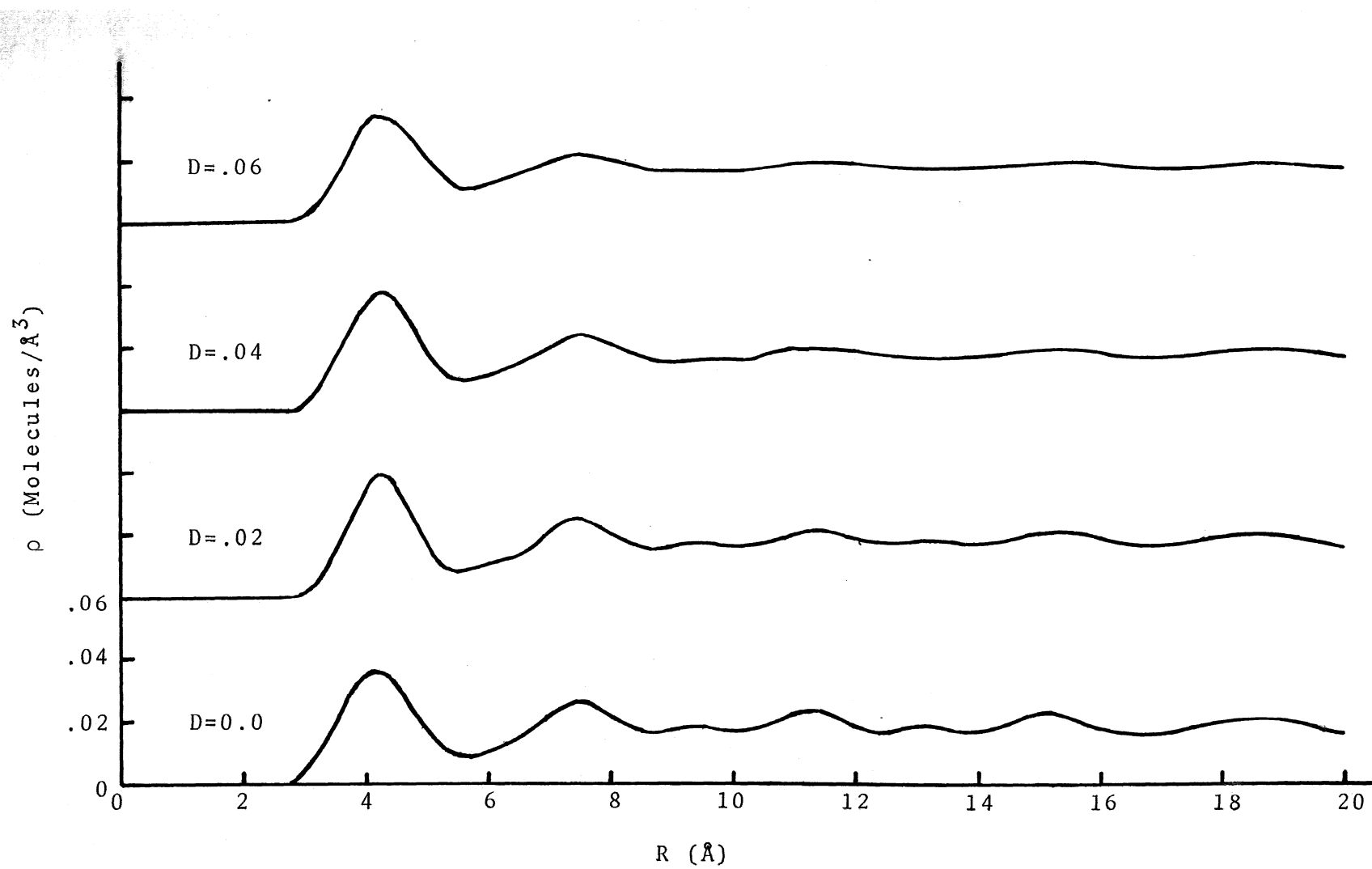


Figure 5. Molecular Pair Distribution,  $T^*=0.7$ ,  $V^*=1.4$

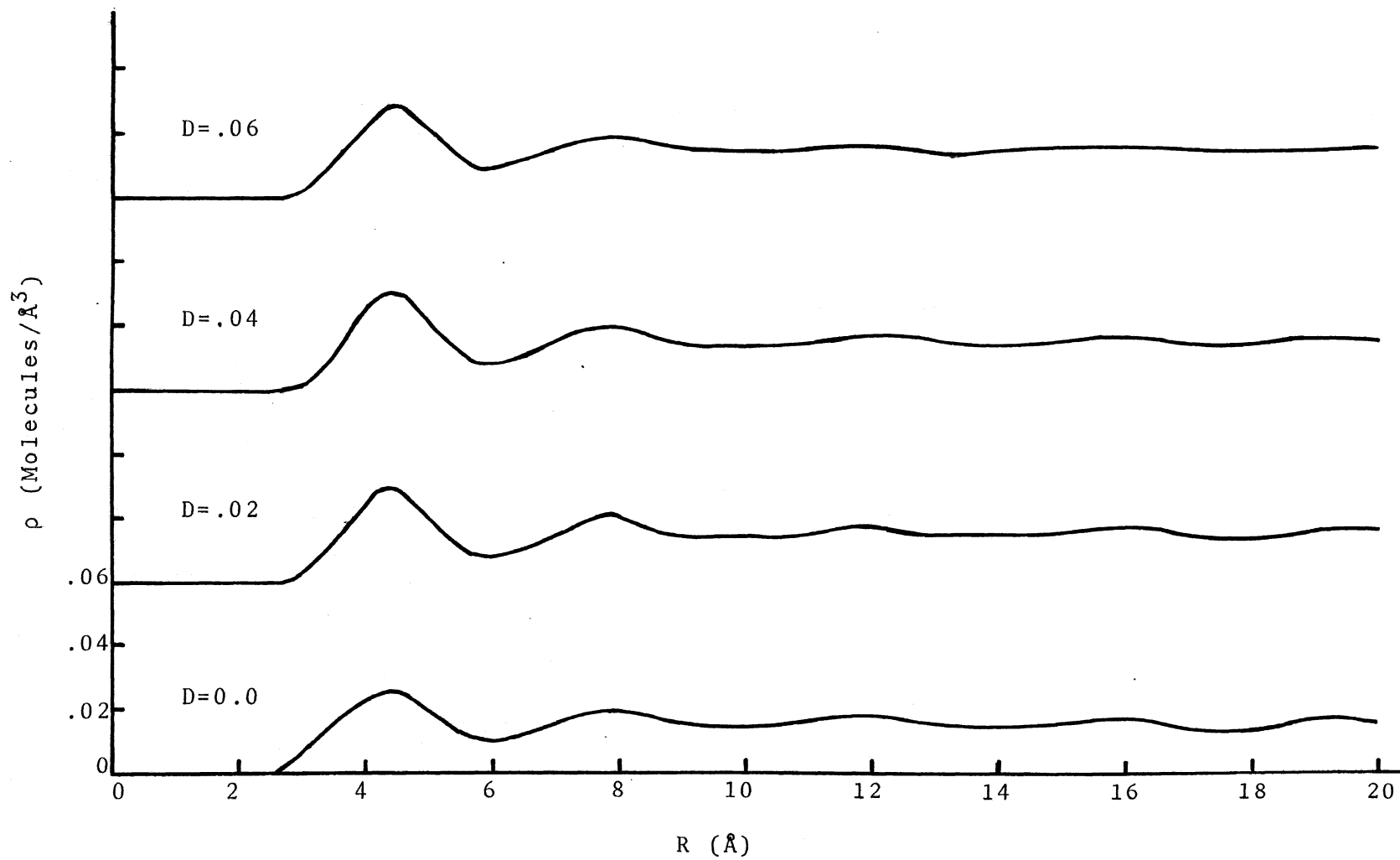


Figure 6. Molecular Pair Distribution,  $T^*=.7$ ,  $V^*=1.6$



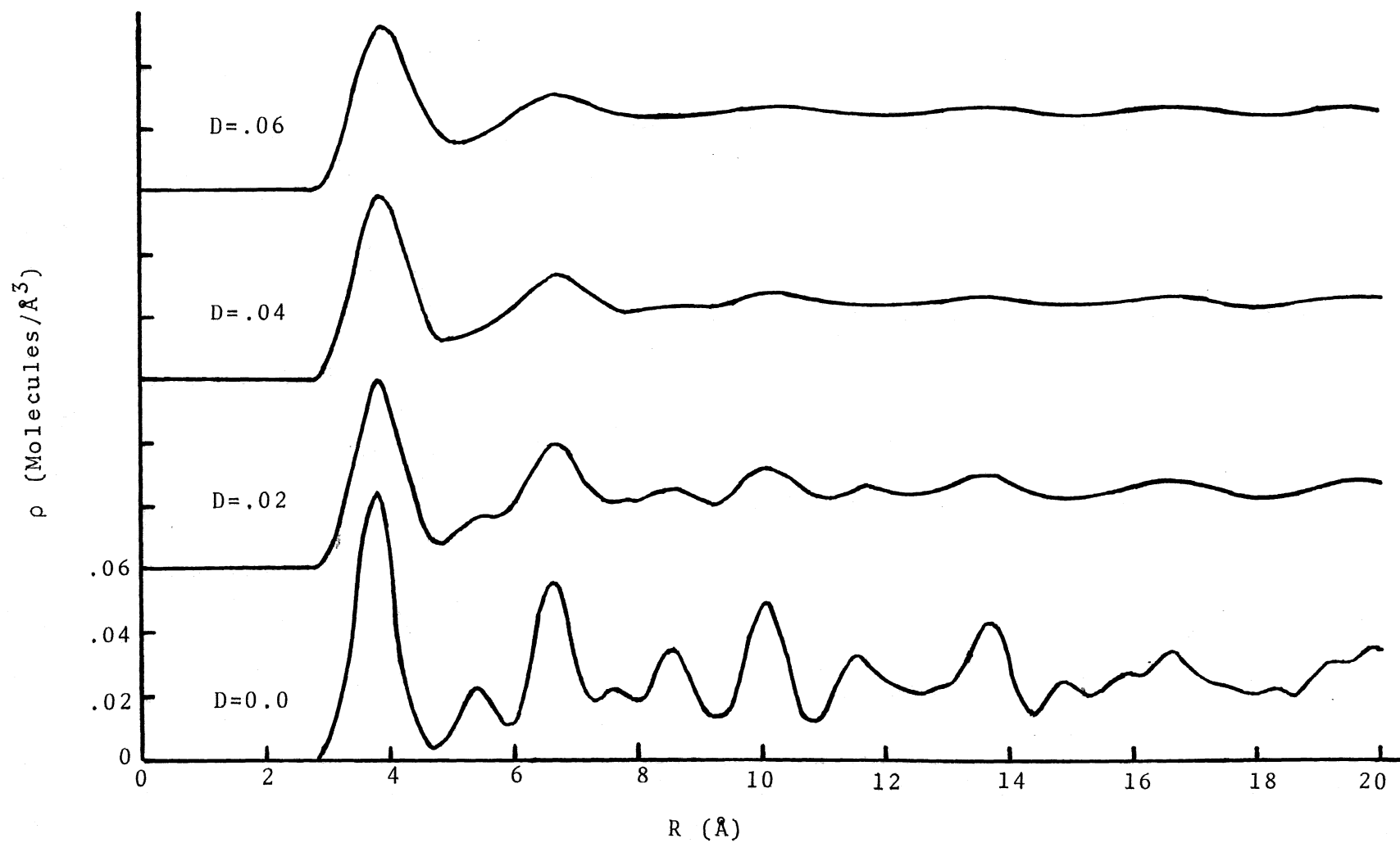


Figure 7. Molecular Pair Distribution,  $T^*=1.2$ ,  $V^*=1.0$

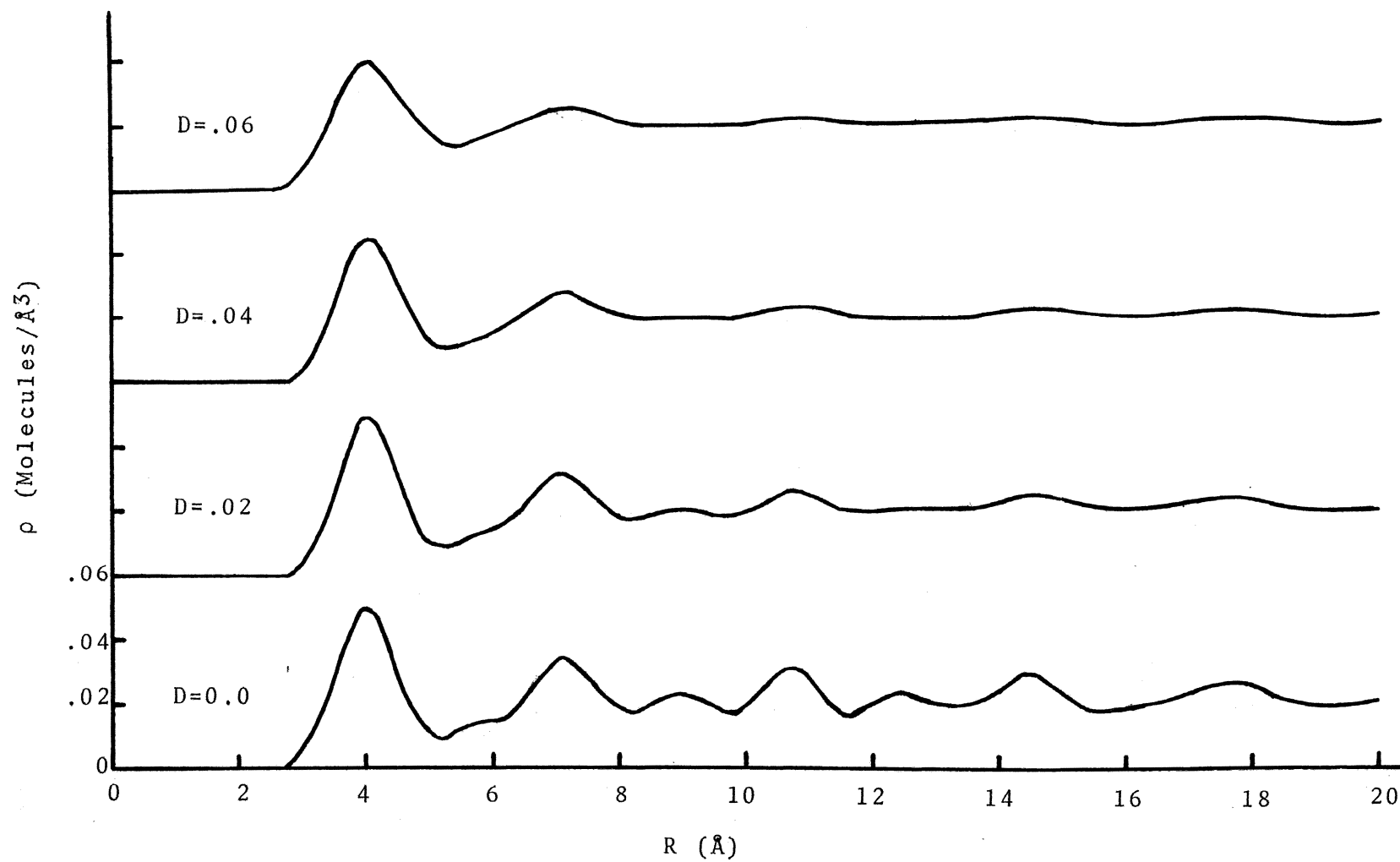


Figure 8. Molecular Pair Distribution,  $T^*=1.2$ ,  $V^*=1.2$

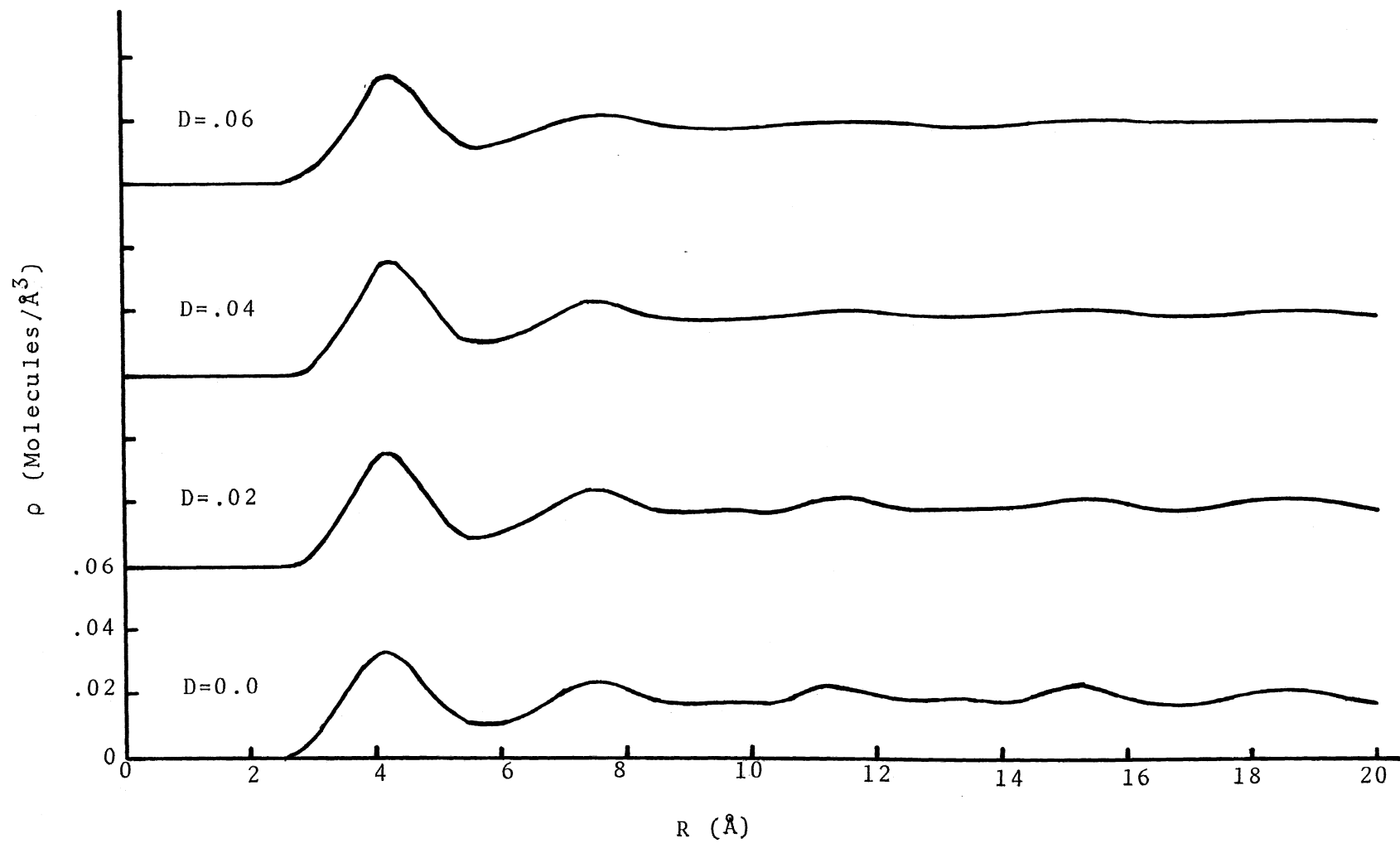


Figure 9. Molecular Pair Distribution,  $T^*=1.2$ ,  $V^*=1.4$

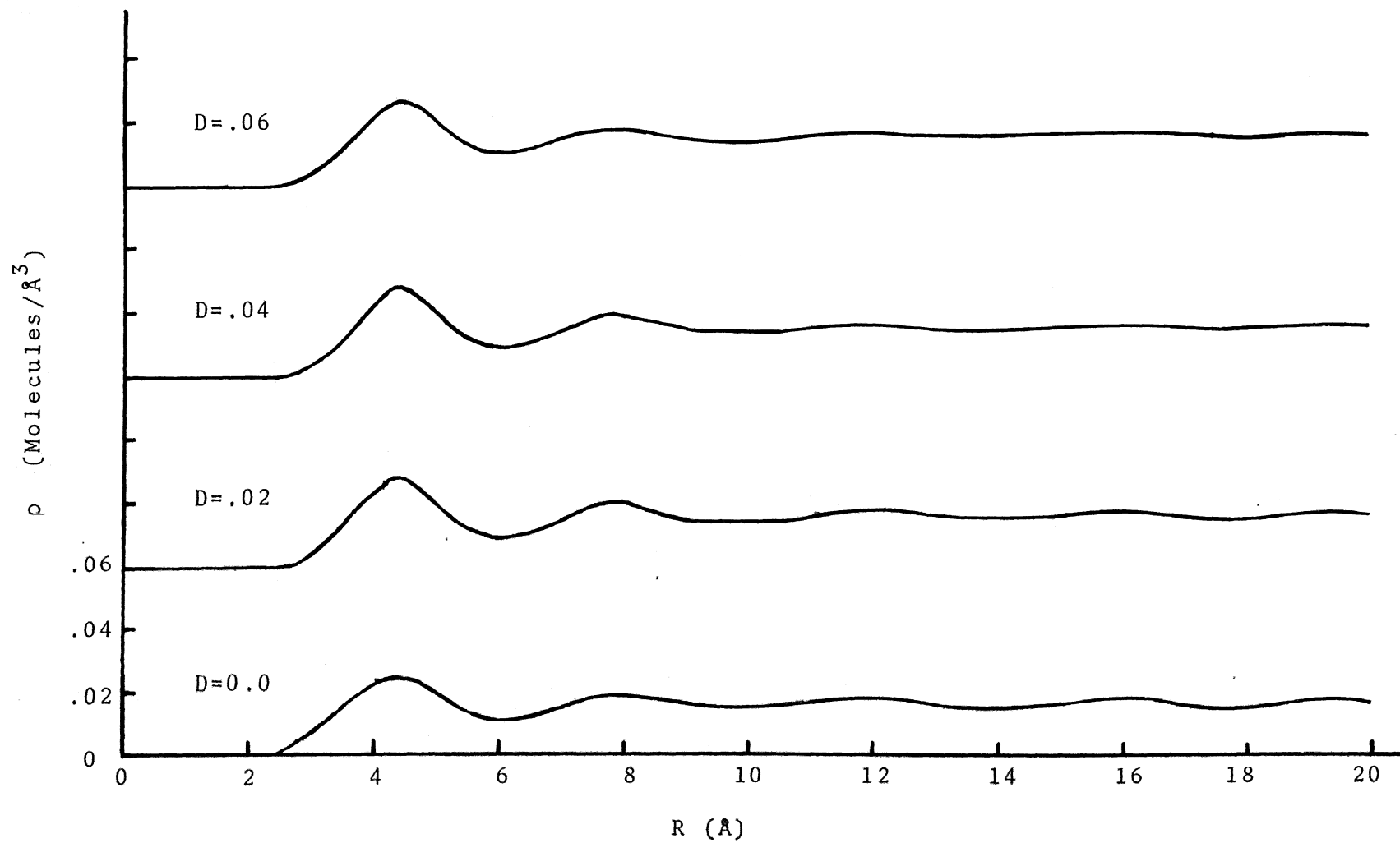


Figure 10. Molecular Pair Distribution,  $T^*=1.2$ ,  $V^*=1.6$

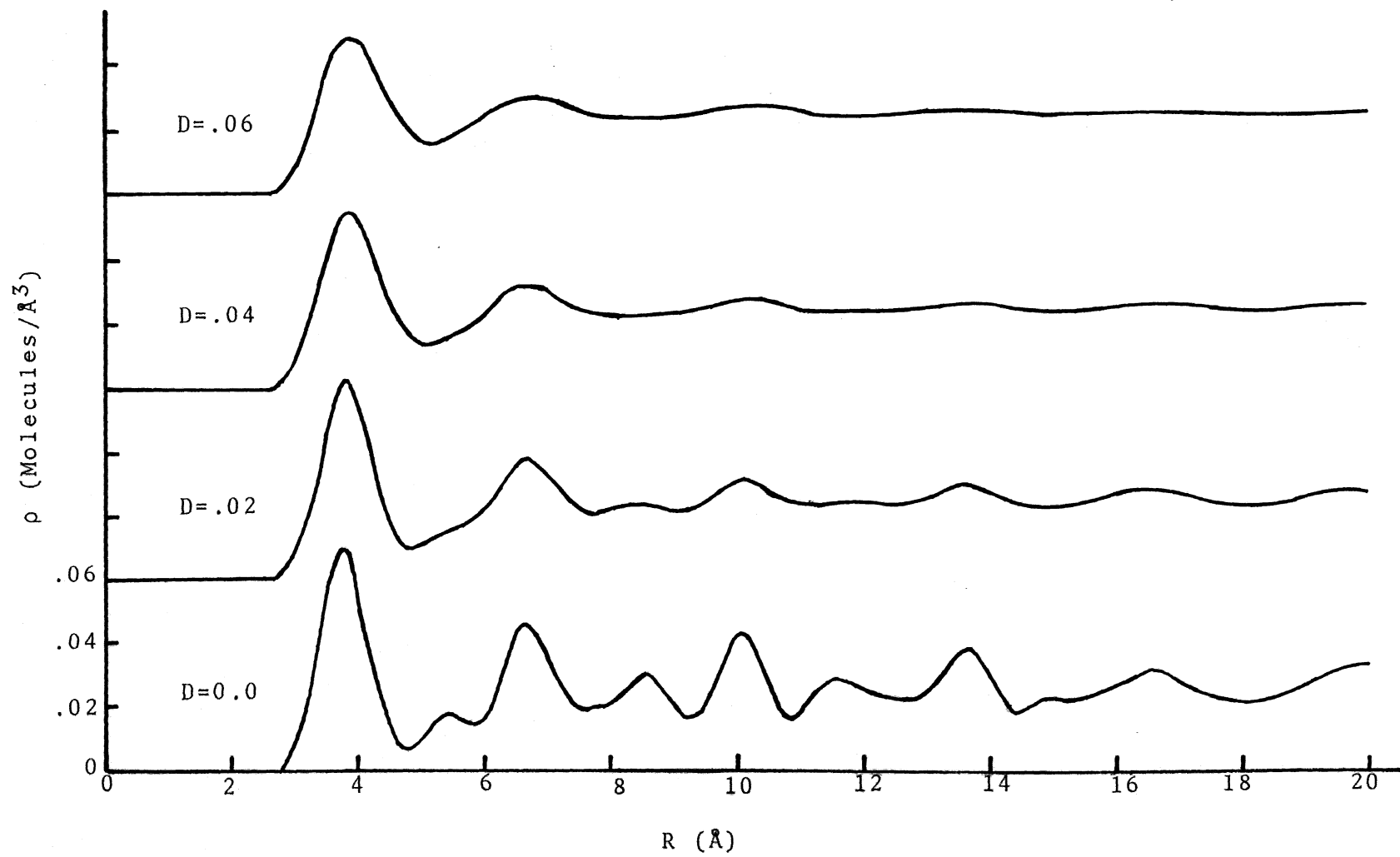


Figure 11. Molecular Pair Distribution,  $T^*=2.0$ ,  $V^*=1.0$

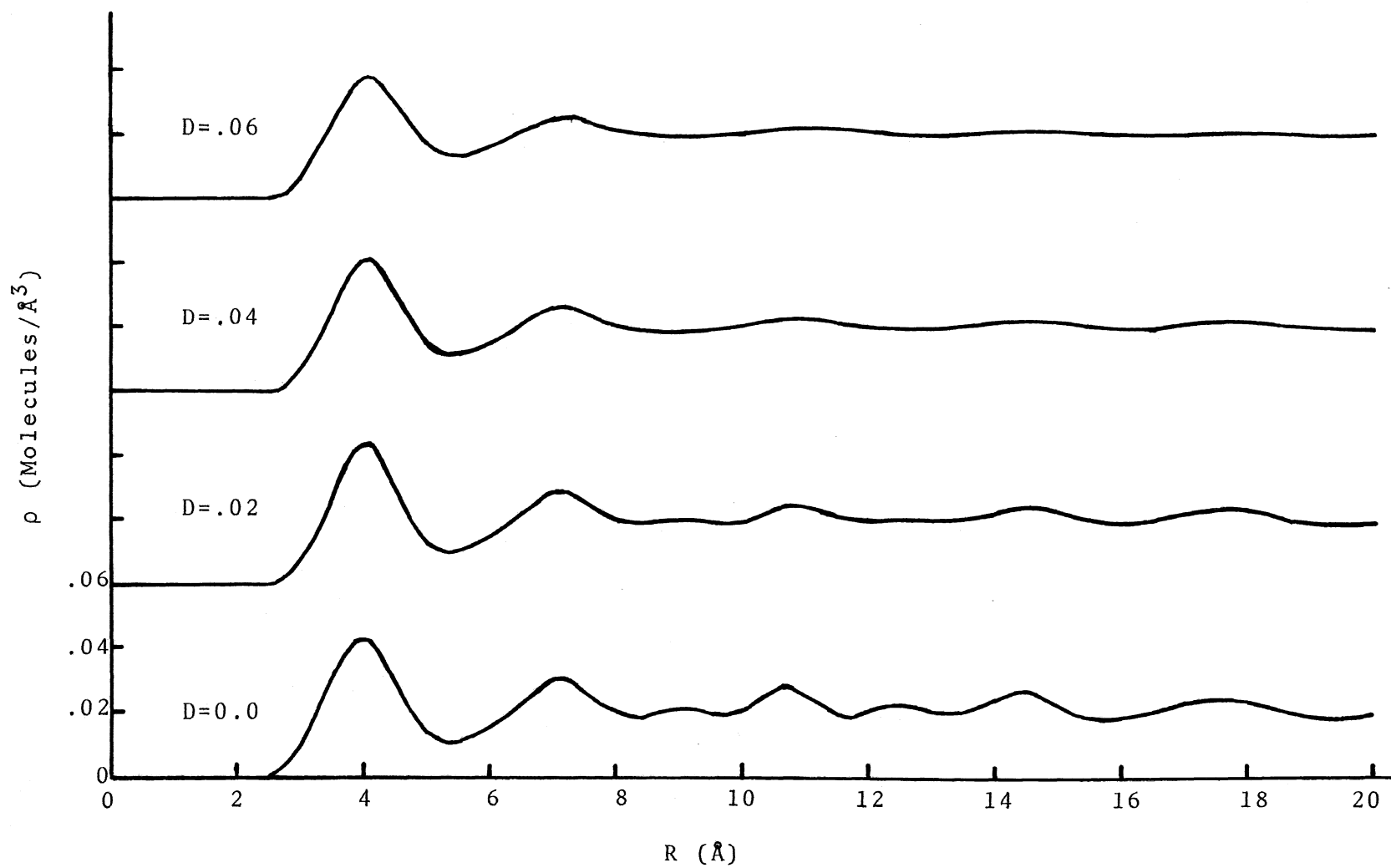


Figure 12. Molecular Pair Distribution,  $T^*=2.0$ ,  $V^*=1.2$

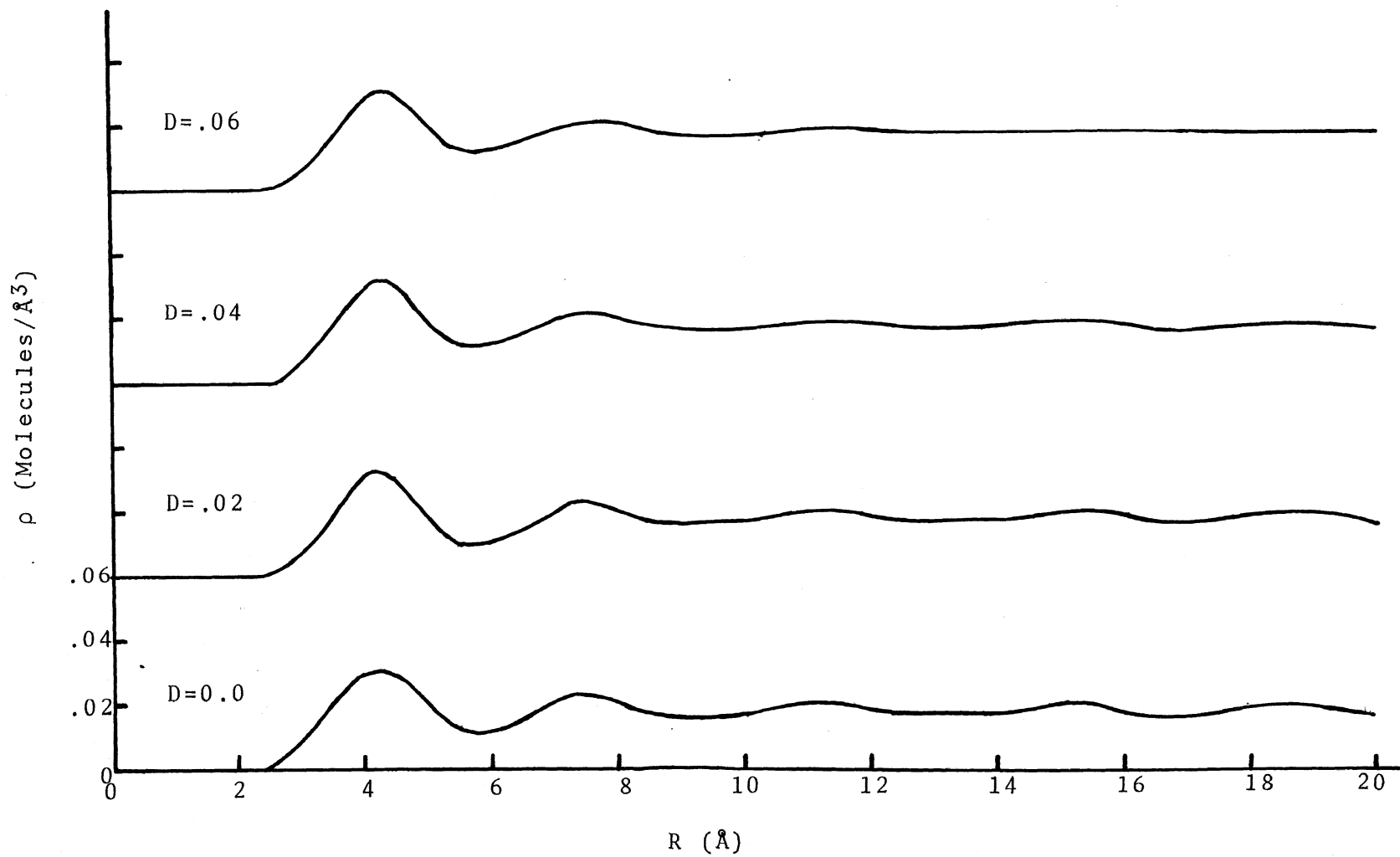


Figure 13. Molecular Pair Distribution,  $T^*=2.0$ ,  $V^*=1.4$

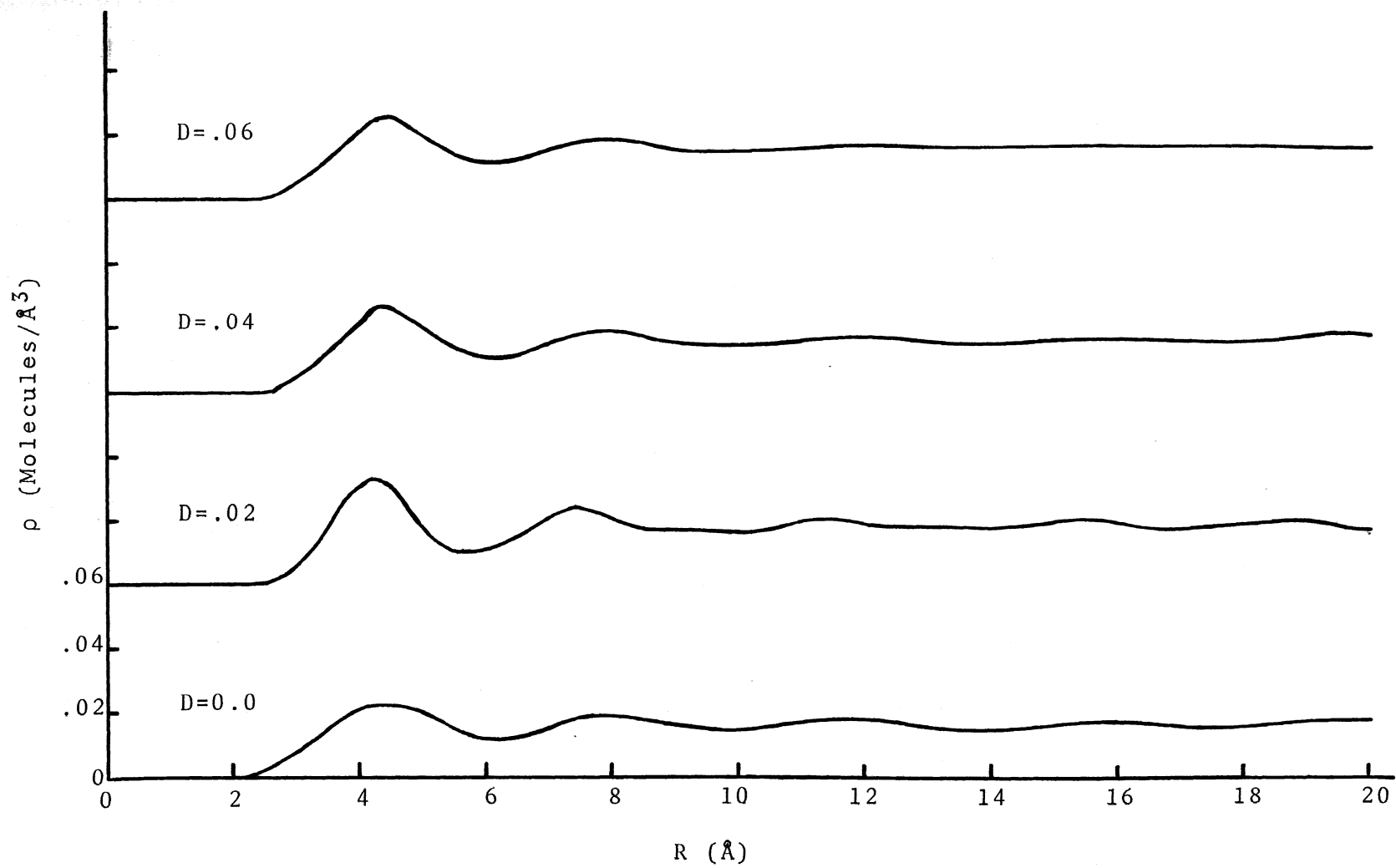


Figure 14. Molecular Pair Distribution,  $T^*=2.0$ ,  $V^*=1.6$



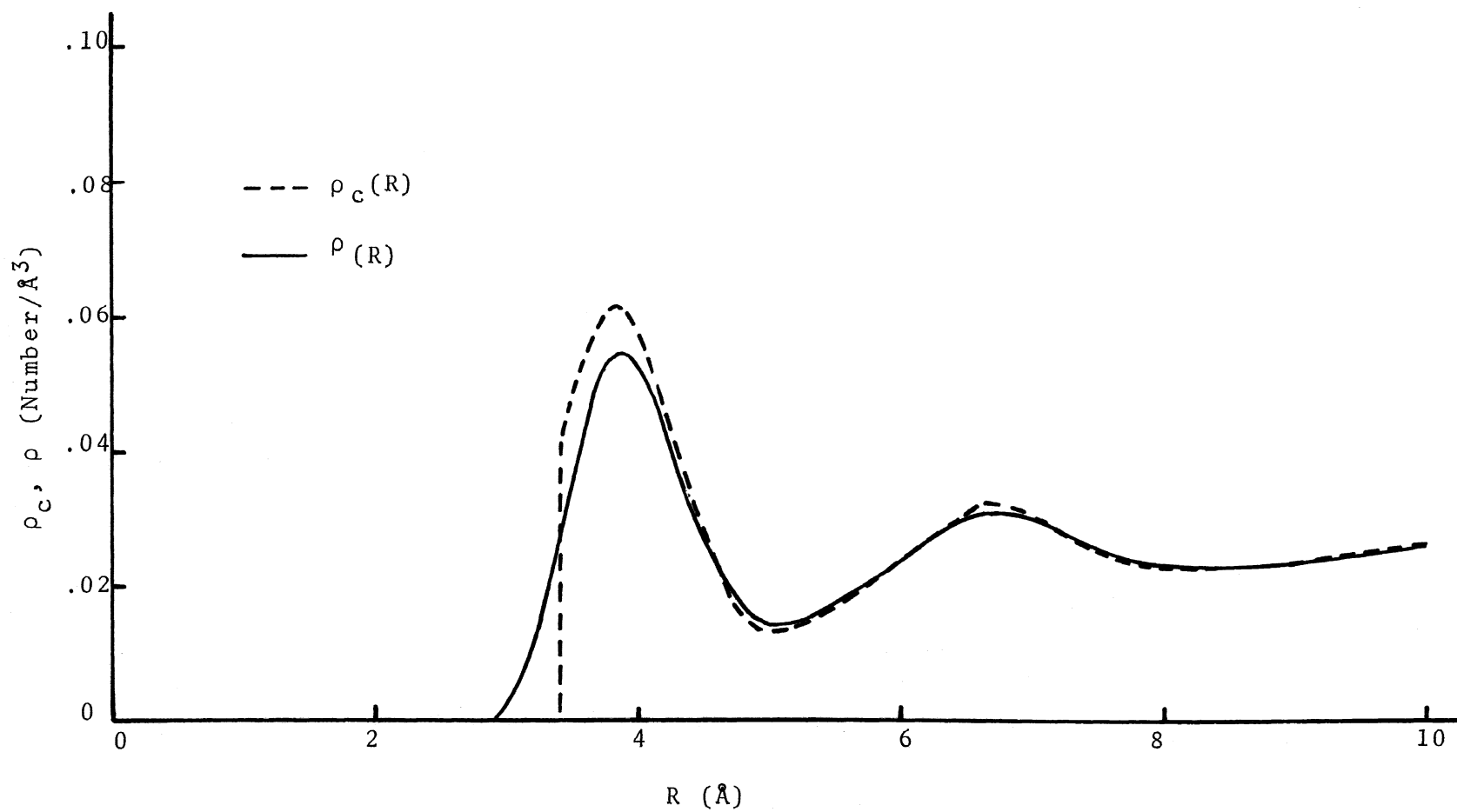


Figure 15.  $\rho(R)$  and  $\rho_c(R)$ ,  $D=.06$ ,  $T^*=.7$ ,  $V^*=1.0$

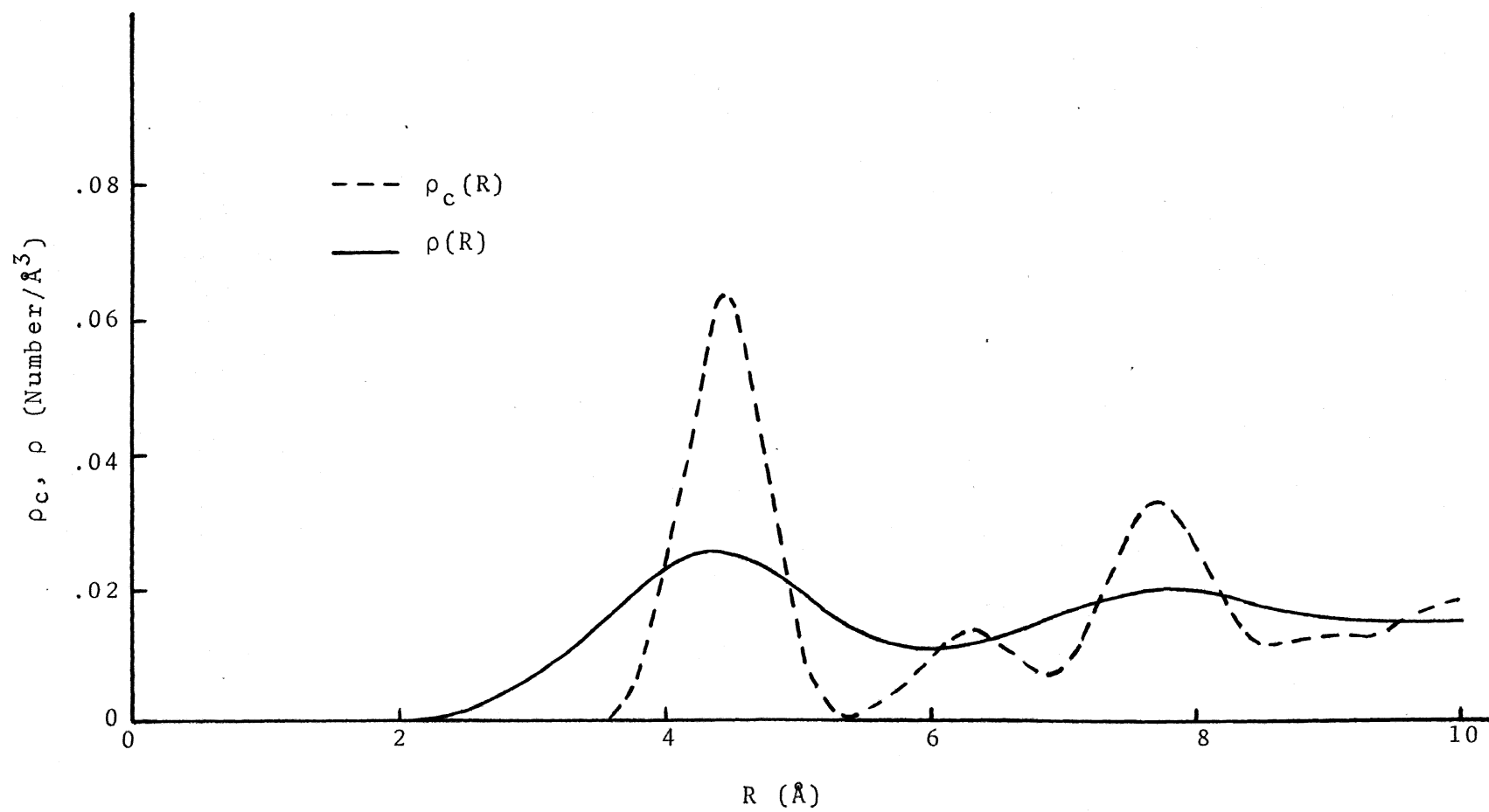


Figure 16.  $\rho(R)$  and  $\rho_c(R)$ ,  $D=.02$ ,  $T^*=2.0$ ,  $V^*=1.6$

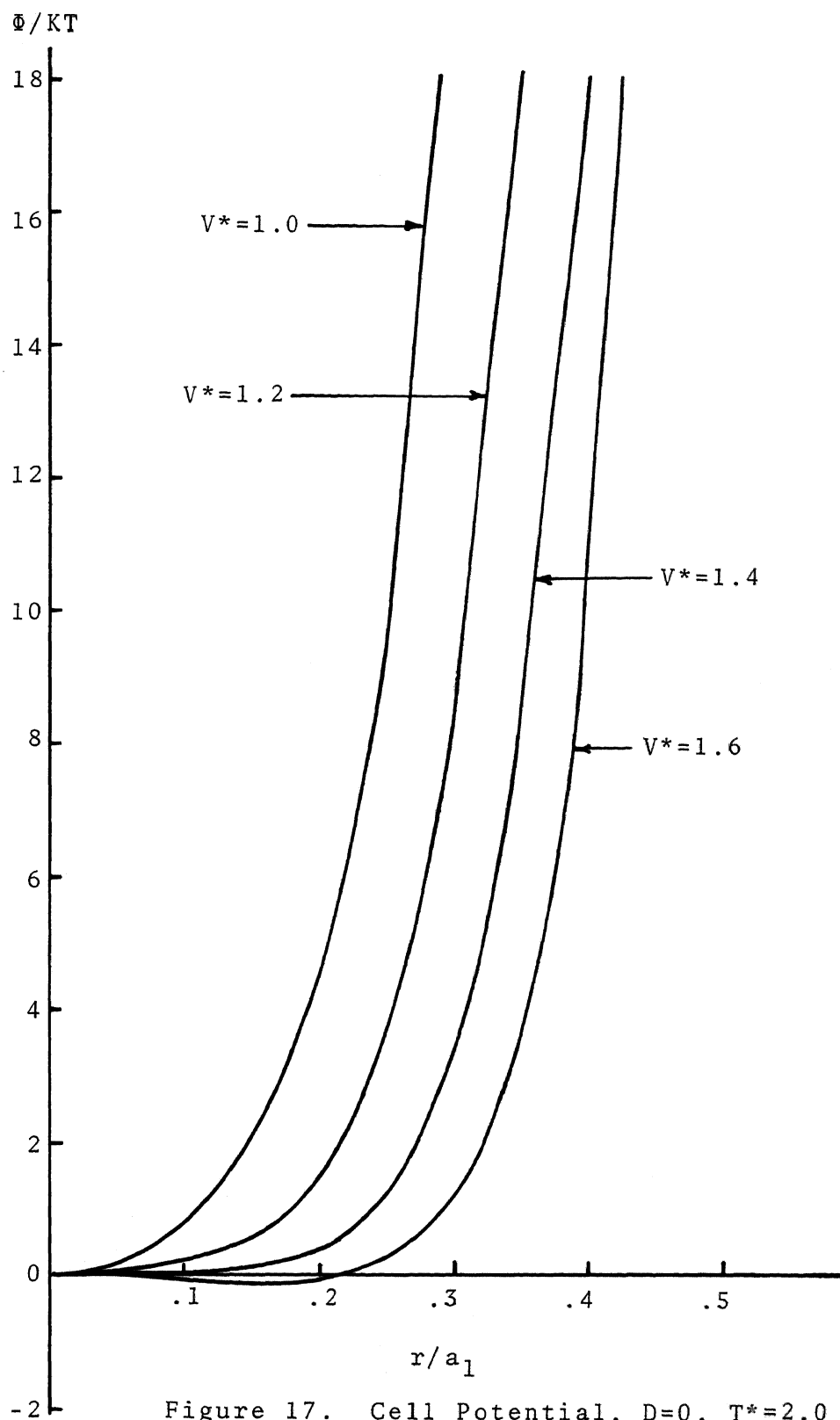


Figure 17. Cell Potential,  $D=0$ ,  $T^*=2.0$

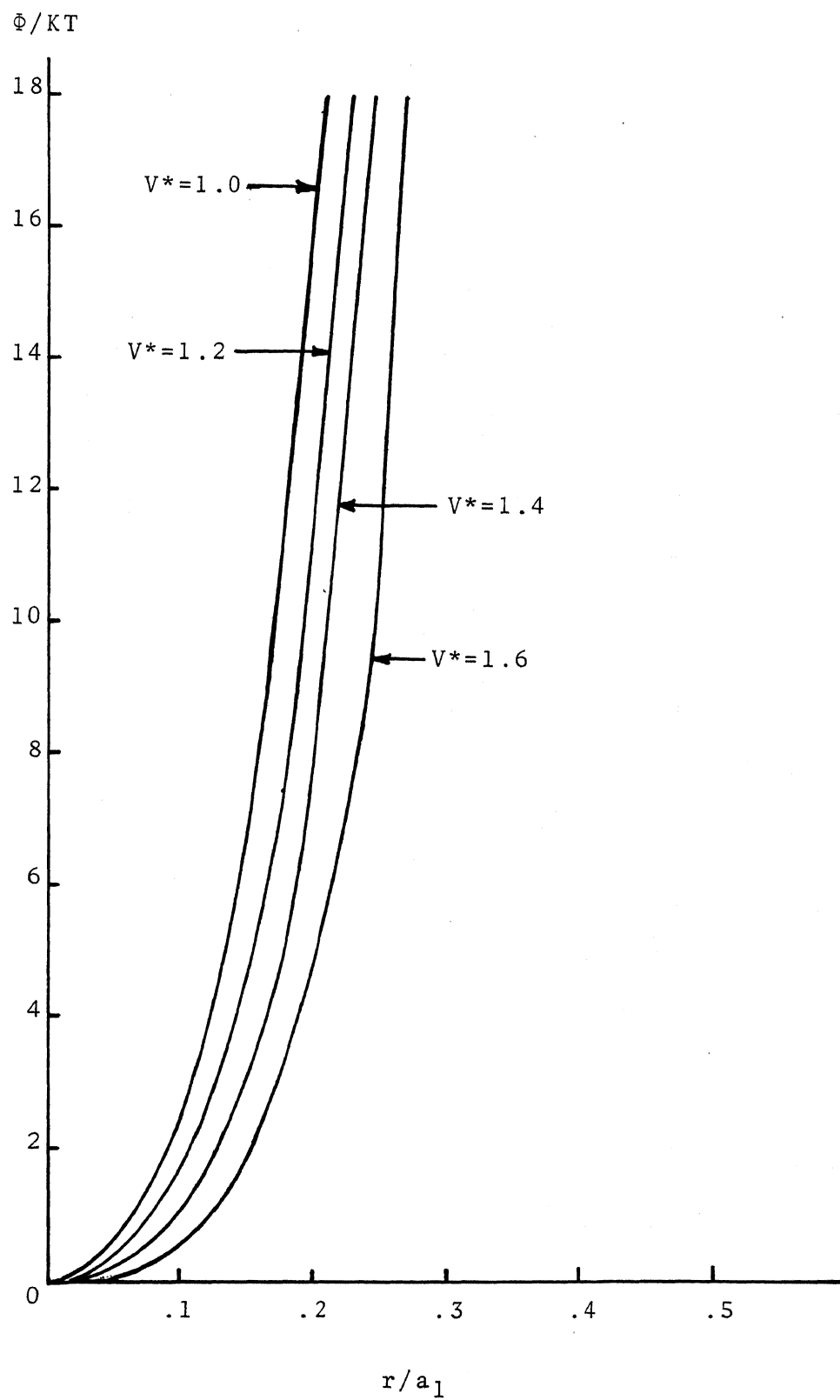


Figure 18. Cell Potential,  $D=.06$ ,  $T^*=.7$

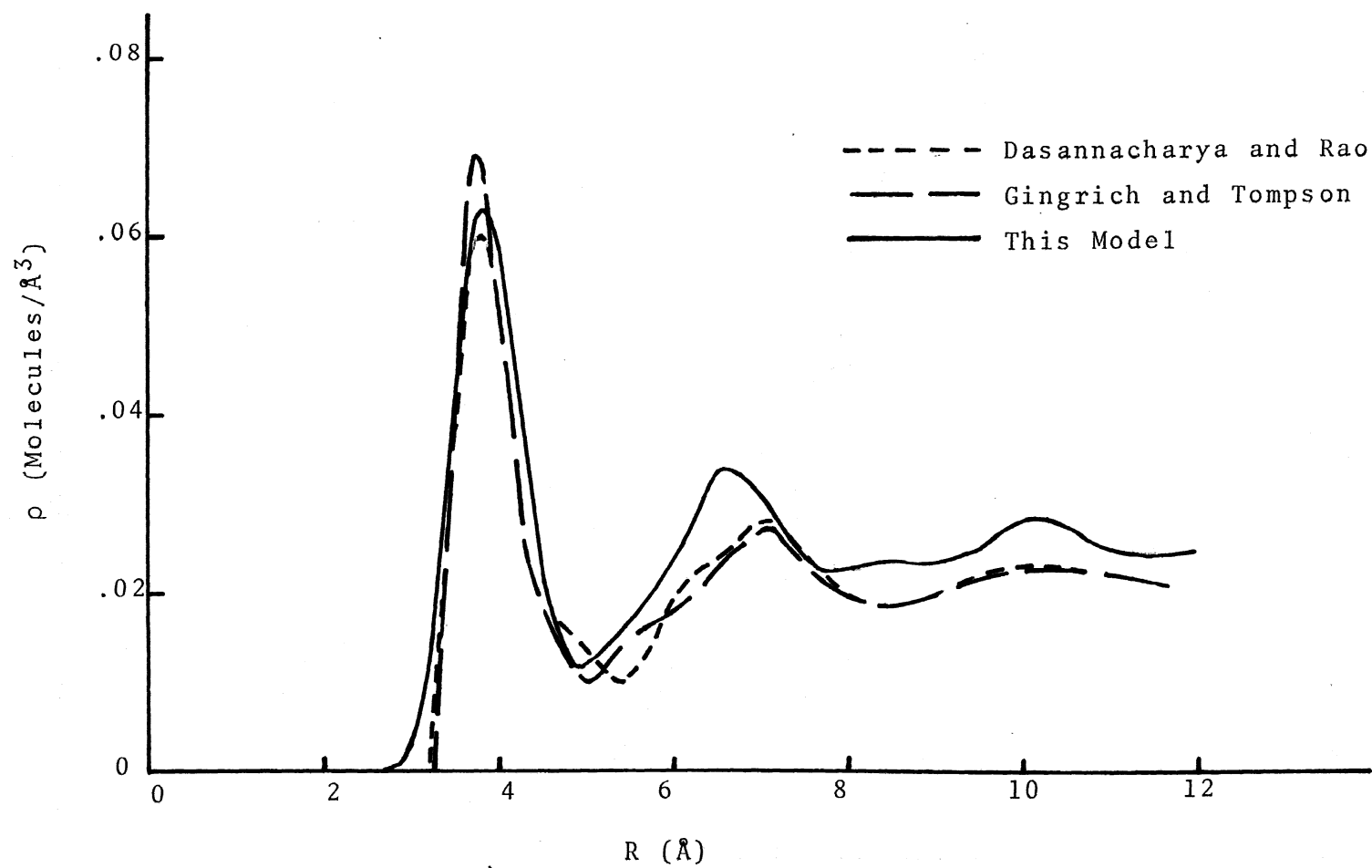


Figure 19. Calculated  $\rho(R)$  Compared to Experimental  $\rho(R)$

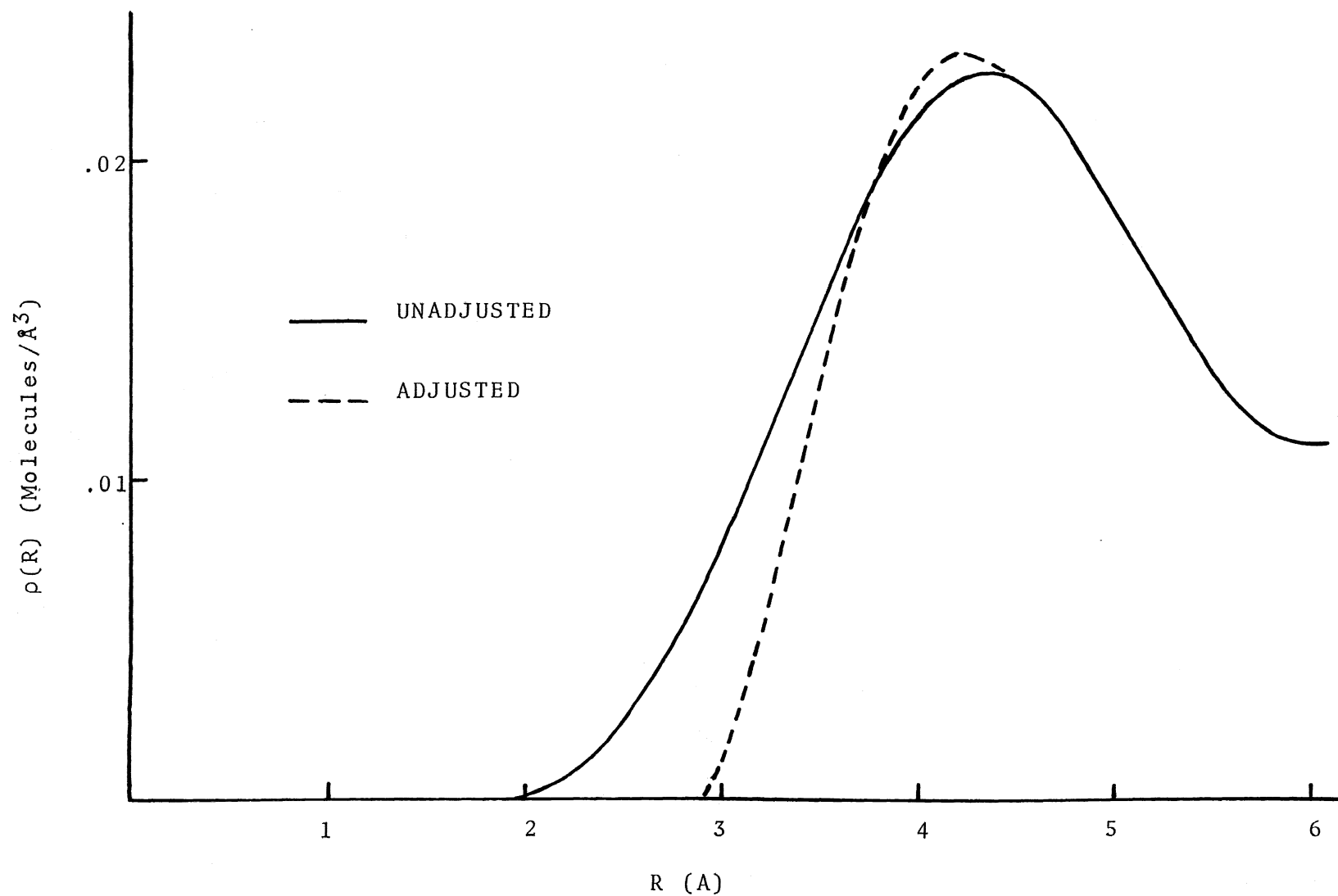


Figure 20. Adjustment of  $p(R)$  in the Most Extreme Case

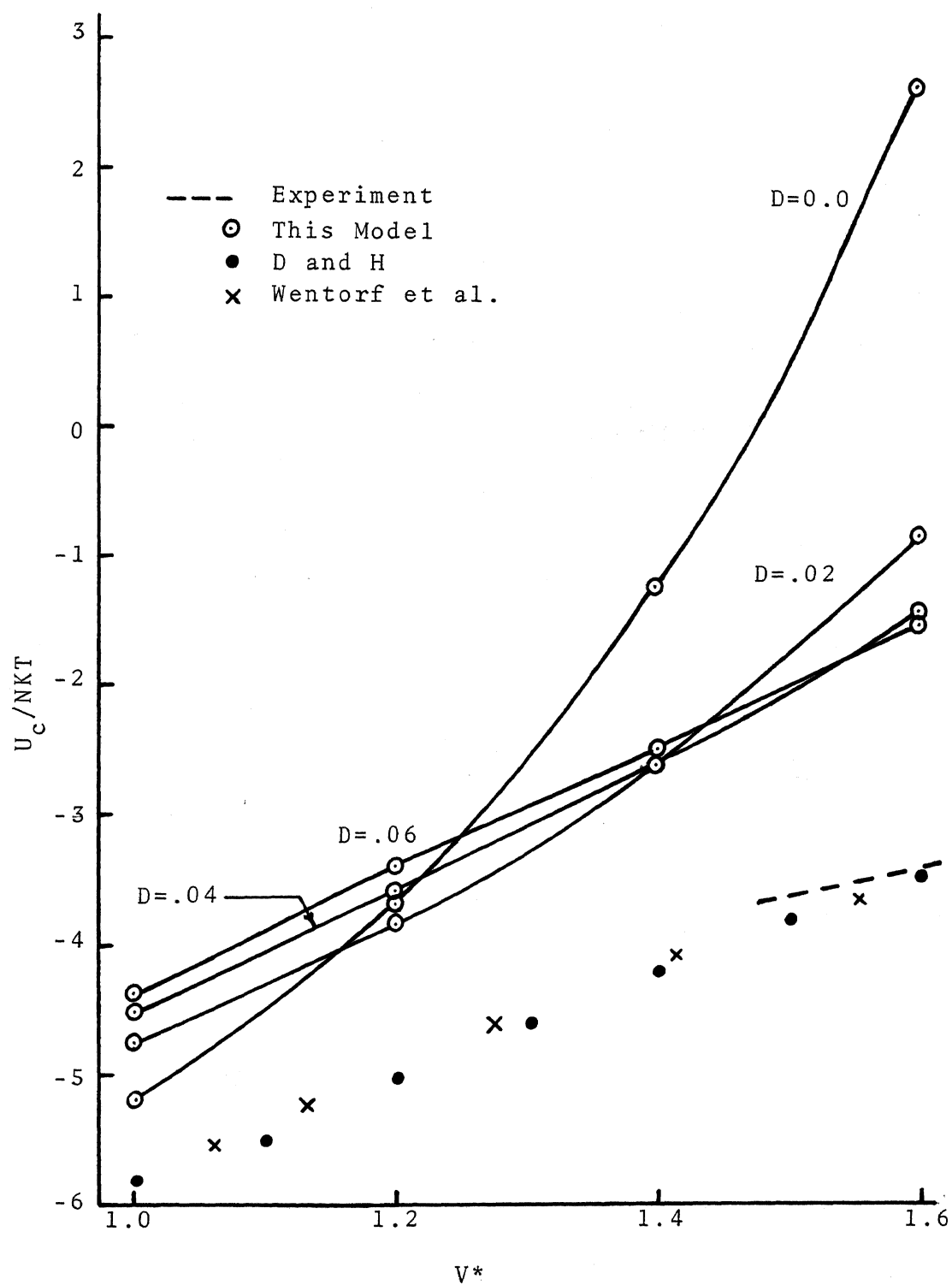


Figure 21. Comparison of  $U_c/NKT$  at  $T^*=1.2$  with Results of Experiment and Other Models

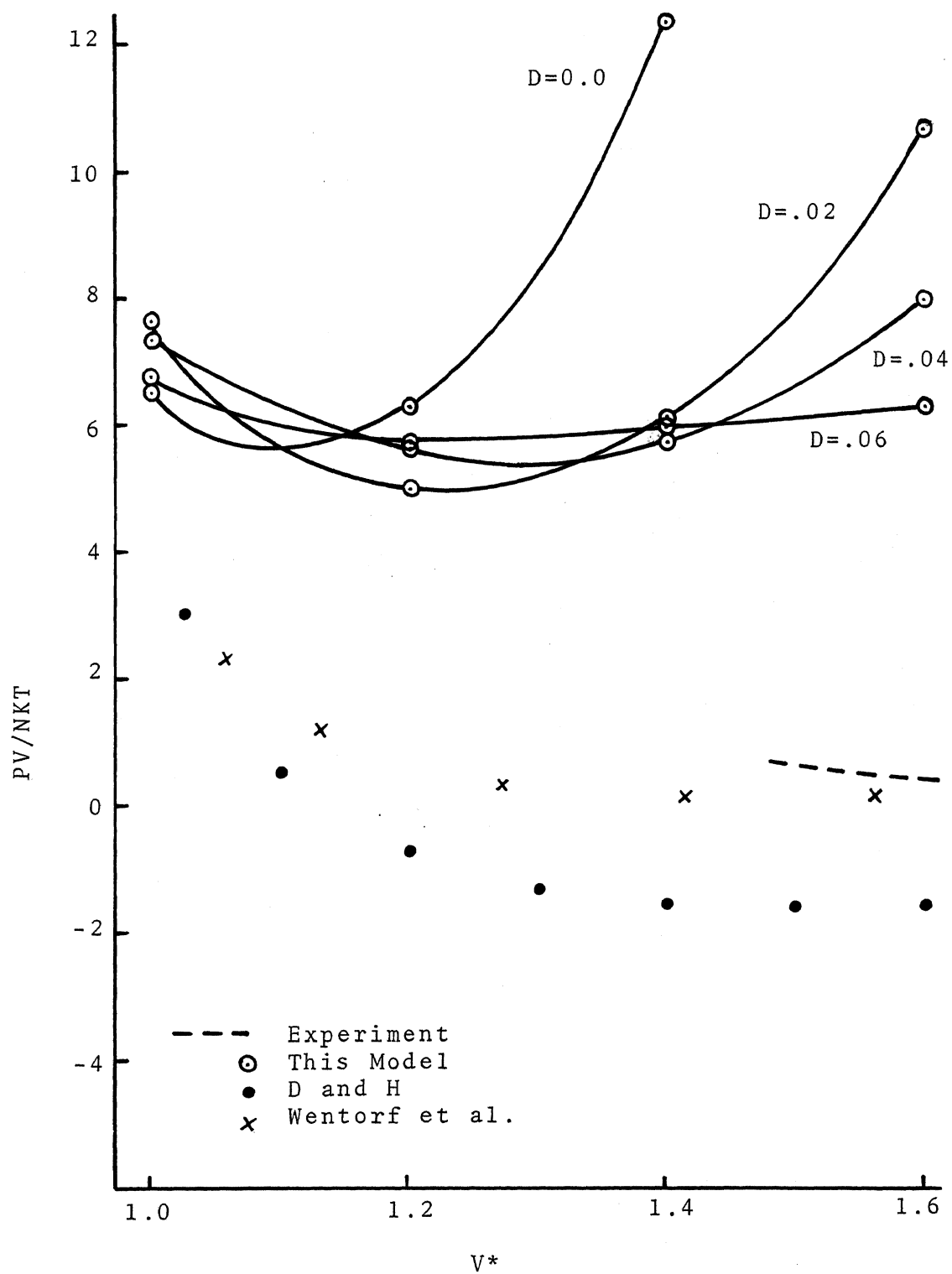


Figure 22. Comparison of  $PV/NKT$  at  $T^*=1.2$  With Results of Experiment and Other Models



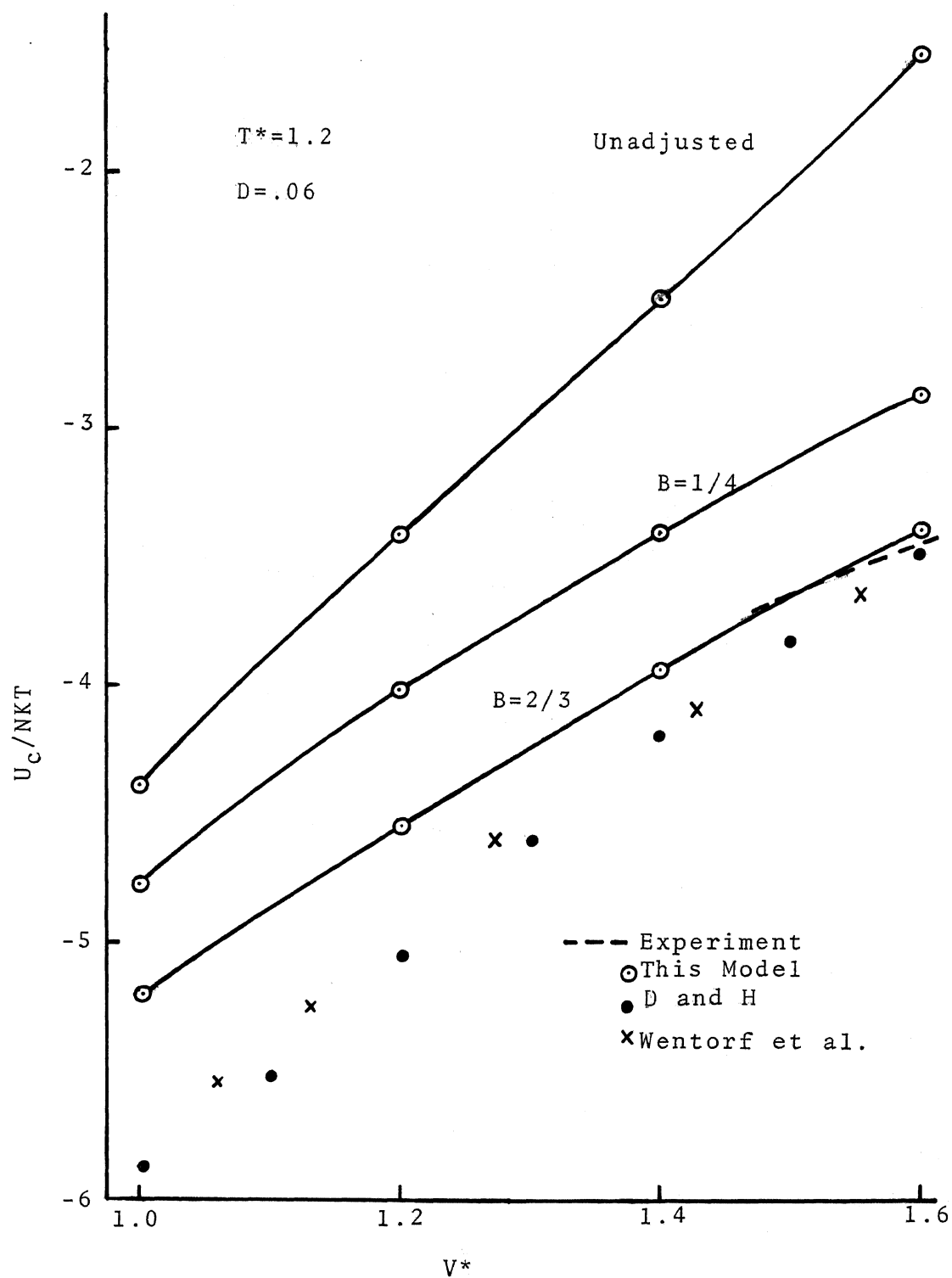


Figure 23. Comparison of Adjusted Values  
 of  $U_c/NKT$  with Results of  
 Experiment and Other Models

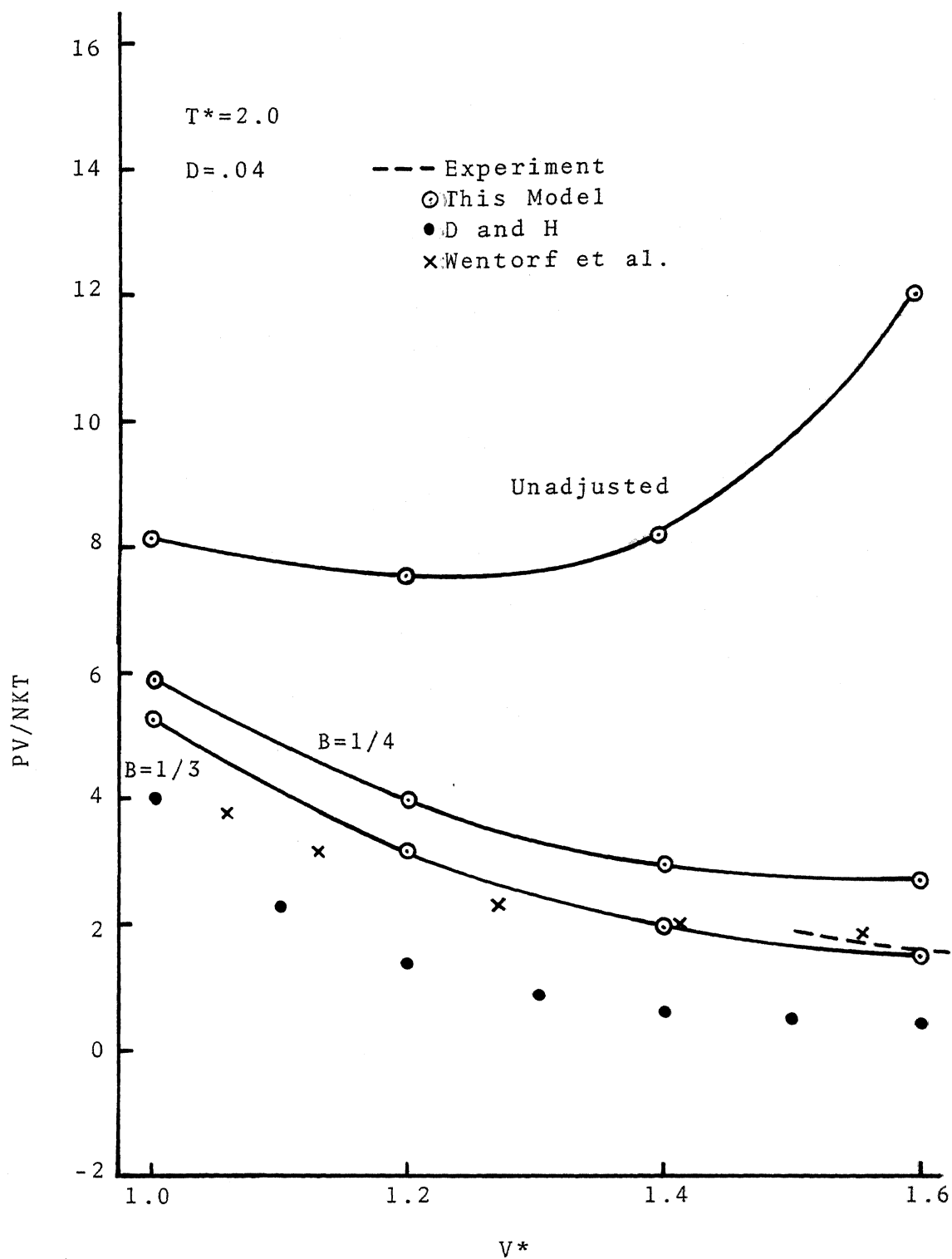


Figure 24. Comparison of Adjusted Values of PV/NKT with Results of Experiment and Other Models

Table V.  $U_c/NKT$  at  $T^* = .7$ 

D	V*	Unadj.	B = 1/4	B = 1/3	B = 1/2	B = 2/3
0.0	1.0	-10.228	-10.341	-10.397	-10.429	-10.487
	1.2	- 8.058	- 8.399	- 8.484	- 8.622	- 8.721
	1.4	- 5.135	- 6.262	- 6.495	- 6.925	- 7.021
	1.6	- .903	- 4.253	- 4.791	- 5.445	- 5.760
.02	1.0	- 9.355	- 9.614	- 9.688	- 9.821	- 9.935
	1.2	- 7.926	- 8.310	- 8.404	- 8.555	- 8.663
	1.4	- 6.197	- 6.852	- 6.983	- 7.163	- 7.262
	1.6	- 4.186	- 5.511	- 5.716	- 5.956	- 6.058
.04	1.0	- 8.978	- 9.278	- 9.364	- 9.518	- 9.650
	1.2	- 7.458	- 7.926	- 8.042	- 8.227	- 8.362
	1.4	- 5.987	- 6.676	- 6.816	- 7.011	- 7.121
	1.6	- 4.482	- 5.573	- 5.745	- 5.946	- 6.028
.06	1.0	- 8.721	- 9.044	- 9.135	- 9.298	- 9.437
	1.2	- 7.132	- 7.641	- 7.768	- 7.971	- 8.119
	1.4	- 5.745	- 6.467	- 6.616	- 6.825	- 6.947
	1.6	- 4.451	- 5.472	- 5.641	- 5.842	- 5.926

Table VI.  $U_c/NKT$  at  $T^* = 1.2$ 

D	V*	Unadj.	B = 1/4	B = 1/3	B = 1/2	B = 2/3
0.0	1.0	- 5.208	- 5.414	- 5.472	- 5.576	- 5.665
	1.2	- 3.698	- 4.254	- 4.388	- 4.598	- 4.749
	1.4	- 1.242	- 2.944	- 3.241	- 3.644	- 3.880
	1.6	2.353	- 1.711	- 2.279	- 2.935	- 3.238
.02	1.0	- 4.776	- 5.087	- 5.174	- 5.327	- 5.456
	1.2	- 3.865	- 4.377	- 4.497	- 4.683	- 4.815
	1.4	- 2.625	- 3.551	- 3.721	- 3.948	- 4.077
	1.6	- .881	- 2.767	- 3.018	- 3.307	- 3.434
.04	1.0	- 4.543	- 4.898	- 4.996	- 5.167	- 5.309
	1.2	- 3.599	- 4.174	- 4.309	- 4.519	- 4.668
	1.4	- 2.604	- 3.500	- 3.667	- 3.893	- 4.022
	1.6	- 1.422	- 2.897	- 3.100	- 3.335	- 3.437
.06	1.0	- 4.383	- 4.764	- 4.869	- 5.049	- 5.198
	1.2	- 3.403	- 4.016	- 4.160	- 4.383	- 4.540
	1.4	- 2.491	- 3.394	- 3.565	- 3.798	- 3.932
	1.6	- 1.534	- 2.866	- 3.060	- 3.286	- 3.387

Table VII.  $U_c/NKT$  at  $T^* = 2.0$ 

D	V*	Unadj.	B = 1/4	B = 1/3	B = 1/2	B = 2/3
0.0	1.0	- 2.412	- 2.703	- 2.783	- 2.924	- 3.042
	1.2	- 1.113	- 1.942	- 2.126	- 2.405	- 2.597
	1.4	1.114	- 1.094	- 1.456	- 1.919	- 2.173
	1.6	5.408	- .274	- .901	- 1.569	- 1.856
.02	1.0	- 2.174	- 2.565	- 2.670	- 2.848	- 2.992
	1.2	- 1.494	- 2.184	- 2.333	- 2.555	- 2.705
	1.4	- .405	- 1.709	- 1.917	- 2.184	- 2.330
	1.6	1.540	- 1.235	- 1.531	- 1.851	- 1.990
.04	1.0	- 2.015	- 2.457	- 2.572	- 2.767	- 2.922
	1.2	- 1.353	- 2.086	- 2.244	- 2.479	- 2.638
	1.4	- .612	- 1.744	- 1.933	- 2.178	- 2.314
	1.6	.711	- 1.404	- 1.639	- 1.895	- 2.005
.06	1.0	- 1.903	- 2.378	- 2.500	- 2.702	- 2.862
	1.2	- 1.224	- 1.998	- 2.163	- 2.408	- 2.572
	1.4	- .503	- 1.683	- 1.879	- 2.131	- 2.270
	1.6	.424	- 1.415	- 1.633	- 1.876	- 1.981

Table VIII. PV/NKT at  $T^* = .7$ 

D	V*	Unadj.	B = 1/4	B = 1/3	B = 1/2	B = 2/3
0.0	1.0	3.780	2.705	2.386	1.775	1.197
	1.2	1.557	- .800	- 1.456	- 2.621	- 3.618
	1.4	7.558	1.424	- .003	- 2.253	- 3.910
	1.6	21.683	5.712	2.836	- 1.085	- 3.491
.02	1.0	6.659	4.860	4.318	3.297	2.356
	1.2	1.396	- 1.098	- 1.781	- 2.977	- 3.985
	1.4	1.460	- 2.326	- 3.209	- 4.611	- 5.658
	1.6	5.395	- 1.401	- 2.660	- 4.436	- 5.584
.04	1.0	5.963	4.008	3.422	2.326	1.324
	1.2	2.663	- .229	- 1.018	- 2.393	- 3.544
	1.4	1.952	- 1.990	- 2.917	- 4.390	- 5.489
	1.6	3.455	- 2.223	- 3.307	- 4.848	- 5.852
.06	1.0	5.071	3.061	2.462	1.349	.378
	1.2	3.075	.004	- .828	- 2.274	- 3.478
	1.4	2.534	- 1.567	- 2.538	- 4.085	- 5.241
	1.6	3.319	- 2.105	- 3.175	- 4.714	- 5.727

Table IX. PV/NKT at  $T^* = 1.2$ 

D	V*	Unadj.	B = 1/4	B = 1/3	B = 1/2	B = 2/3
0.0	1.0	6.501	5.140	4.737	3.985	3.297
	1.2	6.300	3.225	2.427	1.074	-.019
	1.4	12.417	4.793	3.213	.874	-.725
	1.6	25.685	7.433	4.623	1.057	-.960
.02	1.0	7.637	5.808	5.273	4.291	3.413
	1.2	4.982	2.178	1.462	.259	-.705
	1.4	6.032	1.385	.424	- 1.015	- 2.021
	1.6	10.660	1.908	.565	- 1.201	- 2.257
.04	1.0	7.277	5.283	4.707	3.660	2.734
	1.2	5.629	2.548	1.765	.456	-.586
	1.4	5.796	1.294	.349	- 1.070	- 2.062
	1.6	7.924	.973	- .140	- 1.620	- 2.515
.06	1.0	6.799	4.718	4.125	3.052	2.114
	1.2	5.867	2.633	1.817	.461	-.612
	1.4	4.972	1.440	.479	- .969	- 1.983
	1.6	7.241	.887	- .181	- 1.617	- 2.496

Table X. PV/NKT at  $T^* = 2.0$ 

D	V*	Unadj.	B = 1/4	B = 1/3	B = 1/2	B = 2/3
0.0	1.0	7.731	6.096	5.628	4.774	4.018
	1.2	9.378	5.313	4.349	2.804	1.635
	1.4	16.413	6.455	4.687	2.264	.746
	1.6	32.661	8.294	5.370	1.998	.272
.02	1.0	8.259	6.215	5.646	4.638	3.774
	1.2	7.253	3.866	3.081	1.831	.890
	1.4	9.305	3.301	2.241	.760	- .200
	1.6	15.710	3.607	2.158	.405	- .558
.04	1.0	8.110	5.875	5.265	4.198	3.297
	1.2	7.517	3.957	3.136	1.835	.860
	1.4	8.182	2.919	1.946	.573	- .324
	1.6	11.943	2.626	1.455	.022	- .777
.06	1.0	7.883	5.512	4.876	3.776	2.857
	1.2	7.689	3.968	3.120	1.786	.796
	1.4	8.444	2.986	1.992	.594	- .313
	1.6	10.607	2.430	1.332	- .032	- .800



Table XI.  $C_v/NK$  at  $T^* = .7$ 

D	$V^*$	Unadj.	$B = 1/4$	$B = 1/3$	$B = 1/2$	$B = 2/3$
0.0	1.0	1.835	1.530	1.442	1.282	1.143
	1.2	2.269	1.557	1.380	1.092	.880
	1.4	3.531	1.709	1.352	.861	.569
	1.6	5.728	1.837	1.267	.619	.321
.02	1.0	1.597	1.262	1.167	1.000	.859
	1.2	1.728	1.139	.998	.775	.613
	1.4	2.167	1.078	.870	.586	.415
	1.6	3.197	1.077	.779	.431	.261
.04	1.0	1.622	1.250	1.142	.963	.809
	1.2	1.723	1.090	.941	.707	.540
	1.4	2.039	.969	.771	.503	.344
	1.6	2.473	.856	.620	.344	.209
.06	1.0	1.641	1.237	1.125	.933	.771
	1.2	1.731	1.070	.915	.674	.504
	1.4	1.904	.918	.728	.464	.313
	1.6	2.238	.791	.572	.312	.185

Table XII.  $C_v/NK$  at  $T^* = 1.2$ 

D	$V^*$	Unadj.	$B = 1/4$	$B = 1/3$	$B = 1/2$	$B = 2/3$
0.0	1.0	1.805	1.437	1.335	1.155	1.003
	1.2	2.545	1.540	1.317	.977	.742
	1.4	4.260	1.693	1.279	.754	.468
	1.6	8.097	1.862	1.210	.541	.263
.02	1.0	1.671	1.237	1.123	.929	.773
	1.2	1.914	1.120	.951	.699	.528
	1.4	2.589	1.065	.824	.517	.346
	1.6	4.293	1.069	.736	.376	.214
.04	1.0	1.708	1.225	1.099	.891	.725
	1.2	1.886	1.066	.893	.638	.466
	1.4	2.226	.925	.713	.441	.290
	1.6	3.927	.844	.583	.300	.172
.06	1.0	1.739	1.217	1.085	.869	.700
	1.2	1.905	1.047	.869	.608	.435
	1.4	2.224	.898	.685	.412	.262
	1.6	2.862	.775	.535	.272	.152

Table XIII.  $C_V/NK$  at  $T^* = 2.0$ 

D	V*	Unadj.	B = 1/4	B = 1/3	B = 1/2	B = 2/3
0.0	1.0	1.759	1.289	1.165	.953	.780
	1.2	2.986	1.513	1.216	.792	.521
	1.4	5.426	1.668	1.162	.583	.305
	1.6	11.887	1.901	1.120	.417	.171
.02	1.0	1.790	1.198	1.052	.815	.634
	1.2	2.212	1.089	.875	.578	.393
	1.4	3.261	1.043	.750	.408	.236
	1.6	6.047	1.056	.666	.288	.138
.04	1.0	1.847	1.186	1.029	.776	.591
	1.2	2.146	1.026	.816	.527	.349
	1.4	2.525	.856	.621	.344	.203
	1.6	4.548	.825	.523	.230	.113
.06	1.0	1.895	1.185	1.022	.767	.587
	1.2	2.183	1.010	.795	.502	.324
	1.4	2.735	.867	.616	.329	.182
	1.6	3.861	.748	.476	.208	.100

## VI. DISCUSSION OF RESULTS

### A. Molecular Pair Distribution Function

The molecular pair distribution functions (Figures 3 to 14) show the expected behavior. At low temperatures and low specific volume several peaks are evident, the first being the sharpest and most prominent. For a given value of  $D$ , the peaks are more diffuse at higher temperatures and higher specific volume. For a given temperature and volume, corresponding peaks become wider and lower as  $D$  increases, consequently fewer peaks are observed.

In all cases part of the peaks are obscured by large adjacent ones so that peaks corresponding to some shells do not appear, i.e., there are considerably fewer peaks in the molecular pair distribution than there are shells in a face-centered cubic lattice for a given range of  $R$ . The pair distribution assumes essentially its average value at the higher values of  $R$ , within approximately two nearest neighbor distances at higher  $T^*$ ,  $V^*$ , and  $D$ . Discernable peaks are still evident at the maximum radial distance considered, 4 to 5 nearest neighbor distances, in the case of lower  $D$  and  $V^*$ .

X-ray and slow neutron diffraction studies provide experimentally determined molecular pair distributions<sup>1-4,36</sup>. Figure 19 compares two experimentally determined  $\rho(R)$  with

that calculated from the model. The curves of Gingrich and Tompson from x-ray scattering and Dasannacharya and Rao from neutron scattering were chosen because they are at least as accurate as other published results and are available in tabular form. Mikolaj and Pings<sup>37,38</sup> have made extensive x-ray measurements in the critical region but they do not overlap in temperature and density with the ranges considered here. Extraneous peaks at low  $R$  unavoidably appear in experimental curves owing to data analysis techniques<sup>22,39</sup>. They have been removed in Figure 19 to avoid confusion.

The comparison curve from this model used in Figure 19,  $D = .04$ ,  $T^* = .7$ ,  $V^* = 1.0$ , most nearly matches the experimental curves. The experimental curves are essentially at the argon triple point ( $T^* = .7$ ,  $V^* = 1.186$ )<sup>31</sup>.

Exact comparison can not be expected from the model considered here, even if there was considerably more agreement in the experimental results. The coordination number of the first peak is  $7 \rightarrow 12$  at the triple point<sup>39,40</sup> depending on the method used to separate the first and second peak in the overlap region, whereas in this model the requirement of one molecule per cell restricts us to exactly 12. The introduction of "holes", i.e., empty cells, into this model might be adequate to take this into account if a more definite figure could be determined experimentally (see Section G).

Quantitative comparison at other temperatures and densities has not been made since experimental curves are not available at the particular values used in this study. Qualitative comparison can be made however.

In most cases the  $D = 0$  and  $D = .02$  results are too sharply peaked. The  $D = .04$  and  $D = .06$  results agree more closely with experimental results. The decrease in peak height and increase in width with increasing temperature is clearly indicated in the x-ray studies of Eisenstein and Gingrich<sup>1</sup>. The x-ray work of Mikolaj and Pings<sup>37</sup> indicates three, perhaps four, peaks within 20 Angstroms at  $T^* = 1.235$ ,  $V^* = 1.71$  which is comparable to our  $T^* = 1.2$ ,  $V^* = 1.6$   $D = .04$  or  $.06$  results.

One property of the molecular pair distributions, calculated from our model, which is at variance with experiment, is the placement of the peaks as a function of radial distance. While in our model increased specific volume results in increased spacing between peaks, experimental evidence indicates little change in placement of peaks with volume change. The change occurs in peak height indicating a change in the associated coordination number. The fixed value for coordination numbers in this model forbid any such behavior in the calculated distribution functions.

Comparison of the cell-center and molecular distributions is shown in Figures 15 and 16. As one would expect, motion of the molecules within the cell results in

the molecular distribution being more diffuse than the cell-center distribution. This is most evident when the cell-center distribution is sharply peaked, i.e., when  $D = 0$  or  $.02$ . Since Dirac delta functions are not readily depicted graphically, the case of  $D = .02$ ,  $T^* = 2.0$ ,  $V^* = 1.6$  is used in Figure 16. At the other extreme, shown in Figure 15, of high values of  $D$ , low temperature and low specific volume, there is very little difference in the two distributions, only a slight flattening of peaks and dips.

These results are readily explained by considering the potential well within the cells in the two situations. In the first case fewer cell centers occur at low values of  $R$ , hence the potential well calculated with molecules at their cell centers is relatively wide as shown in Figure 17 and allows considerable uncertainty in the molecule's position within the cell. One then expects the molecular distribution to vary somewhat from the cell-center distribution. In the second case (high  $D$ , low  $V^*$ ) a considerable number of cell centers are located at  $R$  slightly greater than  $\sigma$ . Calculation of the potential with molecules at their cell centers gives a fairly narrow well, restricting the molecules to positions very close to their cell centers. In this situation the cell-center and molecular distributions are essentially the same as shown by Figure 18.

The cell-center distribution function in Gaussian form has a finite non-zero amplitude for all values of  $R$ ,

even at  $R = 0$ . An extensive overlap of cells is not acceptable, although slight overlap is not significant since in all cases the molecules are essentially confined to  $r < .4a_1$ .

To correct this problem  $\rho_c(R)$  was set equal to zero for  $R < \sigma$ , while the contribution of the first shell to  $\rho_c(R)$  was enhanced sufficiently to retain the original number of cell centers. A similar difficulty was encountered with the molecular pair distribution which prompted the adjustment discussed in Section C.

#### B. Thermodynamic Functions for Unadjusted $\rho(R)$

Calculated values for reduced configurational internal energy  $U_c/NKT$  are given in Tables V, VI, and VII. Table XI compares the values determined from this model and three other cell models with experimental values for argon at or near the triple point. The models of Wentorf et al.<sup>41</sup>, Dahler and Hirschfelder<sup>42</sup> and Levelt and Cohen<sup>35</sup> are all modifications of the LJD model. A detailed discussion and comparison of these various versions has been given by Levelt and Cohen<sup>35</sup>. The values in Table XIV credited to Wentorf et al. and Dahler and Hirschfelder have been linearly interpolated from tabulated data as a function of  $V^*$ , while those of Levelt and Cohen were extrapolated from tabulated data in the range  $T^* = .8 \rightarrow 2.0$ .



The experimental value is that of Hunter and Rowlinson<sup>43</sup>. There is an additional error not indicated in the given value as a result of converting to reduced form. Comments on this are included in Section E. In addition values calculated from  $\rho(R)$  determined experimentally by Gingrich and Tompson<sup>36</sup> and Dasannacharya and Rao<sup>4</sup> are included in the table. It should be noted in these cases the accuracy of the intermolecular potential as well as that of the distribution function is involved.

For all  $D$ , the values of our model are too high, those for low  $D$  being best. This is in contrast to other cell models which give values that are too low.

Table XV compares the values of  $PV/NKT$  with those of other models and experiments near the triple point. For all  $D$ , the results of this model are closer to the experimental value than those of other models. The values from other models were interpolated graphically from tabulated data. Again values calculated from experimental  $\rho(R)$  are included as well as those determined directly by experiment.

The same situation arises here as with internal energy. Results from this model are too high, those of other cell models too low.

Although experimental data are lacking for higher temperatures in the specific volume range  $V^* = 1.0 \rightarrow 1.3$ , extrapolation of existing data indicates values for

$U_c/NKT$  and  $PV/NKT$  above those of LJD type models and below those of this model.

If we consider the results at higher specific volumes and at all temperatures used in this study, we find our model gives results considerably above the experimental values of Michels, Levelt and Wolkers<sup>44</sup> put in reduced form by Levelt<sup>45</sup>. This effect is most pronounced at low values of  $D$ . The LJD type models however, have their best agreement with experimental data in the region of  $V^* = 1.6 \rightarrow 1.7$ . Figures 21 and 22 compare our results at  $T^* = 1.2$ ,  $D = .06$  with experimental values and the models of Wentorf et al. and Dahler and Hirschfelder.

In general, independent particle models, i.e., most cell models, will not give good results for the constant volume specific heat<sup>35</sup> even at high densities where the assumptions are most valid. Likewise this model gives values which do not agree with experiment.

The rapid rise in the internal energy and compressibility factor with increasing specific volume, characteristic of the model proposed here, can be explained in the following way. High  $V^*$  and low  $D$  are conditions which give the widest potential well within the cell. With no coordination between positions in adjacent cells, there is a significant probability that two molecules will be close together or in other words  $\rho(R)$  for  $R < \sigma$  somewhat greater than zero. This leads to a very large repulsive contribution in the internal energy and pressure-volume product.

Table XIV. Comparison of  $U_c/NKT$  Near the Triple Point

Source	$T^*$	$V^*$	$U_c/NKT$	Deviation
This Model, $D = 0.0$	.700	1.185	-8.334	+ .19
$D = .02$	.700	1.185	-8.032	+ .39
$D = .04$	.700	1.185	-7.571	+ .95
$D = .06$	.700	1.185	-7.248	+1.27
Wentorf et al.	.700	1.185	-9.239	- .72
Dahler and Hirschfelder	.700	1.185	-9.323	- .80
Levelt and Cohen	.700	1.185	-9.32	- .80
Experimental (H and R)	.700	1.185	-8.52±.07	- - -
$\rho(R)$ - x-ray (G and T)	.703	1.200	-8.99	- .47
$\rho(R)$ - neutron (D and R)	.705	1.189	-8.58	+ .06

Table XV. Comparison of PV/NKT Near the Triple Point

Source	T*	V*	PV/NKT
This model, D = 0.0	.700	1.200	1.557
D = .02	.700	1.200	1.396
D = .04	.700	1.200	2.663
D = .06	.700	1.200	3.075
Wentorf et al.	.700	1.200	-3.44
Dahler and Hirschfelder	.700	1.200	-4.849
Experimental (H and R)	.700	1.185	.003
$\rho(R)$ - x-ray (G and T)	.703	1.200	.452
$\rho(R)$ - neutron (D and R)	.705	1.189	.916

Recall the Lennard-Jones 6-12 potential (Figure 1) is very high when  $R$  is less than  $\sigma$  by even a small amount. On the other hand low  $V^*$  gives a narrow potential well, therefore lower probability that two molecules are very close ( $R < \sigma$ ) together.

### C. Thermodynamic Functions for Adjusted $\rho(R)$

In order to examine the possibility of extending the range of specific volumes useful for the calculation of thermodynamic properties from this model, the modification of the molecular pair distribution described in Section II-D was applied. This particular type of adjustment was prompted by three considerations. It would qualitatively adjust the three thermodynamic quantities we are considering here so they more nearly conform to experimental values over a wider range of specific volumes. Secondly it is contradictory to allow more than a very low probability that two molecules will approach closer than  $\sigma$  and at the same time assume a Lennard-Jones 6-12 interaction. Thirdly, experimental  $\rho(R)$  show asymmetry of the first peak<sup>1,4,36</sup>, the low  $R$  side having a steeper slope than the high  $R$  side (see Figure 19).

This adjustment does not alter the qualitative features discussed in Section A except slightly increasing the front slope of the first peak as just mentioned. Figure 20 compares the first peak adjusted and unadjusted

for the case in which the modification was most severe,  
 $D = 0$ ,  $T^* = 2.0$ ,  $V^* = 1.6$ .

The parameter  $B$  defines the degree of adjustment. Calculations were made for  $B = 1/4$ ,  $1/3$ ,  $1/2$ , and  $2/3$  in all cases.  $B = 0$  would mean no adjustment.

At the triple point, values of  $U_c/NKT$  calculated from the adjusted  $\rho(R)$  were even better than the unadjusted and hence considerably better than those of other cell models. This is true for all values of  $B$  and  $D$ . Compare data from Tables V, VI, and VII with those of Table XIV.

The PV/NKT data were improved for low values of  $B$ , but were overadjusted for high  $B$  giving essentially at  $B = 2/3$ , the same results as the LJD type models.

At higher temperatures, but with reduced specific volumes in the neighborhood of  $1.0 \rightarrow 1.3$ , it is difficult to say whether the adjusted values are better than the unadjusted since experimental data are not available.

For higher specific volume, greatly improved values of the internal energy and compressibility factor were attained. In most cases very close agreement could be achieved with a properly selected  $B$  value as shown in Figures 23 and 24. There is some inconsistency in that for a given temperature volume and  $D$  factor, the value of  $B$  which gives the closest fit to experimental PV/NKT data might not be the same which best fit  $U_c/NKT$  data. In most instances a choice of  $B$ , which gives a better

value of both properties than either the unadjusted model or other models, was possible.

The specific heat results, while being significantly improved, could not be matched to experimental data over any large range of temperature and volume with fixed values of  $D$  and  $B$ .

As with the order parameter  $D$ , a particular best value of  $B$  could not be readily assigned to particular values of  $T^*$  and  $V^*$ . Either or both parameters may be functions of temperature and density, but experimental data at sufficient points are not available to attempt determination of such functions.

The problem of excessive probability of two molecules being closer than the distance  $\sigma$  together is not unique with this model, but has also been encountered using the integral equation approach for determining  $\rho(R)$  and using the Lennard-Jones 12-6 interaction<sup>46</sup>.

#### D. Comparison of This Model to Other Cell Models

Virtually all cell models assuming independent particle motion are variations or modifications of the Lennard-Jones and Devonshire model. Their principle advantage is the relative simplicity of the calculations. Frequently more rigorous versions give results which compare less favorably with experiment than simple versions<sup>35</sup>.

The calculations of Wentorf et al.<sup>41</sup>, used frequently for comparison in the previous sections, are based on a model essentially the same as the original LJD except three shells of neighbors are used instead of one as in the original work.

Dahler and Hirschfelder<sup>42</sup> calculated the potential in the cell by considering nearest neighbors can assume positions other than their cell centers and using a self-consistent iterative technique which assumes second, third, etc., neighbors to be at their cell centers. One might expect this to be an improvement over the Wentorf model, but values of the thermodynamic functions were less in agreement with experimental values. Note that this model has long range order, but a degree of short range disorder in contrast to the known situation as a liquid. Thermodynamic functions are determined mainly by the short range conditions.

Levelt and Cohen<sup>35</sup> calculated thermodynamic functions for the "neighbor localized" version of the LJD model, which is a first iteration partially accounting for motion of neighboring molecules. The thermodynamic functions don't differ a great deal from Wentorf's values.

Calculation of the thermodynamic functions for the above models is accomplished by assuming independent motion which allows evaluation of the configurational integral and hence the configurational thermodynamic properties.



Evaluation of thermodynamic properties through the pair distribution function by the procedures used in this study do not give the same results as the above method even though very similar assumptions are used in both cases. Using the  $D = 0$  case in the model proposed in this work often gives far different values for thermodynamic quantities than those of the other cell models. This was verified in a slightly different manner by applying the same equations used by Wentorf et al., suitably modified for the Gaussian cell center distribution to determine thermodynamic functions for several values of  $T^*$ ,  $V^*$  and  $D$ . The results obtained did not coincide with our model and were less in agreement with experiment.

As mentioned in Section A, the LJD type models usually agree best with experiment for reduced specific volumes around 1.6 in reference to the quantities  $PV/NKT$  and  $U_c/NKT$ . This borders on a region of contradictory assumptions<sup>35</sup>. At values of  $V^*$  greater than 1.45, the potential well no longer has a minimum at the cell center but a local maximum (see Figure 15). Hence the cell center is no longer the most probable position for a molecule, yet this same potential is calculated assuming molecules are at their cell centers (see Figure 17).

The model considered in this study appears to be most valid as far as calculating thermodynamic properties at lower specific volumes where the assumptions are most valid.

The fact that in most models only a few shells of neighbors are considered, whereas we consider 40, will not affect the calculation of the potential in the cell to any great extent since the effect of shells beyond the third is small and beyond the fifth or sixth, negligible. Most authors compensate for the fact there are long range contributions to the internal energy. The large number of shells are used in our model since  $\rho_c(R)$  must be known beyond the range of  $R$  for which  $\rho(R)$  is to be calculated.

#### E. Accuracy of Results

Because of the complexity of the calculations, it is difficult to give a precise value to the accuracy of the results of this work. All computer calculations were made in double precision. The increments used in the Simpson's rule integrations, which comprise a large part of the calculations, were adjusted so that decreasing them individually by one half, i.e., doubling the number of strips, produced less than a 1% change in the directly calculated thermodynamic quantities. Comparing the number of cell centers and the number of molecules within the maximum radial distance considered showed a discrepancy of less than 1% in all cases and usually less than .4%. Recall that normalizing to one molecule per cell involves the first integration performed. For the case of  $D = 0$  two integrations are eliminated and the number of molecules and cell centers agrees to less than one part in 10,000.

The parameters in the Lennard-Jones potential are not known with an accuracy of better than 1%<sup>35</sup>. Since the final results are not simply related to these quantities, the effect of these uncertainties was not precisely established. Levelt<sup>45</sup> has studied the effect of uncertainty in the Lennard-Jones parameters upon the process of converting experimental quantities to reduced units which may be several percent. In our study a consistent set of values was used in both calculations and conversion to reduced units which may make comparisons more reliable. As shown by the results given in Section C, the thermodynamic properties are very sensitive to small changes in  $\rho(R)$ . In addition their calculation involves another application of the interaction potential and its attendant uncertainty.

Plots of  $PV/NKT$  and  $U_c/NKT$  as functions of  $D$ ,  $T^*$  or  $V^*$  were smooth curves. No scattering, such as might be caused by a random error in the computing process, was apparent.

It is concluded therefore that the error resulting from the computing process and techniques is considerably less than that attributable to uncertainties in the input quantities. For comparison purposes uncertainties in the results as large as a few percent would not affect the conclusions made.

The determination of the specific heat is expected to be considerably less accurate than the other results.

It is derived from the internal energy and will contain any uncertainties in this quantity. In addition since the internal energy was calculated at only three different temperatures, the accuracy of a curve through these points is questionable, although the deviation from a straight line was slight in most cases.

#### F. Selection of Parameters

The values selected for  $T^*$  (.7, 1.2, 2.0) were chosen to study the model under a wide range of conditions and at the same time have some data available from other models and experiment for comparison. The triple point reduced temperature is .700. The value 1.2 is slightly below the critical temperature of 1.26. Thus 2.0 is a temperature considerably above the critical temperature.

The values of  $V^*$  were selected to correspond to the region where the assumptions of this model are most valid and for comparison purposes. Attempts to extend the rather narrow range of specific volumes in either direction resulted in a considerably slower rate of convergence for one or more of the integrations and thus would involve a significant increase in the computer time required.

Selection of values of the order parameter  $D$  was based on the following considerations.  $D = 0$  gives a cell center distribution exactly the same as the LJD model. Values of  $D$  up to about .06 are necessary to provide a  $\rho(R)$  in agreement with experimental curves. Higher values

of D result in slower convergence of the integrations, although this problem can probably be avoided<sup>24</sup>.

The values of B were chosen in order that the resulting range of magnitudes of the thermodynamic quantities overlapped the results of other models and experiment and so that values intermediate to the unadjusted and maximum adjustment results were more or less evenly spaced.

#### G. Possible Improvements in the Model

The obvious way to improve the values of thermodynamic functions calculated with this model would be to find a physically justifiable way to limit the magnitude of  $\rho(R)$  for  $R < \sigma$  to some very small value. The modification necessary to accomplish this is not apparent however. Probably coordination of the positions of molecules in adjacent cells would be required, which no doubt would vastly extend and complicate the calculations.

A close comparison of  $\rho(R)$  calculated from this model and experimentally determined  $\rho(R)$  indicates the rate at which order decreases with R is too slow in this model, i.e., the peak width should increase faster than the square root of R. What a better function would be, or whether something more complicated than a one parameter function is needed, is an open question.

The relaxing of the requirement that each cell contain one molecule, such as the introduction of empty cells or "holes", has been frequently applied to cell

models<sup>35</sup>. Usually this has only a small effect on the thermodynamic functions<sup>31,35</sup>. An improvement in the pair distribution function might result, since as mentioned in Section A, coordination numbers associated with peaks in the experimental distribution functions are less than those of a face-centered cubic lattice. It may be that the calculation of thermodynamic quantities by the method used in this work would be affected by the introduction of holes.

For cell models, thermodynamic properties are usually calculated through evaluation of the configurational integral. In our model these properties are calculated from the molecular pair distribution function. The assumptions in both cases are essentially the same. A detailed study into the reasons these two methods give different results might provide helpful clues to an improved model. In view of the fact our model gives high values for  $PV/NKT$  and  $U_c/NKT$  compared to experiment, and other models give low values in the temperature and density ranges considered here, it appears some compromise approach would give very good results. The nature of the desirable modifications is obscure at present.

The Lennard-Jones potential is known to have some inadequacies<sup>30,47</sup>. A significantly improved two particle interaction would involve more than two parameters and the experience of other workers indicates this often

leads to considerably more work with little or no improvement in results. Three or more particle interactions may be important in real liquids, but to include such considerations vastly complicates any calculation.

## VII. CONCLUSIONS

The model proposed in this study provides a means of calculating molecular pair distribution functions for simple liquids which qualitatively agree with experimentally determined pair distributions. Molecular pair distributions as such are not usually determined for other independent particle cell models. Unrealistic long range order is inherent in the assumptions on which such models are based, however.

Values for the reduced configurational internal energy,  $U_c/NKT$ , and compressibility factor,  $PV/NKT$ , calculated from the derived molecular pair distributions are in agreement with experimental value as well or better than other cell models in the regions where the assumptions are most valid, i.e., at specific volumes (densities) near the triple point volume. The range of volumes, over which useful values of these thermodynamic properties can be calculated, is less than that of other models.

This volume range, however, can be extended by a slight adjustment of the molecular pair distribution function at short radial distances.

The usual method of calculating thermodynamic quantities through the configurational integral does not give the same results as the methods employed in this



study using the molecular pair distribution function even when the initial assumptions of both models are made to coincide. For the two directly calculated properties, the former method yields low values while the latter yields high values compared to experimental measurements. Further investigation into the exact differences in these two approaches might provide insight into an improved model.

No simple modification of the model proposed is evident which would give significantly better results without an increase in the length and complexity of the calculations.

## VIII. APPENDICES

Appendix A. Square Root of R Dependence of Peak Width<sup>21</sup>

Consider a linear chain of labeled molecules, the position of each having an uncertainty  $\delta_i$  with respect to the previous molecule. The actual distance  $d_i$  between the  $i^{\text{th}}$  and the  $(i-1)^{\text{th}}$  molecule is  $a_i - \delta_i/2 < d_i < a_i + \delta_i/2$  where  $a_i$  is the average distance. Let the distance of the  $s^{\text{th}}$  molecule from the first be  $R_s + \xi_s$  where  $R_s = a_1 + a_2 + \dots + a_s$  is the average value and  $\Delta_s$  the uncertainty, i.e.,  $-(\delta_1 + \delta_2 + \dots + \delta_s)/2 < \xi_s < +(\delta_1 + \delta_2 + \dots + \delta_s)/2$ . If the individual uncertainties are independent, average  $\xi = 0$ , but the average of the square is given by

$$\begin{aligned}\overline{\xi_s^2} &= \overline{\Delta a_1^2} + \overline{\Delta a_2^2} + \dots + \overline{2\Delta a_1 \Delta a_2} + \dots \\ &= \overline{\Delta a_1^2} + \overline{\Delta a_2^2} + \dots + \overline{\Delta a_s^2}\end{aligned}\tag{A1}$$

where the  $\Delta a_i^2$  are the actual deviations from the average positions.

If a correlation between  $\xi^2$  and  $R_s$  exists, it must be of the form  $\overline{\Delta_s^2} = 2DR_s$  since  $R_s = a_1 + \dots + a_s$ , where  $2D$  is a constant.

A very simple illustrative case is when  $a_1 = a_2 = \dots = a$  and  $\delta_1 = \delta_2 = \dots = \delta$ . Then  $R_s = sa$

$$\overline{\xi_s^2} = s \overline{(\Delta a)^2}, \text{ i.e.,}$$

$$\overline{\xi_s^2}/R_s = \overline{\delta_2^2}/a \quad \text{or} \quad \overline{\xi_s^2} = (\overline{\delta_2^2}/a)R_s. \quad (\text{A2})$$

Compare with the case of Brownian motion where a resultant displacement  $\xi_s$  in time  $t_s$  from individual jumps  $\Delta a_i$  in time  $T_i$  are related by

$$\overline{\xi_s^2}/2t_s = \overline{(\Delta a_i)^2}/2T_i = D \quad (\text{A3})$$

where  $D$  is called the diffusion constant. In our case  $R_s$  replaces  $t_s$  and hence the term "structural diffusion".

In the model considered here the width of the  $m^{\text{th}}$  peak in the cell-center pair distribution is  $\sqrt{Da_m}$  in Equation (3) and physically is a measure of the uncertainty in the radial position of the cell-centers in the  $m^{\text{th}}$  shell.

For distances greater than some critical value, peaks no longer are resolved, that is for  $R_s$  such that

$$\sqrt{\overline{\xi_s^2}} = \sqrt{2DR_s} \geq R_{s+1} - R_s. \quad (\text{A4})$$

## Appendix B. Reduced Quantities

It is frequently convenient to express thermodynamic quantities in reduced or unitless form by combination with the parameters of the Lennard-Jones potential,  $\sigma$  and  $\epsilon$ , the Boltzmann constant  $K$  and the number of molecules in the system  $N$ . This also allows direct application of the law of corresponding states. The reducing factor for

Table XVI. Factors Used for Reduction

Quantity	Factor
Temperature	$\epsilon/K$
Volume	$N \theta^3$
Density	$1/N \theta^3$
Pressure	$\epsilon/\theta^3$
Compressibility Factor	1
Internal Energy	$N\epsilon$
Specific Heat	$NK$

the various quantities are given in Table XVI. A superscript asterisk indicates a reduced quantity.

### Appendix C. Computer Programs

This appendix contains the two most important computer programs used in this study. The programming language is Fortran IV in both cases.

The first calculates the molecular pair distribution function  $\rho(R)$ , the reduced configurational internal energy  $U_c/NKT$ , and the compressibility factor  $PV/NKT$ . A slightly simplified program was used when  $D = 0$ , since the integration over delta functions could be performed analytically.

The important variables and their program names are

Variable	Symbol in Text	Name in Program
Order parameter	D	D
Nearest neighbor distance	$a_1$	A
Reduced temperature	$T^*$	RETEMP
Reduced specific volume	$V^*$	REVOL
$m^{\text{th}}$ neighbor distance	$a_m$	DIST(M)
$m^{\text{th}}$ coordination number	$z_m$	COORD(M)
Lennard-Jones potential parameters	$\sigma$	SIGMA
	$\epsilon$	EP
Number of shells considered	-	MMAX
Cell-center pair distribution function	$\rho_c(R)$	RHO1
Molecular pair distribution function	$\rho(R)$	RHO

Variable	Symbol in Text	Name in Program
Radial distance from given molecule	R	R
Radial distance from cell center	r	CR
Increment in R for $\rho_c(R)$ calculation	-	DELC
Increment in R for $\rho(R)$ calculation	$\Delta R$	DELTAR
Increment in s	$\Delta s$	DELTAS
Increment in t	$\Delta t$	DELTAT
Increment in k	$\Delta k$	DELTAK
Number of strips in normalization	-	NG
Number of strips in k integration	-	JMX
Number of strips in s integration	-	NOS
Function X(k)	X(k)	XK
Function F(s)	F(s)	FS
Compressibility factor	PV/NKT	PVONKT
Reduced configurational internal energy	U/NKT	EONKT

The second program adjusts  $\rho(R)$  according to Equation (38) and evaluates  $U_c/NKT$ ,  $PV/NKT$  for each four values of the adjustment parameter B. The names used in the program are essentially those of the first program. The additional program variable B, however, corresponds to  $1/B$  in the text.

The programming parameters are given in Tables III and IV.

C  
C  
C  
C  
C  
C  
C  
C  
C  
C  
C

CALCULATION OF RADIAL DISTRIBUTION FUNCTION  
AND THERMODYNAMIC FUNCTIONS FOR A LATTICE  
MODEL LIQUID

RADIAL DEPENDENT GAUSSIAN CELL-CENTER  
PAIR DISTRIBUTION FUNCTION

LENNARD-JONES INTERACTION POTENTIAL

IMPLICIT REAL\*8(A-H,O-Z)  
COMMON SIGMA,TEMP,A,DR,H(9)  
COMMON CR(800),FCR(800),RHO1(800),GRHO1(800)  
COMMON R(400),FR(400),RHO(400),GRHO(400)  
COMMON S(60),FS(60),FSA(60),DELTAS,DELTAK  
COMMON MAXR,NDP  
COMMON NIC,NI,NOS,JMX  
DIMENSION FINT(200),FK(200),PK(200)  
DIMENSION AREA(900)  
DIMENSION EX(100)  
DIMENSION DIST(60),COORD(60)  
MMAX=40  
SIGMA=3.405  
TWO=2.  
READ (1,10) D,RETEMP,REVOL  
READ (1,1430) MO,(H(I),I=1,6)  
PI=3.14159265358979  
READ (1,520) (COORD(M),M=1,MMAX)  
TEMP=119.8\*RETEMP  
A=SIGMA\*((DSQRT(TWO)\*REVOL)\*\*(1./3.))

C  
C  
C  
C  
C

PROGRAMMING PARAMETERS

MAXD=6  
IF (REVOL-1.5) 52,57,57  
52 IF (REVOL-1.3) 53,56,56  
53 IF (REVOL-1.1) 54,55,55  
54 DEN=12.  
GO TO 59  
55 DEN=16.  
GO TO 59  
56 DEN=20.  
GO TO 59  
57 DEN=24.  
59 CONTINUE  
DELC=(A-SIGMA)/DEN  
NICT=A/DELC  
NICT=4\*(NICT/4)  
ZERO=A-NICT\*DELC  
NDP=(MAXD\*A-ZERO+.0001)/DELC  
NDP=2\*(NDP/2)

```

NI=100
DELTAK=.2
DELTAS=DELC
JMX=70
DELTAT=2.*DELTAS
DELTAR=2.*DELTAS
TMAX=25.0
RMAX=22.0
MAXR=(RMAX-ZERO)/DELTAR
MAXR=2*(MAXR/2)
WRITE (3,900)
WRITE (3,910) MMAX,NI,NOS, JMX
WRITE (3,920) TMAX,RMAX,DELC,DELTAS,DELTAT,DELTAR
WRITE (3,210)
WRITE (3,530) TEMP
WRITE (3,540) RETEMP
WRITE(3,550) REVOL
WRITE (3,560) A

```

C  
C  
C  
C

# DETERMINATION OF GAUSSIAN RHOC(R)

```

DD=D/3.
WRITE (3,590) D
WRITE (3,580)
NDK=-5
24 CONTINUE
DO 511 I=1,NDP
CR(I)=I*DELC+ZERO
RC=CR(I)
SRHO=0
DO 501 M=1,MMAX
IF (NDK) 599,599,598
599 IF (M-1) 598,598,1501
598 CONTINUE
EM=M
IF (EM-13.9) 533,532,532
532 IF (EM-28.9) 535,536,536
536 IF (EM-43.9) 537,538,538
538 IF (EM-52.9) 539,542,542
542 IF (EM-57.9) 543,544,544
533 DM=DSQRT(EM)*A
GO TO 534
535 DM=DSQRT(EM+1.)*A
GO TO 534
537 DM=DSQRT(EM+2.)*A
GO TO 534
539 DM=DSQRT(EM+3.)*A
GO TO 534
543 DM=DSQRT(EM+4.)*A
GO TO 534
544 DM=DSQRT(EM+5.)*A

```



```

534 CONTINUE
    DMOA=DM/A
    IF (I-1) 503,504,503
504 WRITE (3,570) M,DM,DMOA,COORD(M)
503 CONTINUE
    COEF=1./(DSQRT(6.*PI*DD*DM)*(DM*DM+3.*DD*DM))
    EXARG=(RC-DM)*(RC-DM)/(2.*D*DM)
    IF (EXARG-50.) 502,502,501
502 EG=DEXP(-1.*EXARG)
    SRHO=SRHO+COEF*EG*COORD(M)
501 CONTINUE
1501 RH01(I)=SRHO/(4.*PI)
511 CONTINUE
    IF (NDK) 1502,1503,1503
1503 WRITE (3,600)
    WRITE (3,610)
1502 CONTINUE
    JMIN=(SIGMA-ZERO+.001)/DELC
    JMM2=JMIN-2
    JMM1=JMIN-1
    EVEN=0
    ODD=0
    DO 2201 JJ=1,JMM1,2
    ODD=ODD+16.*PI*CR(JJ)*CR(JJ)*RH01(JJ)
2201 CONTINUE
    DO 2211 JJ=2,JMM2,2
    EVEN=EVEN+8.*PI*CR(JJ)*CR(JJ)*RH01(JJ)
2211 CONTINUE
    AD=4.*PI*CR(JMIN)*CR(JMIN)*RH01(JMIN)
    CCIG=(ODD+EVEN+AD)*DELC/3.
    IF (NDK) 23,22,22
    23 COORD(1)=12.*COORD(1)/(12.-CCIG)
    NDK=5
    GO TO 24
    22 CONTINUE
    DO 2221 JJ=1,JMM1
2221 RH01(JJ)=0
    DODD=0
    DEVEN=0
    DO 2241 I=1,NDP
    GRH01(I)=4.*PI*CR(I)*CR(I)*RH01(I)
    FCR(I)=CR(I)/A
    WRITE (3,1620) CR(I),FCR(I),RH01(I),GRH01(I)
    JCUT=MAXR*(DELTAR+.00001)/DELC
    IF (I-JCUT) 367,366,2241
367 IF (I/2.-I/2-.001) 364,364,365
364 DEVEN=DEVEN+2.*GRH01(I)
    GO TO 2241
365 DODD=DODD+4.*GRH01(I)
    GO TO 2241
366 DCHECK=(DODD+DEVEN+GRH01(JCUT))*DELC/3.
2241 CONTINUE

```

C

```

C
C      DETERMINATION OF NORMALIZATION CONSTANT
C
      S6=SIGMA**6
      S12=S6*S6
      GODD=0
      GEVEN=0
      WRITE (3,170)
      WRITE (3,650) MO,(H(I),I=1,6)
      DELR=A/NI
      NG=0
      KMAX=NI*.55267
      DO 1411 K=1,KMAX
      NG=NG+1
      Q=K*DELR
      PEVEN=0
      PODD=0
      DO 1401 J=JMIN,NDP
      RC=J*DELC+ZERO
      AD=RC**8+12.*RC**6*Q**2+25.2*(RC*Q)**4
      T1=AD+12.*RC**2*Q**6+Q**8
      TERM1=S12*T1/((RC*RC-Q*Q)**10)
      TERM2=S6*(RC*RC+Q*Q)/((RC*RC-Q*Q)**4)
      TERM3=-(SIGMA/RC)**12+(SIGMA/RC)**6
      TIM=16.*PI*RHO1(J)*RC*RC
      SSUM=TIM*(TERM1-TERM2+TERM3)/RETEMP
      IF (J/2.-J/2-.001) 1406,1406,1403
1406 IF (J-NDP) 1404,1405,1404
1405 PLAST=SSUM
      GO TO 1401
1404 PEVEN=PEVEN+2*SSUM
      GO TO 1401
1403 PODD=PODD+4*SSUM
1401 CONTINUE
      QR=(2.*Q)/A
      POT=DELC*(PODD+PEVEN+PLAST)/3.
      EXPOT=DEXP(-1.*POT)
      EX(K)=EXPOT
      GINT=Q*Q*EXPOT
      XLPR=-.434294481903251*POT
      WRITE (3,650) NG,Q,QR,POT,EXPOT,XLPR,GINT
      IF (K/2.-K/2-.001) 422,422,423
422 GEVEN=GEVEN+2.*GINT
      GO TO 409
423 GODD=GODD+4.*GINT
409 IF (POT-25.) 1411,1411,12
1411 CONTINUE
      12 VF=4.*PI*DELR*(GODD+GEVEN)/3.
      NG=(NG/2)*2
      WRITE (3,630) VF
      WRITE (3,160) NG
      WRITE (3,700) CCIG
      RHAV=4./((DSQRT(TWO)*A)**3)
      WRITE (3,380) RHAV
C

```

```

C
C      EVALUATION OF F(S)
C
      NMAX=NG
      SX=0
      DO 1004 L=1,NOS
      SX=L*DELTAS
      S(L)=SX
      SODD=0
      SEVEN=0
      COUNTS=0
      DO 31 J=1,JMX
      IF (J-1) 8,9,8
9      PK(1)=DELTAK
      GO TO 115
8      PK(J)=PK(J-1)+DELTAK
115     PKX=PK(J)
      COUNTF=0
      COUNTS=COUNTS+1.
      FODD=0
      FEVEN=0
      DO 211 I=1,NG
      Q=I*DELR
      COUNTF=COUNTF+1
218     FKINT=EX(I)*Q*DSIN(PKX*Q)/PKX
      IF (I-NG) 319,212,319
319     IF (I/2.-I/2-.001) 216,216,217
216     FEVEN=FEVEN+2.*FKINT
      GO TO 211
217     FODD=FODD+4.*FKINT
211     CONTINUE
212     FOFK=(FEVEN+FODD+FKINT)*DELR/3.
      FK(J)=4.*PI*FOFK/VF
100     SINT=FK(J)*FK(J)*PK(J)*DSIN(PK(J)*SX)*4.*PI
      IF (L-NOS) 4,942,942
942     IF (J-1) 43,42,43
42     WRITE (3,1350) SX
      WRITE (3,60)
43     WRITE (3,70) PK(J),FK(J),SINT
4     IF (J-JMX) 6,5,6
6     CONTINUE
      IF (J/2.-J/2-.001) 36,36,37
36     SEVEN=SEVEN+2.*SINT
      GO TO 31
37     SODD=SODD+4.*SINT
31     CONTINUE
5     FSA(L)=((SEVEN+SODD+SINT)*DELTAK)/(3.*8.*PI*PI*PI)
      FS(L)=FSA(L)/SX
1004    CONTINUE
      WRITE (2,1250) (S(L),FS(L),FSA(L),L=1,NOS)
      WRITE (3,1240)
      WRITE (3,1250) (S(L),FS(L),FSA(L),L=1,NOS)

```

C

C  
C  
C

## CALCULATION OF RHO(R)

```

DO 791 I=1,900
791 AREA(I)=0
   MAXJ=NOS/4+1
   DO 311 J=1,MAXJ
   MINA=(J-1)*2
   MINAP2=MINA+2
   MINAP1=MINA+1
   AEVEN=0
   AODD=0
   NOSM1=NOS-1
   NOSM2=NOS-2
   DO 321 I=MINAP1,NOSM1,2
321 AODD=AODD+4.*FSA(I)
   DO 331 I=MINAP2,NOSM2,2
331 AEVEN=AEVEN+2.*FSA(I)
   IF (J-1) 302,322,302
322 AREA(1)=(FSA(NOS)+AODD+AEVEN)*DELTAS/3.
   GO TO 311
302 AREA(J)=(FSA(NOS)+AODD+AEVEN+FSA(MINA))*DELTAS/3.
311 CONTINUE
   AREA(NOS/2+1)=0
   MAXK=NOS/4-1
   DO 341 K=1,MAXK
   AEVEN=0
   AODD=0
   MAXA=NOS-2*K
   MAXAM1=MAXA-1
   MAXAM2=MAXA-2
   DO 351 I=2,MAXAM2,2
351 AEVEN=AEVEN+2.*FSA(I)
   DO 371 I=1,MAXAM1,2
371 AODD=AODD+4.*FSA(I)
   AD=(AODD+AEVEN+FSA(MAXA))*DELTAS/3.
   AREA(NOS/2+1-K)=AREA(1)-AD
341 CONTINUE
   MAXT=(TMAX-ZERO+.001)/DELTAT
   NCR=0
   DO 381 NR=1,MAXR
   XR=NR*DELTAR+ZERO
   TODD=0
   TEVEN=0
   DO 361 NT=1,MAXT
   XT=NT*DELTAT+ZERO
   W=NR+NT
   WW=NR-NT
   LMAX=DABS(W)
   LMIN=DABS(WW)
   XFS=AREA(LMIN+1)-AREA(LMAX+1)
   NCC=((DELTAT+.000001)/DELC)*NT
   TING=XT*XES*RHO1(NCC)

```

```

      IF (NT-MAXT) 305,304,305
305 IF (NT/2.-NT/2-.001) 306,306,303
306 TEVEN=TEVEN+2.*TING
      GO TO 361
303 TODD=TODD+4.*TING
      GO TO 361
361 CONTINUE
304 FU=(TEVEN+TODD+TING)*DELTAT/3.
      RHO(NR)=2.*PI*FU/XR
381 CONTINUE
      WRITE (3,410)
      WRITE (3,420)
      DO 1381 NR=1,MAXR
      XR=NR*DELTAR+ZERO
      CRHO(NR)=4.*PI*XR*XR*RHO(NR)
      GRHOAV=RHAV*4.*PI*XR*XR
      RHNET=RHO(NR)-RHAV
      GRNET=GRHO(NR)-GRHOAV
      QR=XR/A
      R(NR)=XR
      FR(NR)=QR
      WRITE (3,400) QR,XR,RHO(NR),RHNET,GRHO(NR),GRNET
      WRITE (2,1044) QR,XR,RHO(NR),GRHO(NR),NR
1381 CONTINUE
      MAXRM1=MAXR-1
      MAXRM2=MAXR-2
      CODD=0
      CEVEN=0
332 DO 391 NR=1,MAXRM1
      XR=NR*DELTAR+ZERO
      IF (NR/2.-NR/2-.001) 334,334,335
334 CEVEN=CEVEN+2.*GRHO(NR)
      GO TO 391
335 CODD=CODD+4.*GRHO(NR)
391 CONTINUE
      CHECK=(CODD+CEVEN+GRHO(MAXR))*DELTAR/3.
      DEV=CHECK-DCHECK
      PCDEV=DEV*100./DCHECK
      TOTAL=0
      DO 431 M=1,MMAX
431 TOTAL=TOTAL+COORD(M)
      DR=DELTAR
      WRITE (3,430) RHAV
      WRITE (3,370) RMAX,DCHECK
      WRITE (3,390) RMAX,CHECK
      WRITE (3,450) DEV,PCDEV
      CALL THERM2
      WRITE (2,50) NICT,MAXR,DELTAR

```

C

193972

C  
C  
C

## FORMATS

```

10  FORMAT (6F10.4)
50  FORMAT (2I10,4F10.6)
60  FORMAT (24X,'K',21X,'F(K)',14X,'K INTEGRAND'/)
70  FORMAT (5F25.8)
160 FORMAT (//6X,'THE NUMBER OF STRIPS USED IS',I4//)
170 FORMAT (1H1,4X,'POINT',14X,'RADIUS',3X,
1  'FRACTIONAL RADIUS',11X,'POTENTIAL',9X,
1  'PROBABILITY',5X,'LOG PROBABILITY',11X,
1  'INTEGRAND'/)
210 FORMAT (///6X,'PHYSICAL PARAMETERS:')
240 FORMAT (3F20.8)
370 FORMAT (/6X,'THE NUMBER OF CELL CENTERS WITHIN',
1F6.2,'ANGSTROMS IS',F10.4/)
380 FORMAT (/6X,'THE AVERAGE VALUE OF RHO(R) USED',
1  ' IS',F10.6//)
390 FORMAT (/6X,'THE NUMBER OF MOLECULES WITHIN',
1F6.2,'ANGSTROMS IS',F10.4/)
400 FORMAT (F20.8)
410 FORMAT (1H1,9X,'FRACTIONAL',14X,'RADIAL',69X,
1  '(4*PI*R*R)*')
420 FORMAT (12X,'DISTANCE',12X,'DISTANCE',14X,
1  'RHO(R)',6X,'RHO(R)-RHO(AV)',3X,'(4*PI*R*R)',
1  '*RHO(R)',6X,'RHO(R)-RHO(AV)'/)
430 FORMAT (//6X,'THE GIVEN VALUE OF RHO(AV) IS',F12.8)
440 FORMAT (/6X,'THE CALCULATED NUMBER OF MOLECULES',
1  'IN THE FIRST',I4,' SHELLS IS',F8.2)
450 FORMAT (/6X,'THIS IS A DEVIATION OF',F12.8,
1  ' WHICH IS',F10.6,'%')
480 FORMAT (/6X,'THE GIVEN NUMBER OF CELL CENTERS',
1  ' IN THE FIRST',I4,'SHELLS IS',F8.2)
500 FORMAT (6F10.4)
520 FORMAT (3F20.8)
530 FORMAT (/12X,'THE TEMPERATURE IS',F8.2)
540 FORMAT (/12X,'THE REDUCED TEMPERATURE IS',F8.2)
550 FORMAT (/12X,'THE REDUCED VOLUME IS',F8.4)
560 FORMAT (/12X,'THE NEAREST NEIGHBOR DISTANCE IS',F8.4)
570 FORMAT (22X,I2,12X,F8.4,12X,F8.4,14X,F6.2)
580 FORMAT (/12X,'SHELL PARAMETERS:',//18X,'NUMBER',
19X,'MEAN RADIUS',3X,'FRACTIONAL RADIUS',8X,
1  'CELL CENTERS'/)
590 FORMAT (/12X,'THE PARAMETER D =',F6.4)
600 FORMAT (1H1,5X,'THE CELL-CENTER DISTRIBUTION IS',
1  ' AS FOLLOWS: '/')
610 FORMAT (24X,'RADIUS',11X,'FRACTIONAL DISTANCE',
122X,' RHOC(R)',14X,'4*PI*R*R*RHOC(R)'/)
620 FORMAT (F30.4,F30.2,F30.6)
630 FORMAT (///6X,'THE NORMALIZATION CONSTANT IS',F10.6)
650 FORMAT (I10,F20.4,F20.2,4D20.6)
700 FORMAT (6X,'THE NUMBER OF CELL-CENTERS ADJUSTED',
1  ' IS',F8.4//)

```

```

710 FORMAT (3F20.8)
900 FORMAT (1H1,5X,'PROGRAMMING PARAMETERS: '/')
910 FORMAT (12X,'MMAX = ',I4,/12X,'NI = ',I4,/12X,
1 'NOS = ',I4,/12X,'JMX = ',I4)
920 FORMAT (/12X,'T MAX = ',F8.4,/12X,'R MAX = ',
1F8.4,/12X,'DELR = ',F8.6,/12X,'DELTAS = ',
1F8.6,/12X,'DELTAT = 'F8.6,/12X,'DELTAR = ',
1F8.6//)
1042 FORMAT (4F15.8,12X,'RC',I4)
1044 FORMAT (4F15.8,12X,'RHO',I4)
1240 FORMAT (1H1,18X,'S',16X,'F(S)',14X,'S*F(S)')
1250 FORMAT (F20.6,2D20.6)
1350 FORMAT (1H1,5X,'THE TABULATION OF F(K) FOR S=',
1F8.4//)
1400 FORMAT (15X,2F15.6)
1430 FORMAT (I10,6F10.6)
1620 FORMAT (4F30.8)
      STOP
      END

```

C

## SUBROUTINE THERM2

C

C

```

      IMPLICIT REAL*8(A-H,O-Z)
      COMMON SIGMA,TEMP,A,DR,H(9)
      COMMON CR(800),FCR(800),RHO1(800),CRHO1(800)
      COMMON R(400),FR(400),RHO(400),GRHO(400)
      COMMON S(60),FS(60),FSA(60),DELTAS,DELTAK
      COMMON NJ,JMAX
      COMMON NIC,NI,NOS,JMX
      DRAD=A/200
      PI=3.14159265358979
      RETEMP=TEMP/119.8
      BK=1.38046D-16
      EP=119.8*BK
      TWO=2.
      WRITE (3,210)
      REVOL=((A/SIGMA)**3)/DSQRT(TWO)
      WRITE(3,550) REVOL
      WRITE (3,530) TEMP
      WRITE (3,540) RETEMP
      WRITE (3,560) A
      RHAV=4./((DSQRT(TWO)*A)**3)
      WRITE (3,380) RHAV
      RMAX=R(NJ)
      WRITE (3,50) RMAX
      WRITE (3,60) SIGMA,EP
      RV4=REVOL**4
      RV2=REVOL*REVOL

```

C

C  
C  
C

## EVALUATION OF REDUCED LATTICE ENERGY PER MOLECULE

```

C4EVEN=0
C2EVEN=0
C4ODD=0
C2ODD=0
DO 1 J=1,NJ
  RJ=R(J)
  Z=RJ*RJ/(A*A)
  C4INT=4.*PI*RJ*RJ*RHO(J)/(12.*Z**6)
  C2INT=4.*PI*RJ*RJ*RHO(J)/(6.*Z**3)
  IF (J-NJ) 6,7,6
6 IF (J/2.-J/2-.001) 2,2,3
2 C4EVEN=C4EVEN+2*C4INT
  C2EVEN=C2EVEN+2*C2INT
  GO TO 1
3 C4ODD=C4ODD+4*C4INT
  C2ODD=C2ODD+4*C2INT
  GO TO 1
7 C4LAST=C4INT
  C2LAST=C2INT
1 CONTINUE
5 CU4=(C4EVEN+C4ODD+C4LAST)*DR/3.
  CU2=(C2EVEN+C2ODD+C2LAST)*DR/3.
  ADCU4=(4*PI*RHAV*A**12)/(12.*9.*RMAX**9)
  ADCU2=(4*PI*RHAV*A**6)/(6.*3.*RMAX**3)
  CON4=CU4+ADCU4
  CON2=CU2+ADCU2
  REU=6*(CON4/RV4-CON2/RV2)
  WRITE (3,220) RMAX
  WRITE (3,230) CU4
  WRITE (3,240) CU2
  WRITE (3,250)
  WRITE (3,230) ADCU4
  WRITE (3,240) ADCU2
  WRITE (3,270)
  WRITE (3,230) CON4
  WRITE (3,240) CON2
  WRITE (3,260) REU

```

C  
C  
C  
C

## DETERMINATION OF THERMODYNAMIC FUNCTIONS

```

PV4=4.*CON4
PV2=CON2*2.
PVONKT=1.+6.*(PV4/RV4-PV2/RV2)/RETEMP
EONKT=REU/RETEMP
EXPV=PVONKT-1.
EXE=EONKT
WRITE (3,300)
WRITE (3,1310) PVONKT,EONKT
WRITE (3,340)
WRITE (3,1350) EXPV,EXE

```



C  
C  
C  
C

## FORMATS

```

50 FORMAT (/12X,'THE MAXIMUM RADIAL DISTANCE',
1' CONSIDERED IS',F6.2,' ANGSTROMS')
60 FORMAT (//6X,'THE LENNARD-JONES PARAMETERS',
1' ARE:'//12X,'SIGMA=',F6.3,//12X,'EPSILON=',D12.6)
210 FORMAT (1H1,5X,'PHYSICAL PARAMETERS:')
220 FORMAT (/6X,'FOR R(MAX)= ',F8.4)
230 FORMAT (/12X,F15.8,' IS THE COEFFICIENT OF',
1' THE (1/V*)**4 TERM')
240 FORMAT (/12X,F15.8,' IS THE COEFFICIENT OF',
1' THE (1/V*)**2 TERM')
250 FORMAT (/6X,'FROM R(MAX) TO INFINITY')
260 FORMAT (//6X,'THE REDUCED LATTICE ENERGY PER',
1' MOLECULE IS',F15.8/)
270 FORMAT (/6X,'FOR THE TOTAL')
300 FORMAT (///6X,'THE VALUES OF THE THERMODYNAMIC',
1' FUNCTIONS ARE:')
340 FORMAT (///6X,'THE VALUES OF THE EXCESS',
1' (INTERNAL) THERMODYNAMIC FUNCTIONS ARE:')
380 FORMAT (/12X,'THE AVERAGE VALUE OF RHO(R) IS',
1F10.6)
530 FORMAT (/12X,'THE TEMPERATURE IS',F8.2)
540 FORMAT (/12X,'THE REDUCED TEMPERATURE IS',F8.2)
550 FORMAT (/12X,'THE REDUCED VOLUME IS',F8.4)
560 FORMAT (/12X,'THE NEAREST NEIGHBOR DISTANCE IS',
1F8.4)
630 FORMAT (/6X,'THE FREE VOLUME IS',F15.8/)
1310 FORMAT (/12X,'PV/NKT = ',D15.8,//12X,'U*/NKT = ',
1D15.8)
1350 FORMAT (/12X,'PIV/NKT = ',D15.8,//12X,'UI*/NKT = ',
1D15.8/)
      RETURN
      END

```

C  
C  
C  
CADJUSTMENT OF RHO(R) AND CALCULATION OF  
THERMODYNAMIC FUNCTIONS

```

      IMPLICIT REAL*8 (A-H,O-Z)
      DIMENSION Q(320),QHO(320),BB(10)
      COMMON SIGMA,TEMP,A,DR,H(9)
      COMMON R(320),ER(320),RHO(320),GRHO(320)
      COMMON RN(100),RHON(100),GRHON(100)
      COMMON NIS,MAXR,B
      NPACK=4
      DO 4 L=1,NPACK
      READ (1,50) NICT,MAXR,DR
      READ (1,10) D,RETEMP,REVOL
      READ (1,1430) MO,(H(I),I=1,6)
      A1=3.8220
      PI=3.14159265358979
      TEMP=119.8*RETEMP
      TWO=2.
      SIGMA=3.405
      A=SIGMA*(REVOL*DSQRT(TWO))**(1./3.)
      WRITE (3,210)
      WRITE(3,550) REVOL
      WRITE (3,530) TEMP
      WRITE (3,540) RETEMP
      WRITE (3,560) A
      WRITE (3,590) D
      IF (MAXR-180) 6,7,7
6  NIS=NICT/2
      GO TO 9
7  NIS=NICT
9  CONTINUE
      NISO2=NIS/2
      READ (1,90) (Q(I),QHO(I),I=1,MAXR)
      BB(1)=3./2.
      BB(2)=2.
      BB(3)=3.
      BB(4)=4.
      DO 3 IB=1,4
      WRITE (3,80) BB(IB)
      B=BB(IB)
      WRITE (3,40)
      NMI=NISO2-1
      DO 1 I=1,NMI
      ROLD=Q(I)
      DOLD=A-ROLD
      COMP=1.-DOLD/(B*A)
      DNEW=COMP*DOLD
      RNEW=A-DNEW
      RN(I)=RNEW
      RHON(I)=QHO(I)*ROLD*ROLD/(RNEW*RNEW*COMP)
      GRHON(I)=4.*PI*RNEW*RNEW*RHON(I)

```

```

      FRN=RNEW/A
      FRO=ROLD/A
      WRITE (3,20) RNEW,FRN,RHON(I),GRHON(I),ROLD,
1     LFRO,QHO(I)
1 CONTINUE
      COMPN=1.
      RHON(NISO2)=QHO(NISO2)/COMPN
      RN(NISO2)=Q(NISO2)
      DO 2 I=1,NISO2
        R(I)=RN(I)
        FR(I)=R(I)/A
        RHO(I)=RHON(I)
        GRHON(I)=4.*PI*R(I)*R(I)*RHO(I)
2 CONTINUE
      I=NISO2
      RNEW=RN(I)
      FRN=RN(I)
      FRO=FRN
      ROLD=RNEW
      WRITE (3,20) RNEW,FRN,RHON(I),GRHON(I),ROLD,FRO,QHO(I)
      NMPL=NISO2+1
      DO 5 J=NMPL,MAXR
        R(J)=Q(J)
        RHO(J)=QHO(J)
5 CONTINUE
      CALL THERM3
3 CONTINUE
4 CONTINUE
10 FORMAT (6F10.4)
20 FORMAT (7F18.8)
30 FORMAT (6I10)
40 FORMAT (//13X,'NEW R',11X,'NEW R/A',8X,
1     'NEW RHO(R)',2X,'NEW 4*PI*R*R*RHO',13X,'OLD R'
1     '11X,'OLD R/A',8X,'OLD RHO(R)'/)
50 FORMAT (2I10,F10.6)
80 FORMAT (///6X,'FOR B = ',F8.4//)
90 FORMAT (15X,2F15.6)
210 FORMAT (1H1,5X,'PHYSICAL PARAMETERS:')
530 FORMAT (/12X,'THE TEMPERATURE IS',F8.2)
540 FORMAT (/12X,'THE REDUCED TEMPERATURE IS',F10.4)
550 FORMAT (/12X,'THE REDUCED VOLUME IS',F8.4)
560 FORMAT (/12X,'THE NEAREST NEIGHBOR DISTANCE IS',
1     IF8.4)
590 FORMAT (/12X,'THE PARAMETER D =',F6.4)
1430 FORMAT (I10,6F10.6)
      STOP
      END

```

C

C  
C  
C

## SUBROUTINE THERM3

```

      IMPLICIT REAL*8(A-H,O-Z)
      COMMON SIGMA,TEMP,A,DR,H(9)
      COMMON R(320),FR(320),RHO(320),GRHO(320)
      COMMON RN(100),RHON(100),GRHON(100)
      COMMON NIS,NJ,B
      DIMENSION C4I(100),C2I(100),RI(100)
      DIMENSION ZC4(100),ZC2(100)
      DO 2001 I=1,100
      C4I(I)=0
      C2I(I)=0
      RI(I)=R(I)
2001 CONTINUE
      AL=3.8220
      PI=3.14159265358979
      RETEMP=TEMP/119.8
      TWO=2
      REVOL=((A/SIGMA)**3)/DSQRT(TWO)
      RMAX=R(NJ)
      RV4=REVOL**4
      RV2=REVOL*REVOL
      RHAV=4./((DSQRT(TWO)*A)**3)

```

C  
C  
C  
C

## EVALUATION OF REDUCED LATTICE ENERGY PER MOLECULE

```

      ER=RD/B
      C4EVEN=0
      C2EVEN=0
      C4ODD=0
      C2ODD=0
      NISO2=NIS/2
      NDIM=NISO2
      DO 1 J=1,NISO2
      RJ=R(J)
      Z=RJ*RJ/(A*A)
      C4INT=4.*PI*RJ*RJ*RHO(J)/(12.*Z**6)
      C2INT=4.*PI*RJ*RJ*RHO(J)/(6.*Z**3)
      C4I(J)=C4INT
      C2I(J)=C2INT
1 CONTINUE
      CALL TRAP(RI,C4I,ZC4,NDIM)
      CALL TRAP(RI,C2I,ZC2,NDIM)
      CU2=ZC2(NDIM)
      CU4=ZC4(NDIM)
      ADCU4=(4*PI*RHAV*A**12)/(12.*9.*RMAX**9)
      ADCU2=(4*PI*RHAV*A**6)/(6.*3.*RMAX**3)
      NJM1=NJ-1
      NJM2=NJ-2

```

```

N2P1=NISO2+1
N2P2=NISO2+2
C4EVEN=0
C2EVEN=0
C4ODD=0
C2ODD=0
DO 11 J=N2P1,NJM1,2
  RJ=R(J)
  Z=RJ*RJ/(A*A)
  C4INT=4.*PI*RJ*RJ*RHO(J)/(12.*Z**6)
  C2INT=4.*PI*RJ*RJ*RHO(J)/(6.*Z**3)
  C4ODD=C4ODD+4*C4INT
  C2ODD=C2ODD+4*C2INT
11 CONTINUE
DO 21 J=N2P2,NJM2,2
  RJ=R(J)
  Z=RJ*RJ/(A*A)
  C2INT=4.*PI*RJ*RJ*RHO(J)/(6.*Z**3)
  C4INT=4.*PI*RJ*RJ*RHO(J)/(12.*Z**6)
  C2EVEN=C2EVEN+2*C2INT
  C4EVEN=C4EVEN+2*C4INT
21 CONTINUE
ZF=R(NISO2)*R(NISO2)/(A*A)
ZL=R(NJ)*R(NJ)/(A*A)
C2FIR=4.*PI*R(NISO2)*R(NISO2)*RHO(NISO2)/(6.*ZF**3)
C4FIR=4.*PI*R(NISO2)*R(NISO2)*RHO(NISO2)/(12.*ZF**6)
C2LAST=4.*PI*R(NJ)*R(NJ)*RHO(NJ)/(6.*ZL**3)
C4LAST=4.*PI*R(NJ)*R(NJ)*RHO(NJ)/(12.*ZL**6)
ACU4=(C4FIR+C4EVEN+C4ODD+C4LAST)*DR/3.
ACU2=(C2FIR+C2EVEN+C2ODD+C2LAST)*DR/3.
CON4=CU4+ADCU4+ACU4
CON2=CU2+ADCU2+ACU2
REU=6*(CON4/RV4-CON2/RV2)
WRITE (3,1220)
WRITE (3,230) CU4
WRITE (3,240) CU2
WRITE (3,220) RMAX
WRITE (3,230) ACU4
WRITE (3,240) ACU2
WRITE (3,250)
WRITE (3,230) ADCU4
WRITE (3,240) ADCU2
WRITE (3,270)
WRITE (3,230) CON4
WRITE (3,240) CON2
WRITE (3,260) REU

```

C  
C  
C  
C

#### DETERMINATION OF THERMODYNAMIC FUNCTIONS

```

PV4=4.*CON4
PV2=CON2*2.

```

```

PVONKT=1.+6.*(PV4/RV4-PV2/RV2)/RETEMP
EONKT=REU/RETEMP
EXPV=PVONKT=1.
EXE=EONKT
WRITE (3,300)
WRITE (3,1310) PVONKT,EONKT
WRITE (3,340)
WRITE (3,1350) EXPV,EXE

```

C  
C  
C  
C

# FORMATS

```

30 FORMAT (//10X,'RADIAL DISTANCE',6X,'FRACTIONAL',
1' DISTANCE',19X,'RHO(R)',13X,'4*PI*R*R*RHO'//)
40 FORMAT (F25.4,F25.2,2F25.8)
220 FORMAT (/6X,'FROM A TO R(MAX)= ',F8.4)
230 FORMAT (/12X,F15.8,' IS THE COEFFICIENT OF THE',
1' (1/V*)**4 TERM')
240 FORMAT (/12X,F15.8,' IS THE COEFFICIENT OF THE',
1' (1/V*)**2 TERM')
250 FORMAT (/6X,'FROM R(MAX) TO INFINITY')
260 FORMAT (//6X,'THE REDUCED LATTICE ENERGY PER',
1' MOLECULE IS',F15.8/)
270 FORMAT (/6X,'FOR THE TOTAL')
300 FORMAT (///6X,'THE VALUES OF THE THERMODYNAMIC',
1' FUNCTIONS ARE:'//)
340 FORMAT (///6X,'THE VALUES OF THE EXCESS (INTERNAL)',
1' THERMODYNAMIC FUNCTIONS ARE:'//)
1220 FORMAT (/6X,'FROM 0 TO A')
1310 FORMAT (/12X,'PV/NKT = ',D15.8,//12X,'U*/NKT = ',
1D15.8/)
1350 FORMAT (/12X,'PIV/NKT = ',D15.8,//12X,'UI*/NKT = ',
1D15.8/)
RETURN
END

```

C  
C

# SUBROUTINE TRAP(X,Y,Z,NDIM)

C

```

IMPLICIT REAL*8(A-H,O-Z)
DIMENSION X(100),Y(100),Z(100)
SUM2=0
IF (NDIM-1) 4,3,1
1 DO 2 I=2,NDIM
SUM1=SUM2
SUM2=SUM2+.5*(X(I)-X(I-1))*(Y(I)+Y(I-1))
2 Z(I-1)=SUM1
3 Z(NDIM)=SUM2
4 RETURN
END

```

## IX. BIBLIOGRAPHY

1. A. S. Eisenstein and N. S. Gingrich, Phys. Rev., 62, 261 (1942).
2. N. S. Gingrich, "X-ray and Neutron Diffraction Studies of Liquid Structure" in Liquids: Structure, Properties, Solid Interactions, edited by T. J. Hughel (Elsevier, New York, 1965).
3. D. G. Henshaw, Phys. Rev., 105, 976 (1957).
4. B. A. Dassancharya and K. R. Rao, Phys. Rev., 137, A417 (1965).
5. K. Huang, Statistical Mechanics (Wiley, New York, 1967) Chapter 14.
6. J. E. Meyer and M. G. Meyer, Statistical Mechanics (Wiley, New York, 1940) Chapter 13.
7. J. G. Kirkwood, J. Chem. Phys., 3, 300 (1935).
8. J. Yvon, Act. Sci. et Ind., 203 (1935).
9. M. Born and H. S. Green, Proc. Roy. Soc. (London) Ser. A, 188, 10 (1946).
10. N. N. Bogolyubov, Problems of Dynamical Theory in Statistical Physics (State Technical Press, Moscow, 1946).
11. J. K. Percus and G. L. Yevick, Phys. Rev., 110, 1 (1958).
12. D. Henderson and S. G. Davison, "Theory of Liquids," in Physical Chemistry, An Advanced Treatise, Volume II/Statistical Mechanics edited by H. Eyring (Academic Press, New York, 1967), p. 377.
13. J. E. Lennard-Jones and A. F. Devonshire, Proc. Roy. Soc., A163, 53 (1937).
14. J. E. Lennard-Jones and A. F. Devonshire, Proc. Roy. Soc., A165, 1 (1938).
15. N. Metropolis, M. Rosenbluth, A. Rosenbluth, A. Teller and E. Teller, J. Chem. Phys., 21, 1087 (1953).

16. W. W. Wood, J. P. Parker and J. D. Jacobson, *Nuovo Cimento, Suppl.*, 9, 133 (1958).
17. B. J. Alder and T. E. Wainwright, *Nuovo Cimento, Suppl.*, 9, 116 (1958).
18. J. A. Barker, *Aus. J. Chem.*, 13, 187 (1960).
19. J. A. Barker, *Proc. Roy. Soc.*, A259, 442 (1961).
20. J. G. Kirkwood, *J. Chem. Phys.*, 18, 380 (1950).
21. J. Frenkel, *Kinetic Theory of Liquids* (Dover, New York, 1955), p. 112-125.
22. N. S. Gingrich, *Rev. Mod. Phys.*, 15, 90 (1943).
23. T. L. Hill, *Statistical Mechanics, Principles and Selected Applications* (McGraw-Hill, New York, 1956) Chapter 6.
24. L. H. Lund, *J. Chem. Phys.*, 33, 1086 (1960).
25. J. E. Lennard-Jones, *Proc. Camb. Phil. Soc.*, 43, 461 (1931).
26. K. S. Pitzer, *J. Chem. Phys.*, 7, 583 (1939).
27. E. A. Guggenheim, *J. Chem. Phys.*, 13, 253 (1945).
28. I. Z. Fisher, *Statistical Theory of Liquids* (University of Chicago Press, Chicago, 1964).
29. W. Band, *Introduction to Mathematical Physics* (Van Nostrand, Princeton, 1959), p. 111.
30. J. S. Rowlinson, *Liquids and Liquid Mixtures* (Academic Press, New York, 1959), p. 250-254.
31. J. A. Barker, *Lattice Theories of the Liquid State* (Pergamon, New York, 1963).
32. J. O. Hirschfelder, C. F. Curtiss and R. B. Bird, *Molecular Theory of Gases and Liquids* (Wiley, New York, 1954).
33. J. E. Lennard-Jones and A. E. Ingham, *Proc. Roy. Soc.*, A107, 636 (1925).
34. A. Michels, H. B. G. Wijker, H. K. Wijker, *Physica*, 15, 627 (1949).



35. J. M. H. Levelt and E. G. D. Cohen, "Study of Some Theories of the Liquid State" in Studies in Statistical Mechanics, Vol. II, edited by J. DeBoer and G. E. Uhlenbeck (North-Holland, Amsterdam, 1964).
36. N. S. Gingrich and C. W. Thompson, J. Chem. Phys., 36, 2398 (1962).
37. P. G. Mikolaj and C. J. Pings, J. Chem. Phys., 46, 1401 (1967).
38. P. G. Mikolaj and C. J. Pings, J. Chem. Phys., 46, 1412 (1967).
39. C. J. Pings, "Structure of Simple Liquids by X-ray Diffraction" in Physics of Simple Liquids, edited by H. N. V. Temperley, J. S. Rowlinson and G. S. Rushbrooke (North-Holland, Amsterdam, 1968).
40. P. W. Schmidt and C. W. Thompson, "X-ray Scattering Studies of Simple Fluids" in Simple Dense Fluids, edited by H. L. Frisch and Z. W. Salsburg (Academic Press, New York, 1968).
41. R. H. Wentorf, R. J. Buehler, J. O. Hirschfelder and C. F. Curtiss, J. Chem. Phys., 18, 1484 (1950).
42. J. S. Dahler and J. O. Hirschfelder, J. Chem. Phys., 32, 330 (1960).
43. P. J. Hunter and J. S. Rowlinson, "Thermodynamic Functions Along the Orthobaric Liquids Line" in Simple Dense Fluids, edited by H. L. Frisch and Z. W. Salsburg.
44. A. Michels, J. M. Levelt and G. J. Wolders, Physica, 24, 769 (1958).
45. J. M. H. Levelt, Physica, 26, 361 (1960).
46. J. G. Kirkwood, V. A. Lewinson and B. J. Alder, J. Chem. Phys., 20, 929 (1952).
47. E. A. Guggenheim, Elements of the Kinetic Theory of Gases (Pergamon, New York, 1960).

## X. VITA

Jesse Herbert Collins II was born on February 2, 1938, in Springfield, Missouri. He attended Greenwood Training School in Springfield for his primary and secondary education. In September, 1956, he entered the University of Missouri - Rolla, graduating with a B.S. in Physics in 1960. He served eighteen months in the United States Army as a lieutenant in the Corps of Engineers and was employed by McDonnell Aircraft Corporation for approximately two years before returning to the University of Missouri - Rolla in 1963. Since then he has held both teaching and research assistantships.

He is married to the former Nancy Jeanette Rea from Springfield, Missouri, and has twin sons, William and Franklin, presently 12 years old.